

# PHOSPHOLIPASE A<sub>2</sub> AS THERAPEUTIC TARGETS IN PROSTATE CANCER

By

JASON NICHOLAS MOCK

(Under the Direction of Brian S. Cummings)

## ABSTRACT

The ultimate goal of this work is to improve chemotherapy through molecular targeting. Cancer cells undergo a myriad of pathological changes before a solid tumor forms. This is evidenced by dramatic over expression of oncogenes or other enzymes. One such enzyme family is phospholipase A<sub>2</sub> (PLA<sub>2</sub>), which are esterases that cleave phospholipids at the *sn*-2 position to yield a lysophospholipid and a fatty acid. There are six subfamilies of PLA<sub>2</sub>, including calcium-independent PLA<sub>2</sub> (iPLA<sub>2</sub>) and secretory PLA<sub>2</sub> (sPLA<sub>2</sub>). These two subfamilies will be the primary focus of this research. Each of these classes has distinct pathophysiological roles and can be exploited differently.

iPLA<sub>2</sub> are involved in membrane phospholipid homeostasis and signal transduction pathways related to proliferation and migration. Therefore, inhibition of iPLA<sub>2</sub> may halt or slow cancer growth. To test this hypothesis, putative iPLA<sub>2</sub> inhibitors were synthesized and screened for their ability to slow proliferation, inhibit iPLA<sub>2</sub>, and alter the cell cycle in a prostate cancer model.

sPLA<sub>2</sub> are commonly over expressed in prostate tumors as well as other cancers, and appear to have oncogenic properties. We developed liposomes that interact with sPLA<sub>2</sub>, and show that release from these sPLA<sub>2</sub> responsive liposomes (SPRL) can be mediated by sPLA<sub>2</sub>.

*In vitro* evaluation of SPRL, which was performed in several prostate cancer cell lines, showed that these formulations produce levels of cytotoxicity similar to free drug, and uptake of drug and carrier are cell- and carrier-dependent. Cytotoxicity was not different between formulations, nor was cytotoxicity or uptake affected by inhibition of sPLA<sub>2</sub>. This suggests that multiple mechanisms are mediating the observed cytotoxicity. Differential expression of sPLA<sub>2</sub> isoforms as well as the PLA<sub>2</sub> Receptor (PLA<sub>2</sub>R) may be also mediating formulation disposition. Preliminary *in vivo* studies suggest that SPRL are more effective at slowing tumor growth compared to conventional liposome formulations.

In conclusion, this work demonstrates that both iPLA<sub>2</sub> and sPLA<sub>2</sub> can be utilized as targets for molecular based therapeutics for prostate cancer. This targeting strategy may hold tremendous potential not only for the treatment of prostate cancer, but also for other pathologies where PLA<sub>2</sub> are over expressed.

INDEX WORDS: Phospholipase A<sub>2</sub>, prostate cancer, pharmacological inhibitor, calcium- independent PLA<sub>2</sub>, secretory PLA<sub>2</sub>, drug delivery, nanoparticle, liposome, targeting

PHOSPHOLIPASE A<sub>2</sub> AS THERAPEUTIC TARGETS IN PROSTATE CANCER

By

JASON NICHOLAS MOCK

B.S.A.B., University of Georgia, 2008

B.S.A., University of Georgia, 2008

A Dissertation Submitted to the Graduate Faculty of The University of Georgia in  
Fulfillment of the Requirements for the Degree

DOCTOR OF PHILOSOPHY

ATHENS, GA

2012

© 2012

Jason Nicholas Mock

All Rights Reserved

PHOSPHOLIPASE A<sub>2</sub> AS THERAPEUTIC TARGETS IN PROSTATE CANCER

By

JASON NICHOLAS MOCK

Major Professor:

Brian S. Cummings

Committee:

Robert D. Arnold  
Raj Govindarajan  
Timothy E. Long  
Tamas Nagy

Electronic Version Approved:

Maureen Grasso  
Dean of the Graduate School  
The University of Georgia  
August 2012

## ACKNOWLEDGEMENTS

Although this dissertation is the culmination of a degree that will be awarded to me, as an individual, the work herein was in no way an individual effort. Without the help and support of my friends, family, peers, and advisors, I would have had little chance of completing this task.

Firstly, my friends, many of whom are not involved in research, were there as a constant support system. Whether helping me unwind from the lab or forcing me to look at things from a different perspective, these were the individuals who kept my head above water when times were tough. In particular, I would like to thank my girlfriend, Becky Sweet, who, as a fellow graduate student and significant other, was absolutely instrumental to my success. She has been a sounding board for ideas, a source of helpful tips, and a sympathetic ear, but above all else, she has stood by me throughout this process.

My family, including my mother, father, and brother, has been amazing as well. They have known me longer than anyone else, and they know exactly what needs to be said. They were uplifting when I needed encouragement, motivating when I needed a push, and always affable whenever I just needed someone to agree with me. I would like to thank them for helping make me into the man I have become because it was their influence that made me tenacious enough to get to where I am today.

My peers deserve a great deal of recognition as well. Specifically, Bin Sun, Shirley Zhang, and Ibrahim Aljuffali taught me most of the methods that I utilized to complete this research. Additionally, Phillip Callihan helped me with day-to-day trouble shooting and Leah Costyn was instrumental in all of the animal studies I performed. My other labmates, including Narendrababu Kolisetty, Natalie Scholpa, Goudong Zhu, and Stephanie Wilding were also a tremendous help throughout this process.

My graduate committee was also key in shaping me into the scientist I have become. Their pointed questions and sharp input helped me develop a keen insight into research. Dr. Arnold, Dr. Long, Dr. Govindarajan, and Dr. Nagy have all been fantastic stewards along the completion of this degree, and I cannot thank them enough for their willingness to participate in my education.

Finally, I want to give a special thanks to Dr. Brian Cummings. When I met Dr. Cummings just four years ago, I was just a kid with a science degree, but after years of tutelage, I feel confident in saying that I am a scientist. We did not always agree on writing or presentation style, and the road to a Ph.D. can be trying from time to time, but with everything said and done, I could not have asked for a better advisor to instruct me on this project or a better teacher to show me how research should be done. I appreciate all of the time and effort invested into my education, and I am grateful to have had the chance to study here.

## TABLE OF CONTENTS

	Page
ACKNOWLEDGEMENTS.....	iv
TABLE OF CONTENTS.....	vi
LIST OF TABLES.....	viii
LIST OF FIGURES.....	ix
ABBREVIATIONS.....	xii
CHAPTER	
1 INTRODUCTION.....	1
Phospholipase A <sub>2</sub> .....	1
Calcium-Independent PLA <sub>2</sub> .....	6
iPLA <sub>2</sub> and Cancer.....	9
Secretory PLA <sub>2</sub> .....	10
sPLA <sub>2</sub> and Cancer.....	14
Prostate Cancer.....	15
Liposomes and Nanoparticulate Drug Delivery.....	18
Conclusions, Hypothesis and Specific Aims.....	22
2 MATERIALS AND METHODS.....	26

	Materials.....	26
	Methods.....	27
3	INHIBITORS OF iPLA <sub>2</sub> AS ANTINEOPLASTICS.....	41
	Abstract.....	42
	Introduction.....	42
	Results.....	45
	Discussion.....	53
4	EVIDENCE FOR DISTINCT MECHANISMS FOR MEDIATION OF SECRETORY PHOSPHOLIPASE A <sub>2</sub> RESPONSIVE LIPOSOME UPTAKE AND ANTITUMOR ACTIVITY IN A PROSTATE CANCER MODEL.....	54
	Abstract.....	55
	Introduction.....	56
	Results.....	59
	Discussion.....	74
5	MECHANISTIC ROLES OF PHOSPHOLIPASE A <sub>2</sub> RECEPTOR AND GROUP X SECRETORY PHOSPHOLIPASE A <sub>2</sub> IN MODULATING ACTIVITY OF SECRETORY PHOSPHOLIPASE A <sub>2</sub> RESPONSIVE LIPOSOMES IN PROSTATE CANCER CELLS.....	79
	Abstract.....	80
	Introduction.....	81
	Results.....	85

Discussion.....	98
6 SUMMARY.....	103
REFERENCES.....	108
APPENDIX.....	124

## LIST OF TABLES

	Page
Table 1.1: Classification of Phospholipase A <sub>2</sub> .....	4
Table 2.1: Liposome Compositions.....	30
Table 2.2: Primers for RT- and QRT-PCR.....	36
Table 3.1: IC <sub>50</sub> Values for Haloenol Pyranones and Morpholinones in LNCaP and PC-3 Cells.....	49

## LIST OF FIGURES

	Page
Figure 1.1: Basic activity of PLA <sub>2</sub> .....	1
Figure 1.2: The Lands Cycle.....	8
Figure 1.3: Enhanced Permeation and Retention Effect.....	21
Figure 1.4: Mechanism of SPRL.....	25
Figure 3.1: Mechanism of Haloenol Pyranones.....	44
Figure 3.2: Structure of Inhibitors.....	48
Figure 3.3: Cell Morphology in LNCaP.....	50
Figure 3.4: Cell Cycle Analysis in LNCaP.....	51
Figure 3.5: Inhibition iPLA <sub>2</sub> β.....	52
Figure 4.1: Effect of sPLA <sub>2</sub> Inhibition on 6-Carboxyfluorescein (6-CF) Release From SPRL and SSL.....	67
Figure 4.2: Time-dependent Effects of SPRL and SSL on MTT Staining in Human Prostate Cancer Cells.....	68

Figure 4.3: Tandem Tracking of Doxorubicin, SPRL and SSL in PC-3 Cells Using Flow Cytometry and Fluorescence Microscopy.....	69
Figure 4.4: Quantification of Fluorescence of Doxorubicin and DiO in Prostate Cancer Cells Exposed to SPRL and SSL.....	70
Figure 4.5: Time-dependence of DiO Uptake in Prostate Cancer Cells Exposed to SPRL and SSL.....	71
Figure 4.6: Time-dependence of Doxorubicin Uptake in Prostate Cancer Cells Exposed to SPRL and SSL.....	72
Figure 4.7: Effect of Doxorubicin Containing SPRL and SSL on PC-3 Xenograft Tumor Growth.....	73
Figure 5.1: Expression of sPLA <sub>2</sub> in Prostate Cancer Cells.....	90
Figure 5.2: Knockdown of PLA <sub>2</sub> R in PC-3 Cells.....	91
Figure 5.3: Phase contrast microscopy of wild type and PLA <sub>2</sub> R knockdown PC-3 cells treated with SSL and SPRL.....	92
Figure 5.4: Performance of SSL in WT and KD PC-3 Cells.....	93
Figure 5.5: Performance of SPRL-E in WT and KD PC-3 Cells.....	94
Figure 5.6: Performance of SPRL-G in WT and KD PC-3 Cells.....	95
Figure 5.7: Effect of Group X sPLA <sub>2</sub> on Cytotoxicity and Uptake of SSL and SPRL.....	96

Figure 5.8: Potential Drug Delivery Pathways.....97

## ABBREVIATIONS

6-CF: 6-carboxyfluorescein

AA: Arachidonic Acid

AdPLA<sub>2</sub>: Adipose specific phospholipase A<sub>2</sub>

ATP: Adenosine triphosphate

BEL: Bromoenol lactone

cPLA<sub>2</sub>: Cytosolic phospholipase A<sub>2</sub>

DiO: 3,3'-dioctadecyloxycarbocyanine perchlorate

Dox: Doxorubicin

DMSO: Dimethyl sulfoxide

DSPC: Distearoylphosphatidylcholine

DSPE: Distearoylphosphatidylethanolamine

DSPG: Distearoylphosphatidylglycerol

EGF: Epidermal growth factor

ESI-MS: Electrospray ionization mass spectroscopy

GAPDH: Glyceraldehyde 3-phosphate dehydrogenase

HSPG: Heparin sulfate proteoglycan

IC<sub>50</sub>: Half maximum inhibitory concentration

iPLA<sub>2</sub>: Calcium-independent phospholipase A<sub>2</sub>

KD: Knockdown

LPA: Lysophosphatidic Acid

LPC: Lysophosphatidylcholine

MAPK: Mitogen activated protein kinase

MRI: Magnetic resonance imaging  
MTT: 3-(4,5-dimethylthiazol-2-yl)-2,5-diphenyltetrazolium bromide  
PAF: Platelet activating factor  
PBS: Phosphate buffered saline  
PC: Phosphatidylcholine  
PE: Phosphatidylethanolamine  
PEG: polyethylene glycol  
PGE<sub>2</sub>: Prostaglandin E<sub>2</sub>  
PI: Propidium iodide  
PLA<sub>2</sub>: Phospholipase A<sub>2</sub>  
PLA<sub>2</sub>R: Phospholipase A<sub>2</sub> Receptor  
PNPLA: Patatin-like phospholipase domain-containing lipase  
PSA: Prostate specific antigen  
Rac: racemic  
ROS: Reactive oxygen species  
RT: Radiation therapy  
SPION: superparamagnetic iron oxide nanoparticle  
sPLA<sub>2</sub>: secretory phospholipase A<sub>2</sub>  
SSL: sterically stabilized liposomes  
SPRL: secretory phospholipase A<sub>2</sub> responsive liposome  
TG: Triglyceride  
WT: Wild-type

CHAPTER 1  
INTRODUCTION

**Phospholipase A<sub>2</sub>**

Phospholipase A<sub>2</sub> (PLA<sub>2</sub>) are a diverse class of esterases that cleave glycerophospholipids at the *sn*-2 bond to yield a fatty acid and a lysophospholipid (Cummings et al., 2000), as shown in Figure 1.1. Up until 1986, only one mammalian PLA<sub>2</sub> had been discovered, but today, more than 30 isoforms and related enzymes have been identified. These enzymes range in size, location, function, substrate specificity, and calcium requirement, and they are subdivided into six families based on their structure, catalytic mechanism, localization, and evolutionary relationships (Dennis et al., 2011; Murakami et al., 2012).

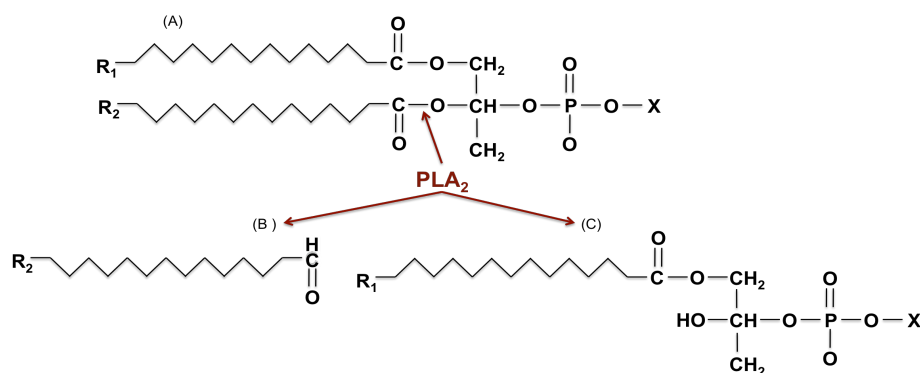


**Figure 1.1 Basic Activity of PLA<sub>2</sub>.** Phospholipase A<sub>2</sub> hydrolyze the ester bond at the *sn*-2 position of glycerophospholipids (A) to release a fatty acid (B) and a lysophospholipid (C).

The six subfamilies of PLA<sub>2</sub> are cytosolic PLA<sub>2</sub> (cPLA<sub>2</sub>), calcium-independent PLA<sub>2</sub> (iPLA<sub>2</sub>), small molecular weight secretory PLA<sub>2</sub> (sPLA<sub>2</sub>), lysosomal PLA<sub>2</sub>, platelet activating factor acetylhydrolases, and the recently discovered adipose specific PLA<sub>2</sub> (AdPLA<sub>2</sub>) (Murakami et al., 2012). Each of these families and their physiological roles will be covered briefly in this section and outlined in Table 1.1 before iPLA<sub>2</sub> and sPLA<sub>2</sub> are expanded on in detail.

The cPLA<sub>2</sub> family contains six isoforms ranging in size from 60-85 kDa. As the name implies, these isoforms are generally localized to the cytosol. They are active in the presence of  $\mu$  M levels of calcium and, with the exception of cPLA<sub>2</sub> $\gamma$ , contain an N-terminal C2 domain for binding two Ca<sup>2+</sup> ions as well as two conserved phosphorylation sites. The conserved Ser/Asp catalytic dyad is similar in structure to that of iPLA<sub>2</sub>, and most cPLA<sub>2</sub> have a preference for choline head groups and arachidonic acid in the *sn*-2 position. As such, these enzymes play an integral role in prostanoid signaling cascades (Dennis et al., 2011; Murakami et al., 2012).

There are currently nine mammalian isoforms of iPLA<sub>2</sub> that have been identified. The catalytic site of iPLA<sub>2</sub> is similar to cPLA<sub>2</sub>, but unlike cPLA<sub>2</sub> these isoforms do not require a calcium cofactor to function and they are generally larger in size, ranging from 84-90 kDa. These enzymes are localized either to the cytosol or the inner side of the cell membrane, and they have little substrate specificity. iPLA<sub>2</sub> are integrally involved in lipid remodeling and the Land's Cycle, shown in Figure 1.2, as well as mediating

cell growth signaling (Dennis et al., 2011; Murakami et al., 2012). This family will be covered in more detail in a later section.

sPLA<sub>2</sub> are considerably different than most other PLA<sub>2</sub>. For instance, they generally have a lower molecular weight, ranging in size from 14-19 kDa. Additionally, their active site has a His/Asp catalytic dyad, as opposed to most other PLA<sub>2</sub>, which have a catalytic serine in their active site. sPLA<sub>2</sub> require mM concentrations of calcium to properly function, and are involved in a variety of physiological and pathological functions (Dennis et al., 2011; Lambeau and Gelb, 2008b), which will be covered in subsequent sections.

Platelet activating factor (PAF) acetylhydrolases are a much smaller family compared to cPLA<sub>2</sub> and iPLA<sub>2</sub>, both in terms of molecular weight and number of isoforms. There are four members of this family, three that are expressed intracellularly, and one secreted form that has generated interest as a drug target for atherosclerosis. All of the members of this family have a catalytic serine and serve the primary function of releasing acetate from the *sn*-2 position of PAF, although they also can catalyze the release of oxidized acyl groups from the *sn*-2 position of phosphocholine (PC) and phosphoethanolamine (PE) (Dennis et al., 2011; Murakami et al., 2012).

There are only two members of the lysosomal PLA<sub>2</sub> family, both of which are structurally very distinct. However, these two are grouped together due to their localization in the lysosome and preference for catalysis in an acidic pH environment. Both of these enzymes, although generally expressed in different cell types, play a role in surfactant metabolism,

specifically catabolic homeostasis of lung surfactants (Dennis et al., 2011; Murakami et al., 2012).

Adipose-specific PLA<sub>2</sub> or AdPLA<sub>2</sub>, were only recently discovered. This enzyme is found abundantly in white adipose tissue and appears to be responsible for supplying arachidonic acid for PGE<sub>2</sub> synthesis within this tissue. Additionally, AdPLA<sub>2</sub> may have roles in energy regulation by cleaving fatty acids from stored triglycerides (TG). Depending on experimental conditions, AdPLA<sub>2</sub> have also shown the ability to hydrolyze the *sn*-1 position of glycerophospholipids, thus the correct classification may PLA<sub>1/2</sub> rather than a traditional PLA<sub>2</sub> (Dennis et al., 2011; Murakami et al., 2012).

**Table 1.1 Classification of Phospholipase A<sub>2</sub> (Continued on Page 5)**

Family	Classification	Gene Name	Other Name
cPLA <sub>2</sub>	IVA	Pla2g4a	cPLA <sub>2</sub> α
	IVB	Pla2g4b	cPLA <sub>2</sub> β
	IVC	Pla2g4c	cPLA <sub>2</sub> γ
	IVD	Pla2g4d	cPLA <sub>2</sub> δ
	IVE	Pla2g4e	cPLA <sub>2</sub> ε
	IVF	Pla2g4f	cPLA <sub>2</sub> ζ
iPLA <sub>2</sub>	VIA	Pla2g6a	iPLA <sub>2</sub> β PNPLA 9
	VIB	Pla2g6b	iPLA <sub>2</sub> γ PNPLA 8
	VIC	Pla2g6c	iPLA <sub>2</sub> δ NTE
	VID	Pla2g6d	iPLA <sub>2</sub> ε Adiponutrin

	VIE	Pla2g6e	iPLA <sub>2</sub> ζ
	VIF	Pla2g6f	iPLA <sub>2</sub> η GS2
	PNPLA 1	Pnpla1	
	PNPLA 5	Pnpla5	GS2-like
	PNPLA 7	Pnpla7	NRE
sPLA <sub>2</sub>	IB	Pla2g1b	Pancreatic sPLA <sub>2</sub>
	IIA	Pla2g2a	sPLA <sub>2</sub>
	IIC	Pla2g2c	
	IID	Pla2g2d	
	IIE	Pla2g2e	
	IIF	Pla2g2f	
	III	Pla2g3	
	V	Pla2g5	
	X	Pla2g10	
	XIIA	Pla2g12a	
	XIIB	Pla2g12b	
PAF-AH	VIIA	Pla2g7	Plasma PAF-AH
	VIIB	paf1h2	PAF-AH II
	VIIIA/B	Pafah1b1/1b2	PAF-AH I α <sub>1</sub> /α <sub>2</sub>
Lysosomal PLA <sub>2</sub>	XV	Pla2g15	LPLA <sub>2</sub>
		Prdx6	aiPLA <sub>2</sub>
AdPLA <sub>2</sub>	XVI	Pla2g16	H-Rev 107

Adapted from Dennis et al. 2011 and Murakami et al. 2012

## Calcium-Independent PLA<sub>2</sub>

Calcium-independent phospholipase A<sub>2</sub> (iPLA<sub>2</sub>) are one of the larger subfamilies of PLA<sub>2</sub>. There are currently between six and nine putative members of the iPLA<sub>2</sub> class, depending on how they are categorized (Dennis et al., 2011; Murakami et al., 2012), which are sometimes referred to as patatin-like phospholipase domain-containing lipases or PNPLA (Kienesberger et al., 2009; Saarela et al., 2008). The moniker PNPLA may be more appropriate than iPLA<sub>2</sub>, as continuing research shows that this subfamily behaves more like conventional lipases than phospholipases, as they can hydrolyze a variety of substrates other than phospholipids, including triglycerides and retinol esters (Rydell et al., 2003; Saarela et al., 2008). However, most iPLA<sub>2</sub> researchers still refer to them by more traditional monikers, specifying isoforms by their group or Greek names (Dennis et al., 2011).

Like their cPLA<sub>2</sub> brethren, iPLA<sub>2</sub> have a catalytic domain that relies on a Ser/Asp dyad (Dennis et al., 2011), as opposed to Ser/His/Asp catalytic triad like most other general lipases (Rydell et al., 2003). Some iPLA<sub>2</sub> also contain a large, unique N-terminal region that may be involved in protein-protein interactions or membrane spanning/binding, and these isoforms primarily function as a phospholipases (this includes PNPLA 6-9, or iPLA<sub>2</sub> β, γ, and δ and Neuropathy target esterase related esterase or NRE). In contrast, enzymes that lack this region function more like lipases (PNPLA 1-5, or iPLA<sub>2</sub> α, ε, ζ, and η and GS-2 like), mostly hydrolyzing triglycerides and lipid

droplets rather than membrane phospholipids (Murakami et al., 2012). On a structural level, regardless of whether the isoform belongs to the PLA<sub>2</sub>-type or lipase-type sub groups, these enzymes all share glycine-rich nucleotide binding domains that are located adjacent to the catalytic domain, and, while unaffected by Ca<sup>2+</sup> concentrations, they are activated several fold by the binding of ATP (Hsu et al., 2009; Ramanadham et al., 1997).

Among iPLA<sub>2</sub> isoforms, iPLA<sub>2</sub> β and γ (Group VIA and VIB, respectively) are the most widely studied isoforms (Dennis et al., 2011; Murakami et al., 2012), but iPLA<sub>2</sub>, in general, are thought to function primarily in a homeostatic role, playing an integral part in normal lipid remodeling and the Land's Cycle (Balsinde et al., 1995; Balsinde and Dennis, 1997), as shown in Figure 1.2. This hypothesis is supported by multiple studies using bromoenol lactone (BEL), an iPLA<sub>2</sub>-selective inhibitor, or antisense oligonucleotide for against iPLA<sub>2</sub>β. The typical result seen in cells under these conditions was a significant decrease in lysophosphatidylcholine (LPC) and arachidonic acid (AA) incorporation into cell membranes (Balsinde et al., 1995; Balsinde and Dennis, 1997). Similarly, others have showed that over expression of iPLA<sub>2</sub>β increased nonselective fatty acid release from cell membranes, which was reversed by the addition of BEL (Atsumi et al., 2000; Murakami et al., 1998). Aside from this canonical function, iPLA<sub>2</sub> are also reported to mediate cell signaling pathways implicated in cell cycle progression (Herbert and Walker, 2006), proliferation (Balboa et al., 2008; Roshak et al., 2000; Song et al., 2007), migration (Ayilavarapu et al., 2010;

Hoeft et al., 2010; Mishra et al., 2008) and apoptosis (Bao et al., 2007; Perez et al., 2006) through the release of fatty acid and lysophospholipid messengers. This suggests that these enzymes have potential roles in cancer cell growth. Also of note, mutations in several different isoforms of iPLA<sub>2</sub> are associated with human diseases including neurodegeneration (Malik et al., 2008; Morgan et al., 2006; Shinzawa et al., 2008; Sina et al., 2009), obesity (Huang et al., 2010; Lake et al., 2005; Liu et al., 2004) and hepatic steatosis (Radner et al., 2012).

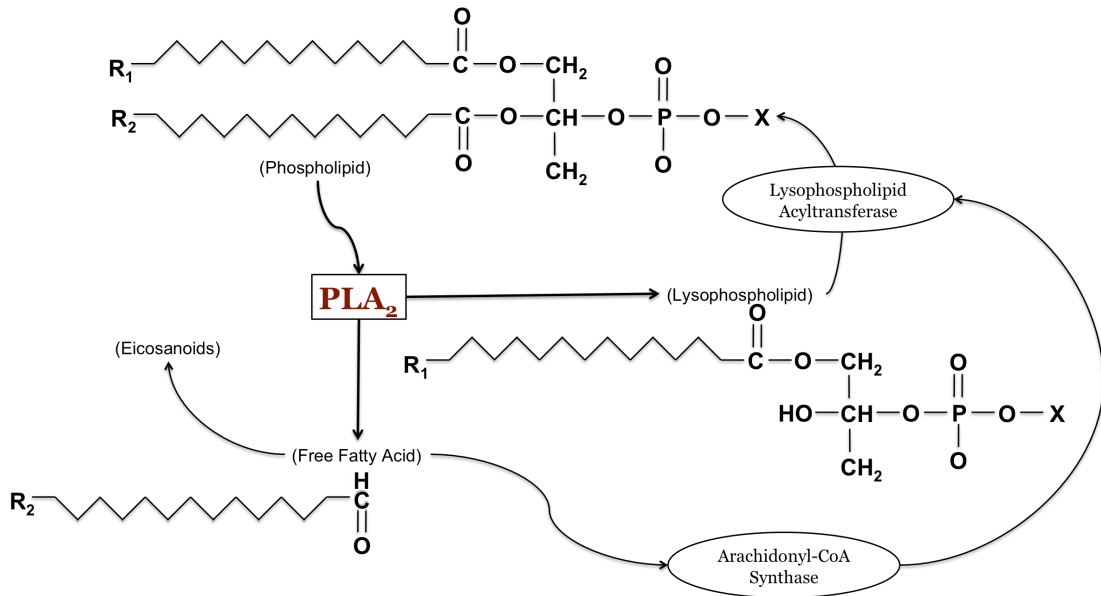


**Figure 1.2 The Lands Cycle.** The Lands cycle is vital to lipid membrane homeostasis and the recycling of phospholipid components. Membrane phospholipids can be hydrolyzed by PLA<sub>2</sub> yielding a fatty acid and lysophospholipid. While both lipid molecules can serve as signaling molecules, they can also be recycled through the Lands cycle, in which lysophospholipid acyltransferase produces new lipids from the existing lysophospholipid and fatty acid pools. Adapted from Zheng et. al 2012.

## **iPLA<sub>2</sub> and Cancer**

iPLA<sub>2</sub> are reported to play a role in cancer cell growth and possibly carcinogenesis. Expression of these enzymes has been noted in several types of cancer cells including pancreatic, kidney, and brain (Ma et al., 1998; Peterson et al., 2007; Zhang et al., 2005). Furthermore, recent studies showed that iPLA<sub>2</sub> $\beta$  knockout mice had a 50% reduction in tumor growth when implanted with ovarian cancer cells compared to WT mice (Li et al., 2010). This is likely due to the decreased generation of LPA and LPC in the microenvironment of the tumors. Other groups have shown that treating ovarian cancer cells with BEL in culture prevents proliferation and results in S- or G2/M-phase arrest. The S-phase arrest can be reversed by the addition of LPA or epidermal growth factor (EGF), suggesting that iPLA<sub>2</sub> likely plays a role in the production of these growth factor (Song et al., 2007). Additionally, other groups have shown strong statistical associations between iPLA<sub>2</sub> over expressing haplotypes and the initiation of colon cancer in humans (Hoeft et al., 2010).

Prostate cancer is particularly of interest to our laboratory, and we have previously shown that inhibition of iPLA<sub>2</sub> in multiple human prostate cancer cell lines results in cell cycle arrest that is both p53-dependent and -independent (Sun et al., 2008). Furthermore, our laboratory also demonstrated that iPLA<sub>2</sub> inhibition of in prostate cancer cells activates p38 mitogen-activated protein kinase (MAPK) through the generation of reactive oxygen species (ROS), suggesting that p38 is involved in the signaling

pathways responsible for the observed cytostasis (Sun et al., 2010). Altogether, these data suggests that iPLA<sub>2</sub> is a viable target for pharmacological intervention of prostate cancer.

### **Secretory PLA<sub>2</sub>**

Secretory phospholipase A<sub>2</sub> (sPLA<sub>2</sub>) are unique members of the PLA<sub>2</sub> superfamily. There are currently 11 mammalian isoforms of sPLA<sub>2</sub> belonging to groups I, II, III, V, X and XII. Of these, groups I, II, V and X are considered “conventional” sPLA<sub>2</sub> (Dennis et al., 2011; Murakami et al., 2012). They cluster on the same chromosome locus and share a variety of structural elements including a His/Asp catalytic dyad, a highly conserved Ca<sup>2+</sup> binding domain, and six absolutely conserved disulfide bonds. Groups III and XII, on the other hand, are structurally distinct, only sharing homology with the aforementioned groups in their Ca<sup>2+</sup> binding loop and catalytic site (Tischfield et al., 1996; Valentin et al., 2000). Additionally, all sPLA<sub>2</sub> share the trait of requiring calcium on the order of mM levels to operate (Dennis et al., 2011; Murakami et al., 2012).

The function, localization, and expression of sPLA<sub>2</sub> are isoform specific and these enzymes play a variety of important roles in many physiological processes and pathologies. sPLA<sub>2</sub> generally function outside of the cell, but depending on the isoform, these enzymes hydrolyze a wide range of substrates; however, all of the groups are interfacially active (Dennis et al., 2011; Murakami et al., 2012).

Group I sPLA<sub>2</sub>, of which IB is the only mammalian isoform, are thought of primarily as digestive enzymes (Seilhamer et al., 1986). Group IB sPLA<sub>2</sub> is secreted by the pancreas as an inactive zymogen, and is cleaved by trypsin in the duodenum to become active. These enzymes have evolved to be more active in the presence of mild detergents, and therefore are well suited for hydrolyzing dietary phospholipids in the presence of bile acids (Kudo et al., 1993; Verheij et al., 1981). Like most of their sPLA<sub>2</sub> brethren, Group IB sPLA<sub>2</sub> has a clear preference for anionic phospholipids.

Group II sPLA<sub>2</sub> are a much larger family in mammals than Group I sPLA<sub>2</sub>, and contains isoforms IIA, IIB, IIC, IID, IIE and IIF (Dennis et al., 2011). Group IIA sPLA<sub>2</sub> was the first isolated of this group (Seilhamer et al., 1989) and is the most widely studied. Unlike Group IB sPLA<sub>2</sub>, Group II sPLA<sub>2</sub> are considered inflammatory sPLA<sub>2</sub>, as they are induced by pro-inflammatory stimuli and are commonly found in excess in the serum of patients with rheumatoid arthritis, Crohn's Disease, atherosclerosis and sepsis (Bingham et al., 1996; Bostrom et al., 2007; Crowl et al., 1991; Fraser et al., 2009; Leistad et al., 2004; Nakano and Arita, 1990; Oka and Arita, 1991; Pfeilschifter et al., 1993; Pruzanski and Vadas, 1988; Rosengren et al., 2006). Of course, these enzymes are not solely expressed in disease states, and, to the contrary, are generally associated with their role in host defense (Nevalainen et al., 2008). Group II sPLA<sub>2</sub> have a strong binding affinity for heparin sulfate proteoglycans (HSPG), which provide support and proximity to the cell membrane (Murakami et al., 1999; Murakami et al., 1998). Furthermore, these enzymes

can also be taken up and degraded via their attachment to HSPG through a caveola-dependent endocytotic pathway (Kim et al., 2001; Murakami et al., 1989). Similar to Group IB sPLA<sub>2</sub>, Group II sPLA<sub>2</sub> have a strong preference for anionic lipids, in particular phosphatidylethanolamine (PE) and phosphatidylglycerol (PG). This preference for PE and PG is useful for their role as a defensive protein, as PE and PG are major components of bacterial membranes (Nevalainen et al., 2008).

There is only one isoform in the Group III sPLA<sub>2</sub> sub-family, which is distinct from those sPLA<sub>2</sub> covered thus far. First, it is a comparatively larger protein, with a molecular weight of 55 kDa. Group sPLA<sub>2</sub> III can cleave both PC and PE effectively and may play a role in arachidonic acid release from the membrane (Murakami et al., 2012). Although Group sPLA<sub>2</sub> III has large N and C terminal regions that are unique to the sPLA<sub>2</sub> superfamily, these epitopes can be cleaved by convertases, leaving an sPLA<sub>2</sub>-domain only form that is still catalytically active (Kim et al., 2001; Murakami et al., 2005).

Group V sPLA<sub>2</sub> is another conventional sPLA<sub>2</sub> group. These enzymes are similar to Group II sPLA<sub>2</sub>, although they are more catalytically active. Like Group II sPLA<sub>2</sub>, they participate in the HSPG-shuttling pathway, but can also function independently of HSPG (Han et al., 1999; Kim et al., 2001; Kim et al., 2002). Physiologically, Group V sPLA<sub>2</sub> function in paracrine eicosanoid synthesis/signaling (Munoz et al., 2006; Wijewickrama et al., 2006) and in the hydrolysis of lipids in lung surfactants and lipoproteins (Hite et al., 1998; Ohtsuki et al., 2006). While many sPLA<sub>2</sub> are noted for their ability to release

arachidonic acid, Group V sPLA<sub>2</sub> have actually displayed a marked preference for lipids with oleic acid in the *sn*-2 position (Murakami et al., 1998).

Similar to Group IB sPLA<sub>2</sub>, Group X sPLA<sub>2</sub> is secreted as a zymogen and is only activated upon proteolytic cleavage (Morioka et al., 2000). Group X sPLA<sub>2</sub> expression is unaltered by pro-inflammatory stimuli. It is the most active sPLA<sub>2</sub> in terms of PC cleavage (Hanasaki et al., 1999) and it is extremely efficient at hydrolyzing lipids in lung surfactants (Hite et al., 1998) and serum lipoproteins (Pruszanski et al., 2005). The promiscuous substrate specificity of Group X sPLA<sub>2</sub> is likely due to its large, open active site that is neutrally charged (Pan et al., 2002). Unlike Groups II and V, Group X sPLA<sub>2</sub> does not participate in the HSPG shuttling pathway, but rather is a substrate for PLA<sub>2</sub>R, a receptor of the C-type lectin superfamily (Hanasaki and Arita, 2002; Lambeau and Gelb, 2008a). Group X sPLA<sub>2</sub> does not have to be catalytically active in order to be taken up by PLA<sub>2</sub>R (Morioka et al., 2000).

Lastly, Group XII sPLA<sub>2</sub> consists of two isoforms, XIIA and XIIB, the latter of which is catalytically inactive (Gelb et al., 2000; Rouault et al., 2003). The exact role of these enzymes have not been elucidated, but the high level of expression of Group XIIA sPLA<sub>2</sub> in a variety of tissues suggests a housekeeping function (Ho et al., 2001). Compared to other sPLA<sub>2</sub>, Group XIIA sPLA<sub>2</sub> has weak catalytic activity in traditional assay conditions (Rouault et al., 2003), making its expression profile and function all the more mysterious.

Overall, sPLA<sub>2</sub> are very diverse in terms of physiological function. While they share many structural similarities, there are important distinctions between groups that lead to differences in substrate specificity and preference as well as binding partners and endocytotic pathways. Although the full extent of the roles of many isoforms has yet to be determined, their evolutionary conservation suggests that they play important parts in processes as distinct as host immunity and defense, digestion, and signal transduction (Dennis et al., 2011; Lambeau and Gelb, 2008a).

### **sPLA<sub>2</sub> and Cancer**

sPLA<sub>2</sub> are commonly over expressed during bouts of inflammation and in inflammatory diseases like arthritis, atherosclerosis and sepsis [41-50]. However, sPLA<sub>2</sub> are also over expressed in a variety of cancers (Dong et al., 2006; Yamashita et al., 1994a) including breast (Yamashita et al., 1994b; Yamashita et al., 1993), colon (Leung et al., 2002), pancreas (Kiyohara et al., 1993; Kuopio et al., 1995; Oka et al., 1990) and prostate (Graff et al., 2001; Jiang et al., 2002; Kallajoki et al., 1998; Sved et al., 2004). Interestingly, it appears that in some instances sPLA<sub>2</sub> play an oncogenic role (Dong et al., 2006; Jiang et al., 2002; Murakami et al., 2005; Sved et al., 2004), and their over expression is correlated to poor clinical prognosis in prostate cancers (Graff et al., 2001). On the other hand, over expression of sPLA<sub>2</sub> in colon cancer appears to have a beneficial clinical correlation (Leung et al., 2002). There are a variety of explanations for both of these phenomena (Nakanishi

et al., 2008; Sonoshita et al., 2001), but for the purposes of this study we will focus on over expression in prostate cancer.

Over expression of sPLA<sub>2</sub>, particularly sPLA<sub>2</sub> IIA, has been observed in prostate cancer for a number of years (Sved et al., 2004). In fact, the up regulation of this enzyme is such a common clinical feature of this disease, research has focused on using serum sPLA<sub>2</sub> levels as a replacement, or partner diagnostic, to the more conventional prostate specific antigen (PSA) test (Dong et al., 2010; Kupert et al., 2011). No clinical diagnostics have been developed to date, but it is apparent that sPLA<sub>2</sub> over expression is associated with aggressive prostate cancer. Others have reported that some tumors show levels of over expression up to 22-fold higher than physiological levels (Sved et al., 2004) and in one study, 91% of high-grade tumors were immunoreactive for sPLA<sub>2</sub> (Jiang et al., 2002). Additionally, primary cultures of cancer cells that over expressed sPLA<sub>2</sub> proliferated twice as fast as those that did not over express the enzyme, and over expression of sPLA<sub>2</sub> was inversely correlated with 5-year survival of prostate cancer patients (Graff et al., 2001). Taken together, these studies suggest that being able to target those tumors that over express sPLA<sub>2</sub> would be most beneficial in those patients with the worst clinical prognosis.

## **Prostate Cancer**

Prostate cancer is one of the most serious afflictions facing the US today. The American Cancer Society estimates that there were over 217,000

new cases of prostate cancer in 2010, and more than 32,000 deaths, making it the most common form of visceral cancer in men (Jemal et al., 2010). European estimates are similarly high, with more than 345,000 new cases and nearly 90,000 deaths annually (Ferlay et al., 2007). Given this kind of volume, it would be difficult to overstates the gravity of this disease on public health in the US and the world, yet traditional treatment approaches leave a great deal to be desired.

Many prostate cancer patients will undergo androgen ablation as the first line of defense against this disease. This is unquestionably the most popular first-line defense among clinicians, and in the vast majority of cases, the only alternative in “watchful waiting.” However, most men that undergo androgen ablation will develop castration-resistant disease within 18-24 months of treatment (Kohli and Tindall, 2010). Thus, these patients will suffer from a variety of unpleasant pharmacological side-effects including malaise, sexual dysfunction, and weakness, and yet the overwhelming majority will still be stricken with more aggressive disease within two year (Kohli and Tindall, 2010; Stavridi et al., 2012).

Radiation therapy (RT) is also commonly utilized to treat prostate cancer. The radiation is generally delivered by external beam or via brachytherapy implant (Boukaram and Hannoun-Levi). Although often effective at shrinking tumors (Al-Mamgani et al.; Boukaram and Hannoun-Levi), RT carries with it many risks and drawbacks, including erectile

dysfunction, radiation proctitis, and increased risk of developing secondary bladder cancer (Abern et al.; Boukaram and Hannoun-Levi).

Radical prostatectomy remains another cornerstone of treatment. This carries with it all of the traditional risks that come with surgery, along with side effects similar to those of androgen deprivation that will last for the lifetime of the patient (Kohli and Tindall, 2010; Stavridi et al., 2012). Moreover, in cases where metastasis may have occurred, and prostatectomy is not curative, chemotherapeutics are routinely used as adjunctive therapy. Although treatment with chemotherapeutics like docetaxel is common, only about 50% of patients respond favorably, and even this slight benefit comes at the price of toxicity (Seruga and Tannock, 2012). The toxic side effects commonly associated with chemotherapy arise because these drugs are most active against rapidly dividing cells, yet most prostate tumor cells have long doubling times, though this may change as the disease progresses (Kohli and Tindall, 2010; Seruga and Tannock, 2012). Even with this knowledge, there is still a great deal of interest in pursuing the development of new small molecule drugs. In fact, the FDA has approved more drugs for the treatment of castration resistant prostate cancer in the last three years than in the last three decades (Galsky et al.), bringing the total number of approved drugs up to 17 according to NCI. Unfortunately, given the similar mechanisms of action of these new compounds, compared to the existing pharmacopeia, they will likely suffer from the same shortcomings and only offer minor improvements in median survival, with the four most recently approved drugs extending the

life of patients with castration resistant tumors an average of 2.4-4.6 months (Crawford and Flaig, 2012). Thus, an altogether different approach to improving the treatment of prostate cancer may be warranted.

### **Liposomes and Nanoparticulate Drug Delivery**

Targeted delivery is a reasonable solution to the problems found in many clinically utilized treatments for prostate cancer. The use of nanoparticles to transport drug specifically to the tumor and deposit it there would increase bioavailability and provide sustained exposure to drug, while limiting systemic toxicity. Considering the growth rates of these tumors and the pathophysiology of the disease, targeted nanoparticulate drug delivery could be ideal for many patients.

The use of nanotechnology in cancer treatment is not a new frontier. Nanoparticles can be broadly defined as constructs with diameters ranging from 1-1000 nanometers. There are countless new technologies currently in development, as well as several formulations that have been in clinical application for years (Schroeder et al., 2012). For example, there is a protein-based nanoparticle containing paclitaxel used to treat metastatic breast cancer (Miele et al., 2009), iron-oxide nanoparticles used to treat anemia in testicular and prostate cancer patients (Duncan and Gaspar, 2011; Shih et al., 2005), and liposomal-doxorubicin has been approved to treat both ovarian cancer and Kaposi's sarcoma (Safra et al., 2000).

Liposomes are lipid-based nanoparticles that can be constructed in a wide range of sizes from a variety of phospholipids, and they usually contain both cholesterol and a polyethylene glycol (PEG) coat (Papahadjopoulos et al., 1991). Their potential as drug carrier vehicles has been postulated in the literature for decades, and like most other drug carriers, liposomes have the potential to provide continuous levels of drug in a desirable range, reduce harmful side effects, the amount of drug needed for efficacy, increase patient compliance by lowering the number of doses necessary, improve administration of drugs with short half-lives and provide a means of targeting specific tissues (Langer, 1998).

Treating cancer with liposomes could take advantage of one, or all of the aforementioned benefits. It has been firmly established, both in the literature and in clinical practice, that liposomes can alter the bioavailability of the drugs they encapsulate, releasing them stably over time (Langer, 1998; Papahadjopoulos et al., 1991; Safra et al., 2000; Schroeder et al., 2012). Furthermore, sequestering drugs from non-target, systemic tissue can greatly reduce dose limiting side effects, like cardiomyopathy in the case of doxorubicin (Barenholz, 2001). This, in and of itself, would allow patients to go longer between doses, and receive a drug for a longer period of time, as chronic toxicity is no longer an issue.

Another advantage of long circulating liposomes is their ability to passively accumulate in solid tumors, like those found in breast and prostate cancer, through a phenomenon known as enhanced permeation and retention

(EPR). This passive targeting results from the aberrant, leaky architecture vasculature and lack of adequate lymphatic drainage that is characteristic of many solid tumors (Maeda et al., 2000), and it is illustrated in Figure 1.3. Combine this with modern, active targeting techniques like conjugation antibodies directed at tumor specific markers, and the ability of liposomes to explicitly target cancer cells could become even more powerful (Langer, 1998). Many types of cancer, including prostate cancer, over express some of the same proteins, which could form the basis for molecular targeting. For example, HER-2/neu, EGF receptors and sPLA<sub>2</sub> (Graff et al., 2001; Mannello et al., 2008; Ow et al.; Schonborn et al., 1995) are all commonly over expressed in several cancers, meaning that a targeted liposomal delivery system specific for one of these markers would likely be effective for multiple types of cancer.

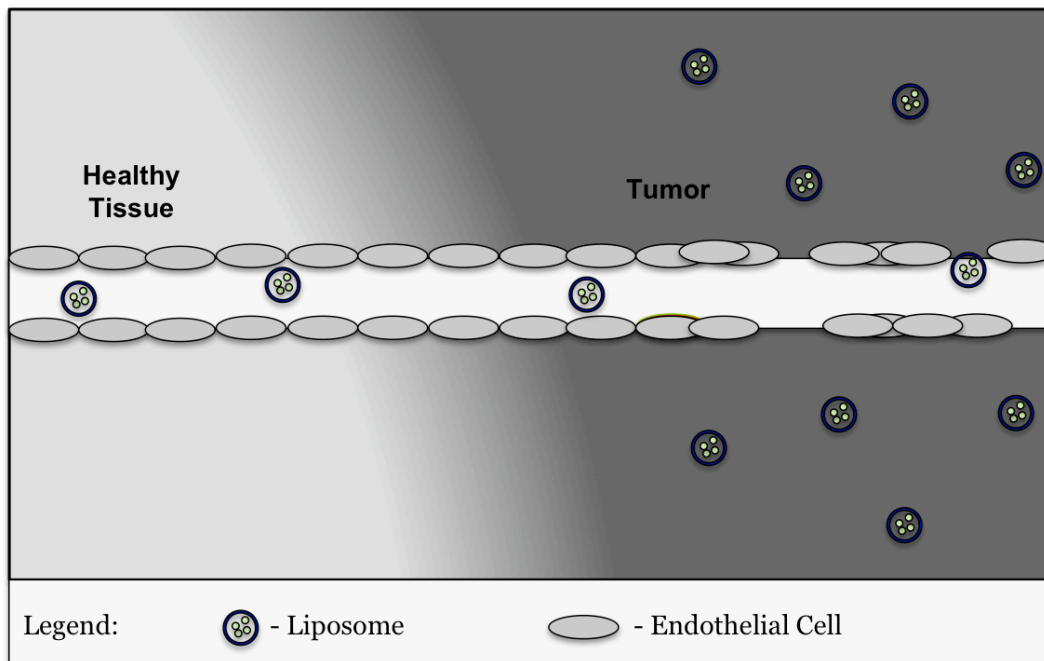


**Figure 1.3 Enhanced Permeation and Retention Effect.** The EPR effect allows nanoparticles to passively accumulate in tumor tissue due to a combination of leaky vasculature and inadequate lymphatic drainage.

There are some disadvantages to drug delivery systems using nanoparticles. These include toxicity of the carrier, the potential for dose dumping, and additional expense (Langer, 1998). Luckily, the phospholipids that make up liposomes are biocompatible and therefore, pose little threat. The potential for dose dumping, on the other hand, is of some concern. Liposomes have the ability to carry therapeutics at an extremely high drug-lipid ratio, and so, unexpected lysis of the vesicles could have toxic ramifications (Barenholz, 2001; Langer, 1998). Finally, a liposomal formulation of a drug would, no doubt, be more expensive than its unencapsulated counterpart.

To date, there have been few clinical advances in terms of nanoparticle-based treatments for prostate cancer. As mentioned above,

iron-oxide nanoparticles have been used in both prostate and testicular cancer patients suffering from anemia (Duncan and Gaspar, 2011; Shih et al., 2005). Additionally, there is ongoing research for improved prostate cancer diagnostics using nanoparticles. These include using superparamagnetic iron oxide nanoparticles (SPIONs) as MRI contrast agents to track lymph node metastasis (Harisinghani et al., 2003), and the potential to engineer nanomaterial-based microfluid devices (Fan et al., 2008) capable of early stage detection of prostate cancer biomarkers like sarcosin (Sreekumar et al., 2009).

### **Conclusions, Hypothesis and Specific Aims**

Given the important roles of PLA<sub>2</sub> and their involvement in cancer as well as other diseases, the goal of this research was to test the hypothesis that PLA<sub>2</sub>, specifically iPLA<sub>2</sub> and sPLA<sub>2</sub>, can be utilized as therapeutic targets for the treatment of prostate cancer. This hypothesis will be tested by addressing the following specific aims.

- **Specific Aim 1:** Evaluate the effectiveness of iPLA<sub>2</sub> inhibitors on cancer cell growth and proliferation.
- **Specific Aim 2:** Demonstrate the ability of sPLA<sub>2</sub> responsive liposomes to treat multiple models of prostate cancer.
- **Specific Aim 3:** Determine the molecular mechanisms that are dictating the behavior of sPLA<sub>2</sub> responsive liposomes.

First, due to its role in lipid homeostasis and growth, iPLA<sub>2</sub> can be targeted in a more traditional pharmacological approach using small molecule inhibitors. Inhibition of iPLA<sub>2</sub> should halt cell growth and prevent cancer cell proliferation. This hypothesis was tested in Aim 1 by screening a library of compounds synthesized by Dr. Timothy Long of the Department of Pharmaceutical and Biomedical Science at the University of Georgia and his students. Putative inhibitors were tested for inhibitory activity against iPLA<sub>2</sub> as well as their ability to halt the cell cycle and prevent proliferation. IC<sub>50</sub> values were determined and compared to the current industry standard for iPLA<sub>2</sub> inhibition, BEL.

Conversely, sPLA<sub>2</sub> will be used as a targeting mechanism for liposomes that are specifically designed to interact with this family of enzymes. These sPLA<sub>2</sub> responsive liposomes (SPRL) should be stable in circulation, but upon entering the microenvironment of the tumor, which is enriched with sPLA<sub>2</sub>, the lipid membrane will be cleaved and destabilized, releasing the interluminal contents. This prospective mechanism is depicted in Figure 1.4 and was studied in Aims 2 and 3. Furthermore, as SPRL will benefit from the passive accumulation of the EPR effect and the selective interaction with sPLA<sub>2</sub>, SPRL should provide increased, sustained drug delivery to the target site as well as decreased systemic toxicity. This hypothesis was first tested in Aim 2 by screening multiple formulations in a model system comprising either tris buffer or media with serum. The performance of each formulation was determined based on an extended

release and degradation profile using established fluorescent tracking techniques and ESI-MS, respectively (Zhu et al., 2011a; Zhu et al., 2011b). Those formulations that were considered sPLA<sub>2</sub> responsive were then tested *in vitro* in three different prostate cancer cell lines to determine their effect on cytotoxicity and uptake. Further *in vivo* evaluation was performed with SPRL to compare efficacy against the clinically utilized standard, SSL. Finally, in Aim 3 both molecular and pharmacological methods were employed to determine what factors (i.e. individual enzymes, enzymatic activity, and membrane receptors) are most influential in determining the behavior of SPRL.

Overall, this dissertation provides evidence that both iPLA<sub>2</sub> and sPLA<sub>2</sub> can be exploited for antineoplastic ends. However, given the relation of both of these enzyme families to other pathologies including neurodegeneration, arthritis, sepsis, atherosclerosis, and other cancers, the benefit and application of this work may be much broader in scope.

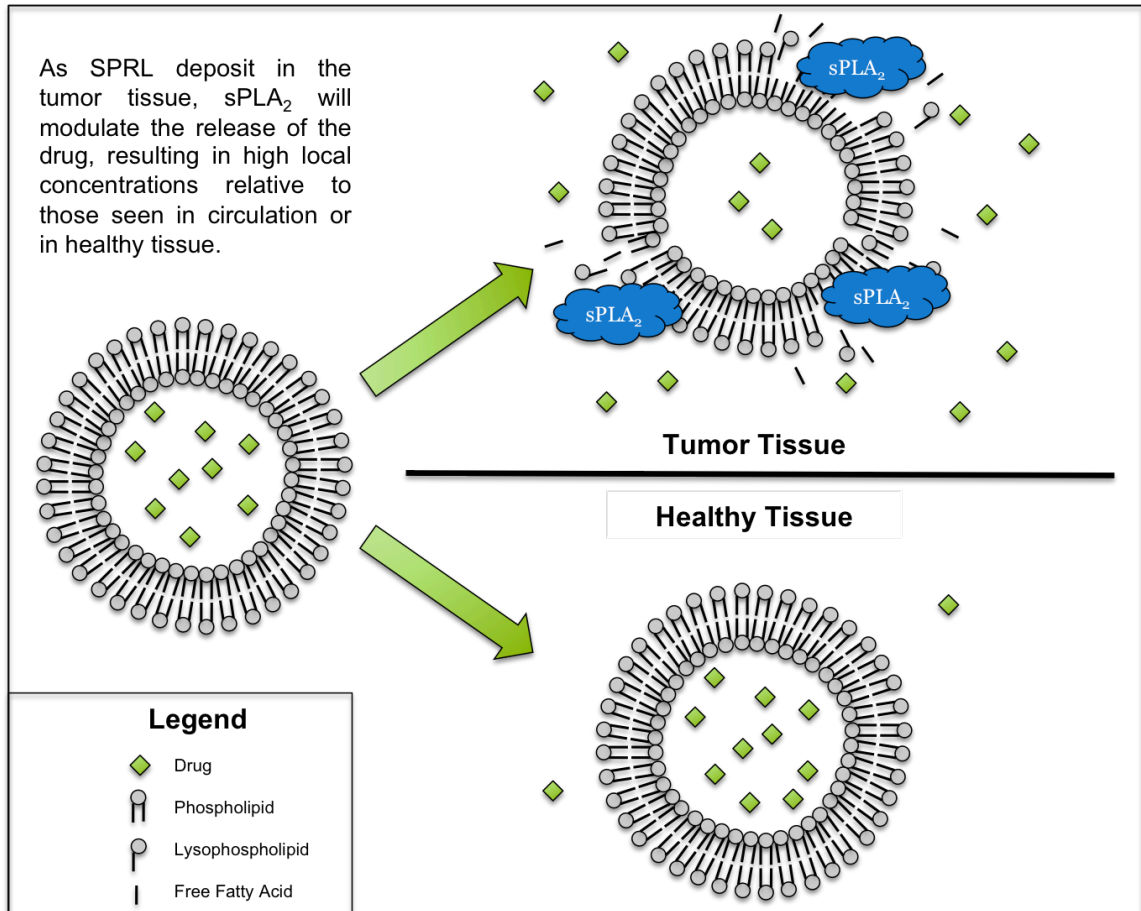


**Figure 1.4 Release from SPRL.** Due to the comparatively high concentration of sPLA<sub>2</sub> found within the tumor, release of drug should only occur within this micro-environment.

## CHAPTER 2

### MATERIALS AND METHODS

#### **Materials**

Distearoylphosphatidylcholine (DSPC), distearoylphosphatidylglycerol (DSPG), distearoylphosphatidylethanolamine (DSPE), and 1,2-distearoyl-*sn*-glycero-3-phosphoethanolamine-N-[poly(ethylene glycol) 2000 (DSPE-PEG) were purchased from Avanti Polar Lipids Inc (Alabaster, USA). 6-Carboxyfluorescein (6-CF) was purchased from Acros Organics (Geel, Belgium). Group III sPLA<sub>2</sub> (bee venom sPLA<sub>2</sub>), E-6-(Bromoethylene)tetrahydro-3-(1-naphthyl)-2H-pyran-2-one or bromoenol lactone (BEL), and propidium iodide (PI) were purchased from Cayman Chemical Company (Ann Arbor, MI). Sephadex G-75 was purchased from Pharmacia (Uppsala, Sweden). LY311727 (sPLA<sub>2</sub> inhibitor) was purchased from Tocris Bioscience (Minneapolis, MN). LNCaP, DU-145 and PC-3 cells were purchased from ATCC (Manassas, VA) and maintained in RPMI 1640, Eagle's Minimum Essential Medium, and F-12K medium supplemented with 10% (v/v) fetal bovine serum and antibiotics, purchased from ATCC as well.

Doxorubicin was purchased from Toronto Research Chemicals (North York, ONT, Canada). 3,3'-Diocetadecyloxacarbocyanine perchlorate (DiO), SuperScript III One-Step RT-PCR with Platinum Taq DNA Polymerase kits, and SuperScript III Platinum SYBR Green One-Step qRT-PCR kits were purchased from Invitrogen (Grand Island, NY). E.Z.N.A. Total RNA Isolation Kit I was purchased from Omega Bio-Tek (Norcross, GA). PCR primers specific for sPLA<sub>2</sub> Groups IB, IIA, V and X, PLA<sub>2</sub>R, and GAPDH were purchased from Integrated DNA Technologies (IDT, Coralville, IA). PLA<sub>2</sub>R shRNA lentiviral particles, control shRNA lentiviral particles, polybrene, and puromycin dihydrochloride were all purchased from Santa Cruz Biotechnology (Santa Cruz, CA). Recombinant human Group X sPLA<sub>2</sub> was purchased from BioVendor R & D (Candler, NC). All other reagents were of analytical quality.

## **Methods**

### *Cell Culture*

All cells were grown in a 37°C incubator at 5% CO<sub>2</sub>. Cells were grown in manufacturer recommended medium (F-12K for PC-3, RPMI 1640 for LNCaP, and MEM for DU-145) supplemented with 10% fetal bovine serum (FBS) and antibiotics. Cells were fed or passaged every 3 days or before reaching 100% confluence.

### *Assessment of iPLA<sub>2</sub> Inhibitor Cytotoxicity*

Putative iPLA<sub>2</sub> inhibitors were brought up in dimethylsulfoxide (DMSO) to specified concentrations. Cells were seeded into 48 well plates at a density of approximately 50,000 cells/ml and allowed to attach for 24 hours. Each well was then dosed with a single inhibitor, ranging in concentration from 1 mM down to 100 pM. At 24, 48 and 72 hours post treatment cells were examined for gross morphological differences and pictures were taken. Additionally, at 24, 48 and 72 hours, 20 µl of 5 mg/ml 3-(4,5-dimethylthiazol-2-yl)-2,5-diphenyltetrazolium bromide (MTT) was added to each well, and cells were incubated at 37°C for 2 hours. After this incubation, media was aspirated and replaced with an equal volume of DMSO and the plates were shaken for 15 minutes to dissolve any precipitate that may have formed. Absorbance was then determined at 544 nm with a FLUOstar OPTIMA plate reader (BMG Lab technologies, Inc., Durham, NC).

### *Cell Cycle Analysis*

Cells were plated in 12 well plates and treated with either 5 or 10 µM of the putative inhibitors. Following a 24-hour treatment, cells were washed twice with PBS and detached using a Cellstripper (Mediatech, Herndon, VA). The cell solution was centrifuged at 400 g for 10 minutes to form a pellet that was then resuspended in sample buffer. Cells were fixed in ice cold ethanol (70% v/v) and then stained with propidium iodide (PI) (50 µg/ml) in sample buffer containing RNase A (100 U/ml) for 30 minutes while being shielded

from light and gently shaken. Samples were stored at 4°C and analyzed within 24 hours using a CyAn flow cytometer (Beckman Coulter, Brea, CA). Data were analyzed using FlowJo software (Tree Star, Inc., Ashland, OR).

#### *iPLA<sub>2</sub> Inhibition Assay*

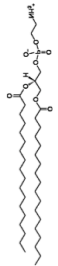
Rat kidney cytosol was isolated using differential centrifugation for the purposes of assessing inhibitor activity due to the known enrichment of iPLA<sub>2</sub>β in this fraction. Aliquots of cytosol were pretreated with inhibitor at concentrations ranging from 0-100 μ M for 30 minutes, at which time arachidonoyl thiol-phosphatidylcholine was added as a synthetic substrate of iPLA<sub>2</sub>. Arachidonoyl thiol-PC can be hydrolyzed by iPLA<sub>2</sub>, causing it to release a free thiol group from the *sn*-2 position. The presence of this thiol can be detected by its interaction with 5,5'-dithiobis(2-nitrobenzoic acid). Activity was measured by determining absorbance at 404 nm and normalized by the protein content of each sample.

#### *Formulation of SSL and SPRL*

SSL and SPRL were formulated as described previously (Zhu et al., 2011a; Zhu et al., 2011b). Based on our previous study we only used two types of SPRL, those containing 10% DSPE (SPRL-E) or 10% DSPG (SPRL-G). These SPRL were chosen as they had the greatest level of 6-CF release in the presence of sPLA<sub>2</sub> and the greatest increase in lipid degradation in our

previous studies (Zhu et al., 2011a; Zhu et al., 2011b). The individual formulations used in this study are described in Table 2.1.

**Table 2.1 Liposome Compositions**

Formulation	Lipid Components	Cholesterol	PEG	Charged Lipid
<b>SSL</b>	<b>1,2-distearoyl-sn-glycero-3-phosphocholine</b> 9 $\mu\text{mol/ml}$	5 $\mu\text{mol/ml}$	1 $\mu\text{mol/ml}$	N/A
<b>SPRL-E</b>	<b>1,2-distearoyl-sn-glycero-3-phosphocholine</b> 8 $\mu\text{mol/ml}$ <b>1,2-distearoyl-sn-glycero-3-phosphoethanolamine</b> 1 $\mu\text{mol/ml}$	5 $\mu\text{mol/ml}$	1 $\mu\text{mol/ml}$	DSPE 
<b>SPRL-G</b>	<b>1,2-distearoyl-sn-glycero-3-phosphocholine</b> 8 $\mu\text{mol/ml}$ <b>1,2-distearoyl-sn-glycero-3-phospho-(1'-rac-glycerol)</b> 1 $\mu\text{mol/ml}$	5 $\mu\text{mol/ml}$	1 $\mu\text{mol/ml}$	DSPG 

#### *Preparation of 6-CF Liposomes*

6-Carboxyfluorescein (6-CF, 100  $\mu\text{M}$ ) solution was prepared by dissolving 6-carboxyfluorescein in 5  $\text{mM}$  Tris-HCl buffer (pH 7.4). Liposomal vesicles were prepared by hydration of thin-film followed by freeze-thawing and extrusion. Briefly, phospholipids, cholesterol or DSPE-PEG (total phospholipid: 10  $\mu\text{mol}$ ) in chloroform were mixed together, and dried under vacuum conditions for 25 minutes using a rotary evaporator to form a thin-

film. The phospholipid film was rehydrated using the previously prepared 100 mM 6-CF solution. The dispersion then underwent 7 freeze–thaw cycles using liquid nitrogen and a 65°C water bath prior to at least five extrusions through double-stacked polycarbonate membranes (80 nm, Osmonics Inc., Minnetonka, MN) using a Lipex extruder (Northern Lipids Inc., Vancouver, BC, Canada) at 65°C. The final liposome sample was stored at 4°C and protected from light under a nitrogen atmosphere until use. Prior to use, total phospholipid was quantified using the Bartlett inorganic phosphate assay (Bartlett, 1959; Zhu et al., 2011b). Free 6-CF was removed by size exclusion chromatography using a Sephadex G-75 column. The mobile phase for these separations consisted of 5 mM Tris-HCl buffer (pH 7.4).

#### *Dox-Loaded and DiO-Labeled Liposomes*

Dox-loaded liposomes were prepared by remote loading using an ammonium sulfate gradient as described previously (Arnold et al., 2005; Haran et al., 1993). Briefly, lipids and cholesterol in chloroform were mixed and subsequently dried using a rotary evaporator. The resulting lipid film was rehydrated in 250 mM ammonium sulfate. This dispersion then underwent 7 freeze-thaw cycles and at least five extrusions as described above. Following extrusion the liposomes were immediately placed on ice for 10 minutes then dialyzed overnight in an isotonic 10% (w/v) sucrose solution to remove excess, unencapsulated ammonium sulfate. Drug loading was performed the following day by adding doxorubicin to the dialyzed liposomes at a 0.2:1

molar ratio. The suspension was mixed and incubated for 1 hour at 65°C with periodic mixing and then immediately put on ice for 15 minutes. The loaded liposomes were then dialyzed overnight in a 10% (w/v) sucrose solution. Doxorubicin loading was quantified spectroscopically in acidified ethanol and lipid concentration determined using the Bartlett assay as described above (Bartlett, 1959; Zhu et al., 2011b).

Fluorescent DiO-labeled liposomes were prepared according to the method of Kamps et al., with slight alterations (Kamps et al., 1997). Briefly, lipids and cholesterol in chloroform were mixed and 1 mol% DiO was added before the solution was evaporated to a lipid film. The resulting film was then rehydrated in PBS or ammonium sulfate depending on whether doxorubicin would subsequently be loaded. The rest of the procedure was the same as above.

### *6-CF Release Assay*

6-CF release from liposomes was determined as previously described (Zhu et al., 2011b). Briefly, liposomal samples (0.05  $\mu\text{mol/ml}$ ) were incubated at 37°C in the presence and absence of Group III sPLA<sub>2</sub> (2.5  $\mu\text{g/ml}$ ) and 100  $\mu\text{M}$  LY311727 in F-12K medium supplemented with 10% FBS. Fluorescent intensity of 6-CF was measured using a Bio-Tec synergy HT spectrofluorometer (BIO-TEK Instruments Inc, Winooski, VT) at excitation and emission wavelengths of 480 and 510 nm, respectively. The time points used to determine fluorescence were 1, 2, 4, 8, 12, 24, 36, 48, 72 and 108 hours.

After determining initial fluorescence at each time point, 10% (v/v) of Triton X-100 was added to the samples to disrupt liposomes and permit calculation of total 6-CF. The percentage of 6-CF leakage was calculated by the equation:

$$\text{Percentage} = [(F_t - F_0) / (F_{\text{Triton}} - F_0)] \times 100\%;$$

where  $F_t$  represents the fluorescent intensity (FI) at a specific time point and  $F_0$  represents FI at time zero.  $F_{\text{Triton}}$  represents FI after addition of Triton x-100.

#### *Assessment of Cytotoxicity of Liposomes*

Cytotoxicity was determined by 3-(4,5-dimethylthiazol-2-yl)-2,5-diphenyltetrazolium bromide (MTT) staining and corroborated with phase contrast microscopy. Cells were seeded in 96 well plates at  $2-3 \times 10^4$  cells per well depending on cell type. After 24 hours cells were incubated with 2.5  $\mu\text{M}$  doxorubicin or the liposomal equivalent and either 0 or 100  $\mu\text{M}$  LY311727. A concentration of 2.5  $\mu\text{M}$  was used as this was the dose that resulted in ~30 to 50% cell kill after 72 hours in these cell lines (data not shown). At 24, 48 and 72 hours 0.25 mg/ml of MTT was added to each well. The plates were then incubated for 2 hours before media was aspirated and replaced with DMSO. Plates were shaken vigorously for 15 minutes to dissolve all precipitates and absorbance was determined at 544 nm with a FLUOstar OPTIMA plate reader (BMG Lab technologies, Inc., Durham, NC).

### *Liposome and Doxorubicin Uptake*

Cells were seeded in 12 well plates at  $7.0-8.0 \times 10^4$  cells per well and allowed to attach for 24 hours. Cells were then treated with PBS, free doxorubicin (Dox), empty liposomes, empty DiO-labeled liposomes, Dox-loaded liposomes or DiO-labeled Dox-loaded liposomes. Free drug and formulations containing drug were dosed at 2.5  $\mu$ M doxorubicin equivalents. Phosphate assays were performed to determine lipid concentrations, and empty and DiO-labeled liposomes were dosed at equal lipid concentrations compared to doxorubicin loaded equivalents,  $\sim 10$  nmol lipid/mL. At 24, 48 and 72 hours post dosing, cells were washed 3 times with ice cold PBS, released from the plate using trypsin/EDTA and pelleted. Pellets were washed again with PBS and suspended in PBS supplemented with 1 mg/ml glucose. Samples were analyzed immediately using a CyAn flow cytometer (Beckman Coulter, Brea, CA). Samples were excited with a 488 nm argon laser and emission was determined at 575 and 613 nm. Only whole cells were analyzed, as determined by forward and side scatter, and at least 5000 events were counted per run. Data was analyzed using FlowJo software (Tree Star, Inc., Ashland, OR).

### *Activity of Liposomes In Vivo*

The activity of SSL and SPRL liposomes *in vivo* was determined by implanting PC-3 cells subcutaneously in 7-8 week old male athymic nude (NCR- nu/nu) mice that were acclimated two weeks after receipt from Taconic

Farms, Inc., (Germantown, NY). Animals were housed and maintained in accordance with an approved Institutional Animal Care and Use Committee (IACUC) protocol at the University of Georgia and in accordance with the U.S. Public Health Service (PHS) Policy on Humane Care and Use of Laboratory Animals. Animals were housed in pathogen-free cages within a light and temperature controlled isolated room and provided with autoclaved rodent chow and autoclaved water *ad libitum*. For tumor implantation, sub-confluent PC-3 cells grown in 10% fetal bovine serum supplemented F-12K were harvested using 0.25% (v/v) trypsin. Cells were counted and suspended in serum free media to a final concentration of  $1 \times 10^7$  cells/mL. Media was mixed with ice-cold Matrigel (1:1, v/v), and 200  $\mu$ L of the mixture was injected subcutaneously into the mouse flank. Tumors were allowed to grow and mice were monitored every other day. Tumor diameters were measured using digital calipers, recorded and tumor volumes were calculated according to the following formula: (larger dimension) x (smaller dimension)<sup>2</sup> x 0.5 (Aljuffali et al., 2011; Geran et al., 1972). When tumors reached  $\sim 400$  mm<sup>3</sup> mice were randomly selected to be treated with 5 mg/kg of doxorubicin or liposomal equivalent *via* tail vein injection once a week. Individual tumor volumes were normalized to their tumor volume on the day treatment was initiated. Treatment continued for 4 weeks (*i.e.*, 5 total doses), tumor dimensions and animals weights were measured every other day. Animals were euthanized roughly 2 weeks after the last treatment.

### *RT- and QRT-PCR*

RT-PCR was performed using Invitrogen's One-Step RT-PCR kit according to manufacturer's recommendations in a Mastercycler Gradient Thermocycler (Eppendorf, Hauppauge, NY). Primers were designed using IDT's primer design software to insure specificity for genes of interest, and primer sequences are shown in Table 3.2. RNA was extracted from samples using the Omega Bio-Tek E.Z.N.A. Total RNA Isolation Kit I according to manufacturer's recommendations.

Results of RT-PCR were run on 1% agarose gels containing ethidium bromide and visualized under UV light. GAPDH was used as a loading control in each experiment.

QRT-PCR was performed in a Bio-Rad iCycler using the primers in Table 3.2. Relative expression values were calculated by  $\Delta\Delta C_t$  using GAPDH as an internal control.

**Table 2.2 Primers for RT- and QRT-PCR**

<b>Primer</b>	<b>Sense</b>	<b>Antisense</b>
sPLA <sub>2</sub> Group IB	5'-AAATGATCAAGTGC GTGATCC-3'	5'-TTGCTGCTACAGGTGATTGC-3'
sPLA <sub>2</sub> Group IIA	5'-ACCATGAAGACCSTCCTACT-3'	5'-GAAGAGGGGACTCAGCAACG-3'
sPLA <sub>2</sub> Group V	5'-GGGCTGCAACATTCGCACAC-3'	5'-CCTCTCTCAGGAACCAGGCAG-3'
sPLA <sub>2</sub> Group X	5'-CCATCGCCTATATGAAATATGG-3'	5'-TAGGAACTGGGGGTAGAAGAG-3'
PLA <sub>2</sub> R	5'-CAGAAGAAAGGCAGTTCTGGATTG-3'	5'-AAAGCCACATCCTGGCTCTGATT-3'
GAPDH	5'-AAGGTCGGAGTCAACGGCT-3'	5'-TGGAAGATGGTGATGGGATT-3'

### *shRNA Knockdown of PLA<sub>2</sub>R*

Cells were plated at  $5 \times 10^4$  cells/ml in 12 well plates and allowed 24 hours to attach. Cells were then infected with various titers of shRNA lentiviral vectors purchased from Santa Cruz Biotechnology Product Number SC-94746-V) coding against PLA<sub>2</sub>R in media containing 5 µg/ml of polybrene. Each virus contained 3 target-specific constructs listed below.

**Sense A:** 5'-GACAAGCCGUUAUGAAAGATT-3'

**Antisense A:** 5'-UCUUUCAUAACGGCUUGUCTT-3'

**Sense B:** 5'- CAAGGAGGUACGCUGUUAATT-3'

**Antisense B:** 5'- UUAACAGCGUACCUCCUUGTT-3'

**Sense C:** 5'- GGAAUCCCUACAAUCGUAATT-3'

**Antisense C:** 5'- UUACGAUUGUAGGGAUUCCTT-3'

**Hairpin:** 5'- GATCCGACAAGCCGTTATGAAAGATTCAA

GAGATCTTTCATAACGGCTTGTCTTTTT-3'

After 24 hours, media containing viruses was aspirated and replaced with fresh, complete media and incubated overnight. The following day, cells were split and seeded into 48 well plates at densities to yield 1-100 cells/ml in media containing 10-20 µg/ml of puromycin dihydrochloride. Individual wells that were able to grow under puromycin selection were expanded. Transcription levels were determined as described above using QRT-PCR. Invitrogen's SuperScript III Platinum SYBR Green One-Step qRT-PCR kit was used according to manufacturer's recommendations in a Bio-Rad iCycler (Bio-Rad, Hercules, CA). Only those samples with the best knockdown

( $\geq 70\%$ ) were maintained. After knockdown was established, cells were maintained in complete F-12K media containing 20  $\mu\text{g/ml}$  puromycin.

*Cytotoxicity of Drug Loaded SPRL and SSL in the Presence of PLA<sub>2</sub>R Knockdown and Exogenous Group X sPLA<sub>2</sub>*

Cytotoxicity was determined as previously described using MTT staining. Wild-type PC-3 and PLA<sub>2</sub>R knockdown cells were seeded into 96 well plates at  $\sim 30,000$  cells/ml and allowed to attach for 24 hours. Cells were then treated with 2.5  $\mu\text{M}$  equivalents of free doxorubicin or doxorubicin encapsulated in SSL, SPRL-E or SPRL-G. At 24, 48 and 72 hours post treatment, cells were stained with MTT at a concentration of 0.25 mg/ml. The plates were then incubated for 2 hours before media was aspirated and replaced with DMSO. Plates were shaken vigorously for 15 minutes to dissolve all precipitates and absorbance was determined at 544 nm with a FLUOstar OPTIMA plate reader (BMG Lab technologies, Inc., Durham, NC).

To determine to effect of Group X sPLA<sub>2</sub> on cytotoxicity, wild-type PC-3 cells were seeded at described above. Before dosing, 10 nM Group X sPLA<sub>2</sub> was added to each well. Cells were treated with liposomes and MTT assays were performed 24 hours later.

*Uptake of Liposomes and Drug in the Presence of PLA<sub>2</sub>R Knockdown and Exogenous Group X sPLA<sub>2</sub>*

Wild-type PC-3 and PLA<sub>2</sub>R knockdown cells were seeded in 12 well plates at  $7.0\text{-}8.0 \times 10^4$  cells per well and allowed to attach for 24 hours. Cells were then treated with PBS, free doxorubicin (Dox), empty liposomes, empty DiO-labeled liposomes, Dox-loaded liposomes or DiO-labeled Dox-loaded liposomes. Free drug and formulations containing drug were dosed at  $2.5 \mu\text{M}$  doxorubicin equivalents. Phosphate assays were performed to determine lipid concentrations, and empty and DiO-labeled liposomes were dosed at equal lipid concentrations compared to doxorubicin loaded equivalents,  $\sim 10 \text{ nmol lipid/mL}$ . At 24, 48 and 72 hours post dosing, cells were washed 3 times with ice cold PBS, released from the plate using trypsin/EDTA and pelleted. Pellets were washed again with PBS and suspended in PBS supplemented with  $1 \text{ mg/ml}$  glucose. Samples were analyzed immediately using a CyAn flow cytometer (Beckman Coulter, Brea, CA). Samples were excited with a 488 nm argon laser and emission was determined at 575 and 613 nm. Only whole cells were analyzed, as determined by forward and side scatter, and at least 5000 events were counted per run. Data were analyzed using FlowJo software (Tree Star, Inc., Ashland, OR).

As with the cytotoxicity studies, to determine to effect of Group X sPLA<sub>2</sub> on uptake, wild-type PC-3 cells were seeded at described above. Before dosing,  $10 \text{ nM}$  Group X sPLA<sub>2</sub> was added to each well. Cells were treated with liposomes and uptake was assessed 24 hours later.

### *Statistical Analysis*

All *in vitro* experiments were completed at least three times (n = 3) in triplicate. *In vivo* studies were performed with four to five mice per treatment group. Results are shown as the average of all replicates  $\pm$  SEM. Results were compared using Student's T-test or one-way ANOVA, where applicable, and considered significant if  $p \leq 0.05$ .

## CHAPTER 3

### INHIBITORS OF iPLA<sub>2</sub> AS ANTINEOPLASTICS<sup>1</sup>

---

<sup>1</sup> Mock, Jason, Taliaferro, John, Lu, Xaio, Patel, Sravan, Cummings, Brian and Long, Timothy. 2012, *Bioorganic and Medicinal Chemistry Letters*, 22, 4852-4858. Reprinted here with permission of publisher.

## Abstract

Haloenol pyran-2-ones and morpholin-2-ones were synthesized and evaluated as inhibitors of cell growth in two different prostate human cancer cell lines (PC-3 and LNCaP). Analogs derived from L- and D-phenylglycine were found to be the most effective antagonists of LNCaP and PC-3 cell growth. Additional studies reveal that the inhibitors induced G2/M arrest and the (S)-enantiomer of the phenylglycine-based derivatives was a more potent inhibitor of cytosolic iPLA<sub>2</sub>b.

## Introduction

Haloenol pyranones are serine protease inhibitors capable of alkylating the active site of these enzymes following hydrolysis and unmasking of a reactive  $\alpha$ -haloketone functional group, as illustrated in Figure 3.1 (Chakravarty et al., 1982; Daniels et al., 1983; Daniels and Katzenellenbogen, 1986; Rai and Katzenellenbogen, 1992; Rando, 1974; Reed and Katzenellenbogen, 1991; Sofia and Katzenellenbogen, 1986). Although there are numerous chemicals in this class, the most widely studied is bromoenol lactone (BEL). However, BEL is more commonly utilized for its ability to inhibit Ca<sup>2+</sup>-independent phospholipase A<sub>2</sub> (iPLA<sub>2</sub>), as opposed to its properties as a serine protease inhibitor. BEL is a relatively potent inhibitor of iPLA<sub>2</sub>, and it displays enantiomer-based selectivity, with (R)- and (S)-inhibiting iPLA<sub>2</sub>  $\gamma$  and  $\beta$ , respectively (Jenkins et al., 2002; Kinsey et al., 2005;

Sun et al., 2001). The mechanisms involved in this selectivity are still under study.

iPLA<sub>2</sub> plays a role in a variety of pathologies where oxidative stress and inflammation are present including cardiovascular disease (McHowat and Creer, 2004), Alzheimer's (Hoozemans et al., 2001; Sun et al., 2005) and Parkinson's Disease (Farooqui and Horrocks, 2006; Farooqui et al., 2006), diabetes mellitus (Ma et al., 1998; Ma et al., 1999; Ramanadham et al., 2003; Song et al., 2005) and carcinogenesis (Song et al., 2007; Sun et al., 2001; Zhang et al., 2005; Zhang et al., 2006). The use of BEL as a pharmacological probe has helped to establish these roles; however, there is still a largely untapped potential for chemicals in this class to be used as pharmaceuticals, owing to their selectivity for iPLA<sub>2</sub>. Although iPLA<sub>2</sub> play important roles in membrane homeostasis, it has become evident that they may also play oncogenic roles in several types of cancer, participating in cell cycle progression (Herbert and Walker, 2006), proliferation (Balboa et al., 2008; Roshak et al., 2000; Song et al., 2007), migration (Ayilavarapu et al., 2010; Hoeft et al., 2010; Mishra et al., 2008) and apoptosis (Bao et al., 2007; Perez et al., 2006). Others have found that knocking out iPLA<sub>2</sub> reduced tumor burden in a ovarian cancer mouse model by 50% (Li et al., 2010), and there are strong statistical correlations between iPLA<sub>2</sub> expression and colon cancer initiation in humans (Hoeft et al., 2010). Moreover, these PLA<sub>2</sub> are often found in greater abundance in cancer cells (Cummings et al., 2000; Dong et

al., 2006), providing a therapeutic window in which inhibition of iPLA<sub>2</sub> may result in cancer cell death or cytostasis.

To this end, Dr. Timothy Long's laboratory in the Department of Pharmaceutical and Biomedical Science at the University of Georgia synthesized a library of putative iPLA<sub>2</sub> inhibitors. These novel halonalenol pyranones and morpholinones were evaluated in two prostate cancer cell lines, PC-3 and LNCaP, for their ability to slow growth, alter the cell cycle, and inhibit iPLA<sub>2</sub> activity. While the biological screening of these compounds is the basis of this chapter, the synthesis (carried out by Timothy Long, John Taliaferro, Xiao Lu, and Sravan Patel) was also presented in the same publication. As the synthesis was performed in another laboratory, but is pertinent to the work presented below, it is presented in the appendix.

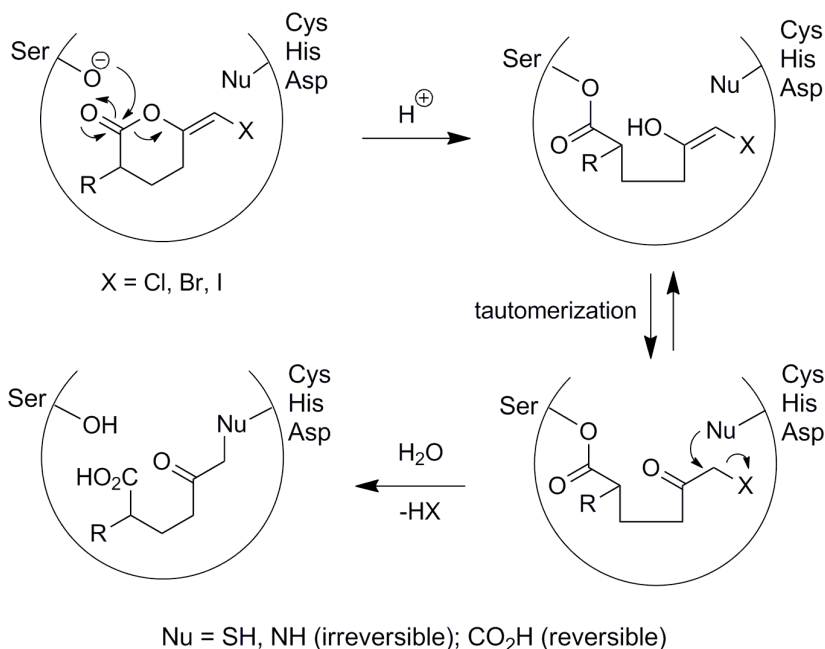


**Figure 3.1 Mechanism of Haloenol Pyranones.** The active site is alkylated following ring hydrolysis of the inhibitor. This inhibition of the serine is reversible.

## Results

Inhibitory concentrations ( $IC_{50}$ s) for cell growth were determined at 24, 48 and 72 hours in LNCaP and PC-3 cells using MTT staining. BEL served as a haloenol standard of comparison. The results of these experiments are shown in Table 3.1 and the structure of each of the inhibitors can be found in Figure 3.2. BEL was found to inhibit growth in the range of 5-13  $\mu$ M and 14-34  $\mu$ M in LNCaP and PC-3 cells, respectively. This is in agreement with previously reported findings from our laboratory (Sun et al., 2008). Comparison of the novel compounds to BEL showed that unsubstituted analogs were equally efficacious, while substitutions at the  $\alpha$ -position slightly enhanced activity, lowering the  $IC_{50}$ s to 6-27  $\mu$ M in PC-3 cells.

The morpholinone analogs also demonstrated antineoplastic activity that, like BEL, was enantiomer specific. Two of these derivatives, 14a and 14b, reduced the  $IC_{50}$  to 3  $\mu$ M at select time points and appeared to act more rapidly than the other compounds being tested. 14b, the (R)- enantiomer was more effective than the (S)- enantiomer, 14a, and this may be due to the higher proteolytic susceptibility of 14b.

Several of the other analogs proved to be less potent than BEL, including those derived from L-Pha and Gly-, 16 and 17, respectively. However, the N-benzyl L-Phg-based analog, 20, was the most potent compound screened, with  $IC_{50}$ s in the 1-4  $\mu$ M range. This compound elicited sustained decreases in cell growth in both cell lines over the entire time course studied. Cell morphology was also monitored throughout this time

course to check for signs of gross cytotoxicity. Representative images of LNCaP cells treated with haloenol pyranones and morpholinones are shown in Figure 3.3.

To determine whether the observed decreases in cell growth were caused by cytotoxicity or cytostasis, cell cycle changes were assessed by flow cytometry and propidium iodide (PI) staining. In LNCaP cells, there was an increase in cell number in the G1 phase. Additionally, both 14a and 14b caused complete cell cycle arrest at 10  $\mu$ M. The increase in S phase seen at these concentrations is likely due to a lack of cells entering G2/M phase. This could be the result of cytotoxic effects caused by DNA hypoploidy. Examples of other agents that block mitosis by inhibiting chromosome replication include DNA alkylating agents and antagonists of glutathione S-transferase (Wu et al., 2004). Results of cell cycle analysis are shown in Figure 3.4.

Finally, rac-BEL, rac-4, 14a, and 14b were tested for their ability to inhibit iPLA<sub>2</sub> $\beta$ . The cytosolic fraction of rat kidney isolates were treated with these compounds for 30 minutes in doses ranging from 0-100  $\mu$ M. Both BEL and 4 demonstrated similar dose dependent activity as shown in Figure 3.5. 14a showed less activity than the previous pyranone-based antagonists, and 14b had little to no inhibitory activity. Again, this agrees with what would be expected, as it is well documented that (S)-BEL is selective against iPLA<sub>2</sub> $\beta$ , while (R)-BEL is selective for iPLA<sub>2</sub> $\gamma$  (Jenkins et al., 2002; Kinsey et al., 2005; Sun et al., 2001; Sun et al., 2008; Sun et al., 2010). Thus, we would not

expect to see activity from (R)-14b in the cytosolic fraction, as iPLA<sub>2</sub> $\gamma$  should only be present in microsomal fractions.

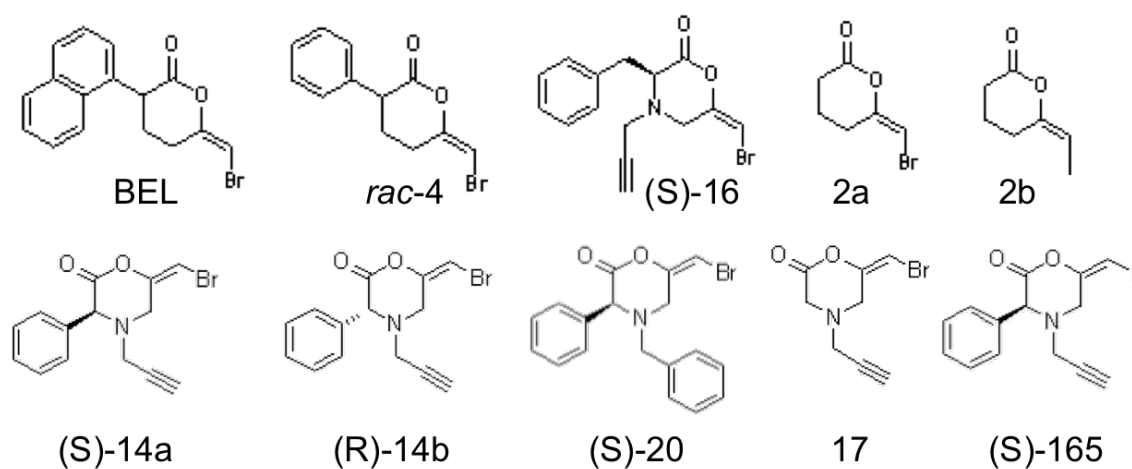


**Figure 3.2 Structure of Inhibitors.** The chemical structure of each of the putative inhibitors is displayed above. BEL, shown in the top right, served as the basic scaffold on which the other compounds were patterned.

**Table 3.1 IC<sub>50</sub> Values of Haloenol Pyranones and Morpholinones in LNCaP and PC-3 cells.** Concentrations are shown in  $\mu$  M. IC<sub>50</sub>s were calculated from nonlinear regressions using GraphPad Prism software.

Compound	LNCaP			PC-3			
	hours	24	48	72	24	48	72
<i>rac</i> -BEL		13	5	9	34	26	14
<b>2a</b>		10	5	5	19	23	14
<b>2b</b>		9	5	7	32	15	16
<i>rac</i> -4		31	5	4	27	10	6
( <i>S</i> )-14a		8	3	3	15	13	5
( <i>R</i> )-14b		6	6	3	8	6	3
( <i>S</i> )-15		26	23	20	21	21	25
( <i>S</i> )-16		41	26	32	33	57	39
<b>17</b>		25	29	28	13	10	7
( <i>S</i> )-20		3	4	3	4	1	4

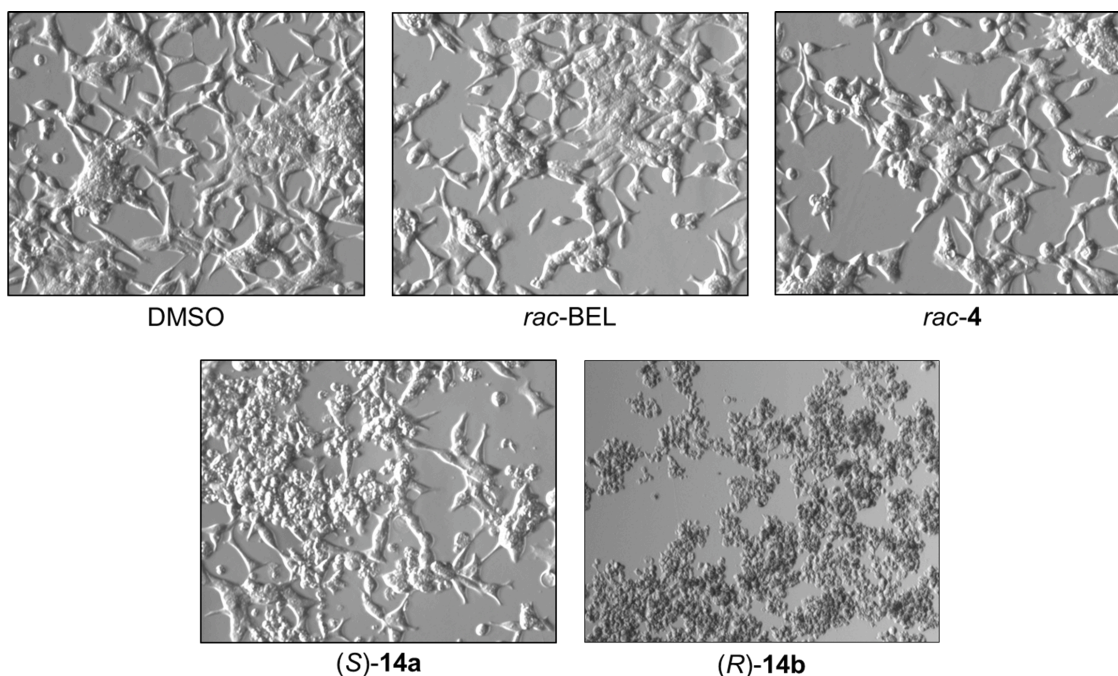


**Figure 3.3 Cell Morphology in LNCaP.** LNCaP cells were exposed to racemic BEL (*rac*-BEL), *rac*-4, S-14a or R-14b at 5  $\mu$ M for 72 hours prior to analysis of cell morphology by phase contrast microscopy at 350X magnification. Neither BEL nor *rac*-4 cause any overt changes in morphology compared to vehicle control (DMSO). 14a causes some rounding and clumping of cells, suggesting cell death or apoptosis, and this clumping and rounding becomes more evident with 14b.

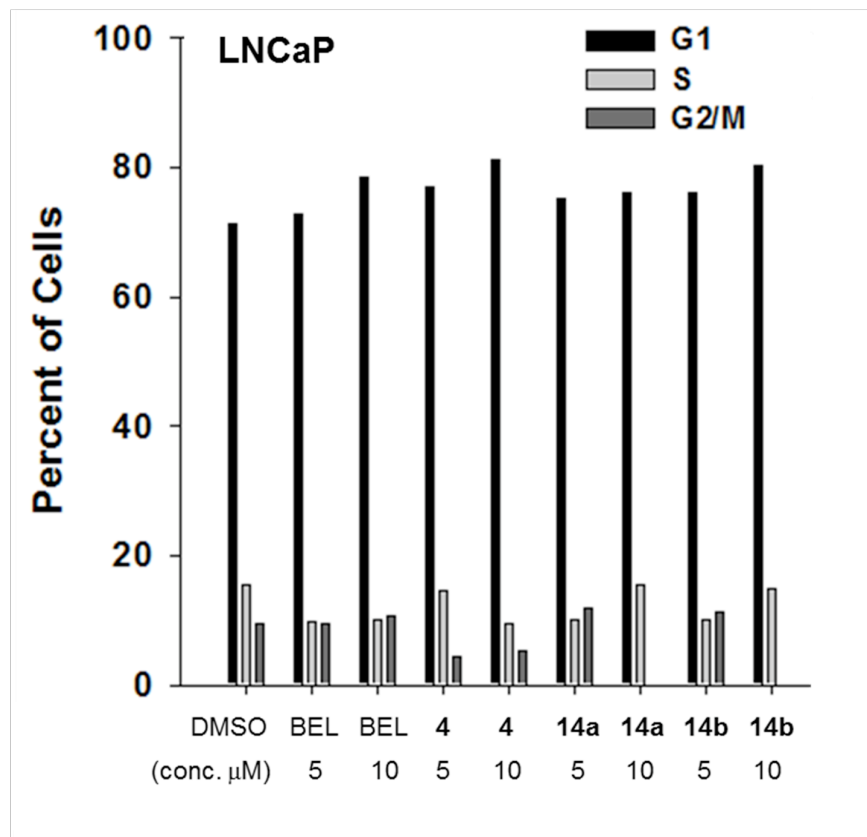


**Figure 3.4 Cell Cycle Analysis in LNCaP.** At each dose, most compounds cause an increase in the number of cells in G1. At 10  $\mu\text{M}$ , both 14a and 14b cause arrest in S-phase and a complete blockage of G2/M.

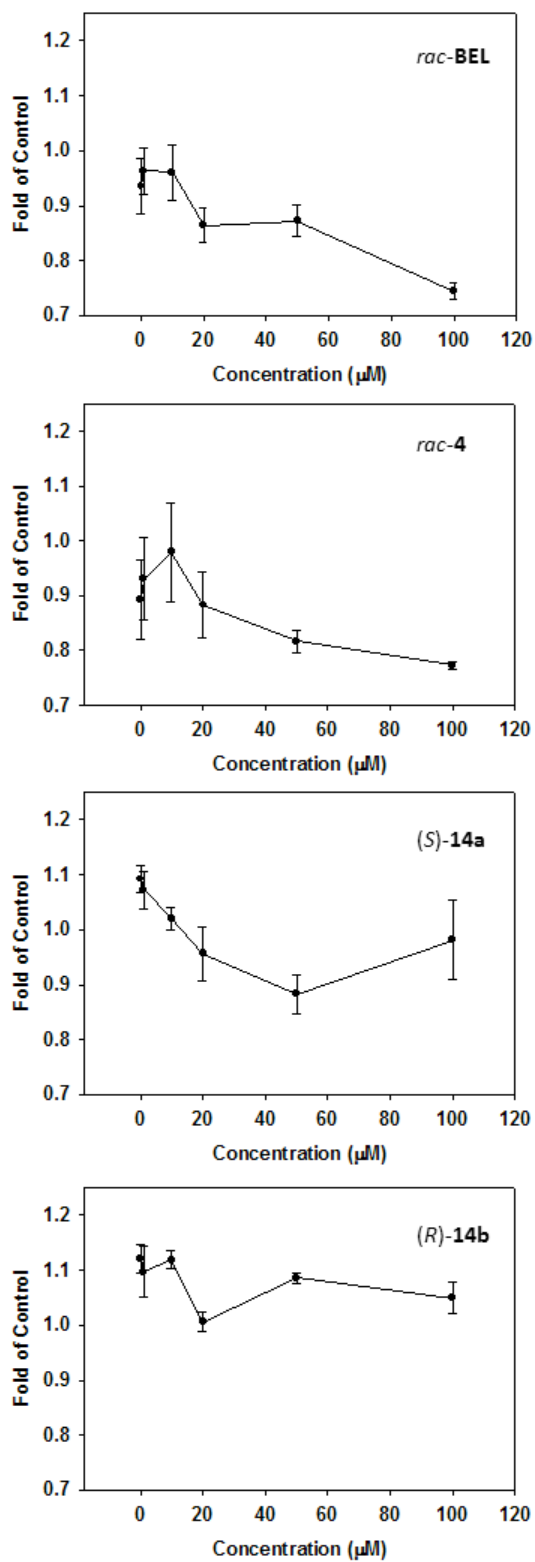


**Figure 3.5 Inhibition of iPLA<sub>2</sub> β.** Both BEL and 4 show activity as an inhibitor of iPLA<sub>2</sub> β, as dose 14a, to a lesser extent. 14b showed no inhibitory activity in this assay.

## Discussion

Novel haloenol pyranones and morpholinones were effective at halting prostate cancer cell growth and inhibiting iPLA<sub>2</sub>. However, a definitive correlation between this putative cause and effect could not be made. Analysis of cell cycle and iPLA<sub>2</sub> inhibition suggest that some of these compounds, 14 specifically, may be working directly or indirectly to damage DNA. Gluathione S-transferase, which also is known to be inhibited by halenol lactones (Wu et al., 2004), plays a role in protecting DNA from oxidative damage and therefore may be involved in this potential mechanism.

It became apparent during these studies that the chemical instability of these compounds would prevent them from reaching clinical application. A viable prostate cancer therapeutic candidate must be able to survive in circulation to reach the tumor site, and given the tendency of these compounds to degrade in solution, it is unlikely that they could be utilized as drugs. However, their use as research tools to probe the roles of iPLA<sub>2</sub>, oxidative stress, and other serine proteases in tumorigenesis may still prove to be of great value to in the field of drug discovery.

## CHAPTER 4

### EVIDENCE FOR DISTINCT MECHANISMS FOR MEDIATION OF SECRETORY PHOSPHOLIPASE A<sub>2</sub> RESPONSIVE LIPOSOME UPTAKE AND ANTITUMOR ACTIVITY IN A PROSTATE CANCER MODEL<sup>2</sup>

---

<sup>2</sup> Mock, Jason, Costyn, Leah, Wilding, Stephanie, Arnold, Robert and Cummings, Brian. Submitted to *Integrative Biology*, 05/04/2012

## **Abstract**

Secretory phospholipase A<sub>2</sub> (sPLA<sub>2</sub>) cleave phospholipids at *sn*-2 ester bonds, releasing lysophospholipids and fatty acids, and are over expressed in several pathologies, including inflammation, arthritis, sepsis and breast and prostate cancers. Herein we evaluated the therapeutic activity of liposomes engineered to be responsive to different sPLA<sub>2</sub> isoforms compared to clinically used standard sterically stabilized liposomes (SSL) *in vitro* and *in vivo*, and assess difference in role of sPLA<sub>2</sub> in the mechanism of uptake and delivery of these nanoparticles. Exposing sPLA<sub>2</sub> responsive liposomes (SPRL) to sPLA<sub>2</sub> increased the release of intraluminal entrapped contents in a time-dependent manner that was inhibited by the sPLA<sub>2</sub> inhibitor LY3117272. Treatment of prostate cancer cells with doxorubicin encapsulated in SSL and SPRL resulted in cytotoxicity in LNCaP, DU-145 and PC-3 cells lines comparable to free drug. Interestingly, cytotoxicity was not altered by sPLA<sub>2</sub> inhibition. Tracking of drug and liposome delivery using fluorescence microscopy and flow cytometry, we demonstrated that drug uptake was liposome-dependent, as encapsulation of doxorubicin in SPRL resulted in 1.5 to 2-fold greater intracellular drug levels compared to SSL. Liposome uptake was cell-dependent and did not correlate to doxorubicin uptake; however, doxorubicin uptake was generally greatest in PC-3 cells, followed by DU-145 cells and then LNCaP cells. In almost all cases, uptake of one of our formulations, SPRL-E, was greater than SSL. The therapeutic activity of SPRL *in vivo* was demonstrated using a mouse xenograft model of human prostate cancer, which showed that doxorubicin entrapped within SPRL decreased tumor

growth compared to SSL, suggesting that SPRL are more effective at slowing tumor growth than a SSL formulation similar to the FDA approved DOXIL™. Collectively, these data show the therapeutic activity of SPRL compared to SSL, yield insights into the mechanisms of action of these nanoparticles and suggest that SPRL could be useful for treatment of other pathologies that over express sPLA<sub>2</sub>.

## **Introduction**

Pathological changes in physiology can be exploited to enhance the delivery and efficacy of drugs encapsulated in nanoparticles. Long-circulating nanoparticulate drug carriers, such as pegylated, sterically-stabilized liposomes (SSL), can stably entrap drug, alter drug disposition, improve activity and minimize toxicity (Arnold et al., 2005). However, the inability to accurately control drug-release kinetics has limited their clinical potential (Drummond and Mason, 2007). Secretory phospholipase A<sub>2</sub> (sPLA<sub>2</sub>) degrade phospholipids at the *sn*-2 ester position to release a fatty acid and a lysophospholipid (Lambeau and Gelb, 2008b). They require calcium for their enzymatic activity, and play diverse roles in several physiological functions, such as degradation of dietary phospholipids, defense against bacterial infections and arachidonic acid production (Lambeau and Gelb, 2008b; Murakami et al., 2012). sPLA<sub>2</sub> are also hypothesized to promote inflammatory diseases, such arthritis, atherosclerosis, sepsis, and cancers (Bostrom et al., 2007; Fraser et al., 2009; Graff et al., 2001; Leistad et al., 2004; Pruzanski and Vadas, 1988; Rosengren et al., 2006). Recent evidence,

including that from our laboratory, has hypothesized that the over expression of sPLA<sub>2</sub> in these pathologies makes them good targets to control drug release from lipid-based nanoparticles, such as liposomes (Andresen et al., 2005; Zhu et al., 2011a; Zhu et al., 2011b).

sPLA<sub>2</sub> are becoming of note in cancer biology because recent studies show that these enzymes are over expressed in prostate (Dong et al., 2006; Jiang et al., 2002; Kallajoki et al., 1998) and several other cancers (Kiyohara et al., 1993; Kuopio et al., 1995; Oka et al., 1990; Yamashita et al., 1994a; Yamashita et al., 1994b; Yamashita et al., 1993). Moreover, it is usually the more aggressive, high-grade metastatic prostate tumors that over express sPLA<sub>2</sub> and increased expression is inversely correlated to 5-year survival (Graff et al., 2001; Jiang et al., 2002; Sved et al., 2004). This suggests the hypothesis that targeting liposomes to interact with sPLA<sub>2</sub> would be most beneficial in those patients with the worst clinical prognosis.

We recently hypothesized that the increased expression of sPLA<sub>2</sub> in prostate cancer could be exploited by designing nanoparticle-based therapies that contain phospholipids targeted to sPLA<sub>2</sub> (*i.e.*, those with short *sn*-2 acyl chain and anionic polar head groups). In studying this hypothesis we tested 17 different formulations that differed in terms of the lengths of the fatty acyl chain present in the phospholipids, types of polar head groups and the presence and absence of polythethylene glycol and cholesterol (Zhu et al., 2011a; Zhu et al., 2011b). Our goal was to identify formulations that were selectively degraded by sPLA<sub>2</sub> compared to clinically standard SSL. We used

electrospray ionization-mass spectrometry to assess liposome degradation and release of 6-carboxyfluorescein (6-CF) as a surrogate marker of drug release. These studies resulted in the identification of sPLA<sub>2</sub> responsive liposomes (SPRL), whose degradation and release of payload was increased significantly in the presence of exogenously added sPLA<sub>2</sub>. Two of these SPRL, termed E and G for the presence of ethanolamine and glycerol head groups, had significantly greater levels of lipid degradation and payload release compared to the all the others studied. Unfortunately, these studies were limited in that experiments were not performed in cells or animals, and that release was not correlated to any marker of therapeutic potential.

With the limitations of the previous study in mind, the goal of this study was to determine the therapeutic potential of SPRL *in vitro* and *in vivo*. We also identified sPLA<sub>2</sub>- and cell-dependent differences in the cytotoxicity, uptake and delivery of SRPL and SSL to investigate differences in the mechanisms mediating the distinct behavior of these formulations. In particular, the ability, or lack thereof, of each formulation to be taken up by cells in culture, whether this uptake of particles would correspond to increases in drug delivery, and whether these results would translate *in vivo* was assessed. Differences in formulation behavior at this level were used to assess differing delivery mechanisms and molecular interactions. It is our hope that the increased understanding of these mechanisms gained from this study will serve as a basis for targeting strategies not only for cancers, but also for other pathologies where sPLA<sub>2</sub> are over expressed.

## Results

### *sPLA<sub>2</sub>-dependent release from SPRL and SSL*

Our laboratory previously designed liposomes whose degradation and release of intraluminal contents was increased in the presence of sPLA<sub>2</sub> isoforms compared to SSL formulations (Zhu et al., 2011b). These liposomes were called sPLA<sub>2</sub> responsive liposomes (SPRL) to denote their preference, as opposed to selectivity, for sPLA<sub>2</sub>. Unfortunately, our previous study was limited in that it did not test the effect of sPLA<sub>2</sub> inhibition on the release of intraluminal contents, nor did it assess the therapeutic activity of SPRL in a model of disease. To address these limitations we tested the hypothesis that LY311727, a broad-spectrum sPLA<sub>2</sub> inhibitor, prevented the release of 6-CF, which was used as a drug marker, from SSL and two different formulations of SPRL (SPRL-E and SPRL-G). As mentioned above, SPRL-E and SPRL-G were used based on our recent publication showing that these formulations yielded the highest responsiveness to sPLA<sub>2</sub> compared to SSL (Zhu et al., 2011b). The differences between these liposome formulations are shown in Table 2.1. As shown in Figure 4.1, 6-CF release in the absence of sPLA<sub>2</sub> was minimal up to 108 hours in media containing 10% FBS. Exposure of formulations to 2.5 µg/ml sPLA<sub>2</sub> increased 6-CF release in all formulations. sPLA<sub>2</sub>-mediated release from SSL was significantly greater than that from untreated liposomes starting at 48 hours. In contrast, significant increases compared to control were seen in SPRL-E and G treated liposomes at time points as early as 24-36 hours. The overall release of 6-CF was less than

20%, which is consistent with the non-burst slow release profile reported in our previous study (Zhu et al., 2011b).

Treatment of SSL with LY311727 decreased 6-CF release roughly 50% compared to SSL treated with sPLA<sub>2</sub> alone (Figure 4.1A). In contrast, exposure of SPRL-E and G to LY311727 reduced 6-CF release almost to control levels. These data support our previous observations that 6-CF release from SPRL is more dependent on sPLA<sub>2</sub> than SSL.

#### *Anti-tumor activity of SPRL and conventional liposomes in human prostate cancer cell lines*

The anti-tumor activity of SPRL was initially determined *in vitro* using multiple prostate cancer cell lines. Prostate cancer cell lines used were chosen because this cancer is reported to over express sPLA<sub>2</sub> at levels 5-20 fold higher than normal prostate tissue and because sPLA<sub>2</sub> expression correlates to poor prognosis and decreased survival (Jiang et al., 2002). Thus, they represent excellent models to assess the therapeutic activity of these liposomes.

Therapeutic activity was first assessed by measuring the cytotoxicity of free doxorubicin, a commonly used anti-cancer drug, or doxorubicin encapsulated in SSL or SPRL-E or G (Figure 4.2). Free doxorubicin induced a concentration-dependent decrease in MTT staining that was also cell specific (data not shown). As expected, MTT staining and potency (IC<sub>50</sub>) of doxorubicin was cell (LNCaP, DU-145 and PC-3) dependent. For example,

doxorubicin induced roughly 60, 70 and 80% decreases in MTT staining in LNCaP cells at 24, 48 and 72 hours, respectively (Figure 4.2A). In contrast, MTT levels were significantly greater in DU-145 cells at these same time points (Figure 4.2B), and similar to controls in PC-3 cells after 72 hours of exposure to free doxorubicin (Figure 4.2C).

Similar to their responses to free doxorubicin, each cell line responded differently to SSL and SPRL-E and -G. For the most part, exposure of LNCaP cells to doxorubicin encapsulated in SSL or SPRL-E or G resulted in decreases similar to that seen with free drug (Figure 4.2A). In contrast to LNCaP cells, exposure of DU-145 cells to doxorubicin encapsulated in SSL, SPRL-E and -G resulted in significantly lower levels of MTT staining compared to free doxorubicin at 24 and 48 hours (Figure 4.2B). A similar trend was seen in PC-3 cells, but only at 24 hours. Interestingly, there did not appear to be a formulation-dependent difference in cytotoxicity.

LY311727 was used to assess the role of sPLA<sub>2</sub> activity in cytotoxicity. Treatment of cells with 100 mM LY311727 prior to exposure to doxorubicin alone or doxorubicin encapsulated in SSL or SPRL did not alter MTT staining compared to cells exposed to these compounds alone, with the exception of SPRL-G in LNCaP cells (Figure 4.2D). LY311727 did not decrease MTT staining alone, and its ability to inhibit sPLA<sub>2</sub> activity was verified in separate experiments (data not shown).

### *Tandem tracking of liposomes and doxorubicin in human prostate cancer cell lines*

Flow cytometry and fluorescent microscopy were used to simultaneously track carrier and payload delivery. Figure 4.3 represents scatter plots and microscopy images demonstrating the fluorescence of doxorubicin and DiO labeled liposomes in PC-3 cells after 72 hours of exposure. Figure 4.3A represents cells treated with empty (unlabeled) liposomes demonstrating a lack of both doxorubicin fluorescence on the X-axis and DiO fluorescence on the Y-axis. Figure 4.3B represents the change in fluorescence on the Y-axis in PC-3 cells treated with DiO labeled liposomes, as indicated by an increase in staining in the upper left hand quadrant compared to Figure 4.3A. Figure 4.3C represents PC-3 cells treated with liposomes containing only doxorubicin. An increase in fluorescence can be observed in the lower right hand quadrant compared to control cells. Figure 4.3D represents cells treated with DiO labeled liposomes containing doxorubicin. As expected, increased fluorescence was seen in the upper right hand quadrant compared to control. Fluorescent intensities of both DiO and doxorubicin were time- and concentration-dependent and linear over the dose ranges tested (data not shown). These data demonstrate that drug and nanoparticle delivery to cells could be tracked simultaneously.

Fluorescence microscopy was used to verify the flow cytometry results (Figure 4.3E-H). For these experiments, all cells were fixed and stained with DAPI after 72 hours of exposure to various treatments. Figure 4.3E

represents control PC-3 cells. Blue stained, normal nuclei are clearly discernible as a result of the DAPI staining. Figure 4.3F represents PC-3 cells exposed to DiO only labeled SPRL-E, demonstrating increased green fluorescent staining compared to control cells. Figure 4.3G represents cells exposed to SPRL-E loaded with doxorubicin. While doxorubicin fluorescence is usually red, in this case it appears purple when overlaid with the DAPI stain as both signals co-localize to the nucleus. Figure 4.3H represents cells exposed to DiO labeled SPRL-E liposomes containing doxorubicin. Evidence can be seen of cells staining for green fluorescence representing SPRL-E, as well as cells staining for doxorubicin. Additionally evidence of altered nuclear morphology can be seen, supporting the conclusion that these liposomes induced cell death.

Having demonstrated the presence of nanoparticle and drug uptake in cells, we used flow cytometry to compare cell- and nanoparticle-dependent differences in fluorescence at 24, 48, and 72 hours (Figure 4.4). Doxorubicin fluorescence was lowest in LNCaP cells and greatest in PC-3 cells, as can be seen in Figure 4.4A. Likewise, DiO fluorescence was generally greater in PC-3 cells, but similar in LNCaP and DU-145 cells, with the exception of SPRL-G fluorescence, which was equal in all three cell lines (Figure 4.4B). DiO fluorescence for SPRL-E was visibly greater in each cell line, compared to SSL and SPRL-G, especially in LNCaP and PC-3 cells. In general, the level of doxorubicin fluorescence correlated with DiO fluorescence in both SSL and SPRL-E, but this correlation was not observed for SPRL-G.

Cytotoxicity may alter liposome uptake. This is especially relevant as LNCaP cells had increased levels of cytotoxicity compared to DU-145 and PC-3 cells. To assess liposome uptake in cells in the absence of cytotoxicity we determined time-dependence differences in fluorescence in cells exposed to liposomes labeled only with DiO (Figure 4.5). Exposure of LNCaP cells to DiO-labeled SSL resulted in comparable levels of fluorescence at 24, 48 and 72 hours (Figure 4.5A). The levels of fluorescence were similar to cells exposed to SSL containing both DiO and doxorubicin (Figure 4.4B). DiO fluorescence in LNCaP cells was also similar to that seen in DU-145 and PC-3 cells exposed to SSL (Figure 4.5B and C), with the exception of slightly greater levels in PC-3 cells at 72 hours. DiO fluorescence was similar in all cells lines exposed to SPRL-G at all time points measured, which agrees with data reported in Figure 4. In contrast, DiO fluorescence was significantly ( $p \leq 0.05$ ) greater in cells exposed to SPRL-E, compared to SSL and SPRL-G. Interestingly, DiO fluorescence was higher in LNCaP cells exposed to SPRL-E at all time points, compared to DU-145 or PC-3 cells.

It is also possible that labeling liposomes with DiO may alter doxorubicin fluorescence. Thus, the fluorescence of doxorubicin was determined in cells after exposure to doxorubicin alone, or doxorubicin encapsulated in SSL, SPRL-E and SPRL-G (Figure 4.6). Doxorubicin fluorescence was lower in LNCaP cells exposed to SSL, compared to cells exposed to doxorubicin alone, or to SPRL formulations (Figure 4.6A). There was a time-dependent decrease in doxorubicin fluorescence in LNCaP cells,

with significantly ( $p \leq 0.05$ ) lower levels being observed at 48 and 72 hours, compared to 24 hours. There were no differences in fluorescence between the formulations tested at 48 and 72 hours.

Exposure of DU-145 and PC-3 cells to doxorubicin alone resulted in greater levels of fluorescence, compared to LNCaP cells, at all time points tested (Figure 4.6B and C). Once again fluorescence was lower in cells exposed to SSL, and unlike LNCaP cells, this trend was maintained at both 48 and 72 hours. For the most part, fluorescence was similar in DU-145 and PC-3 cells exposed to doxorubicin alone or that encapsulated in SPRL-E or G, with the exception of 24 hours in PC-3 cells. These data suggest that the uptake of SSL and SPRL is cell- and formulation-dependent.

#### *In vivo evaluation of SPRL and SSL*

While our *in vitro* data was promising, *in vivo* evaluation is better for suggesting real clinical utility. For these studies, we used a human PC-3 xenograft model in nude mice, as PC-3 cells are our most aggressive cell line. Additionally, LNCaP cells do not readily form tumors in this model and DU-145 are slower growing. For the purpose of testing, we evaluated the SPRL-E formulation, given its comparatively high levels of uptake, and the SSL formulation as a clinically relevant comparison. Treatment of mice, *via* tail vein injection, with doxorubicin encapsulated in SSL resulted in slight decreases in tumor volume compared to controls after 21 days and 3 treatments (Figure 4.7A). Tumor volume continued to increase in SSL

treated mice throughout the length of the study, but was decreased compared to control after 35 days. In contrast, treatment of mice with doxorubicin encapsulated in SPRL-E resulted in significantly lower tumor volumes than either control or SSL treated mice. Tumor volume was lower than controls and SSL at day 17 and remained lower than controls even after treatment was stopped at 21 days. Body weights were not significantly different between control, SSL and SPRL-E exposed mice after 21 days, and only slightly lower in treated groups after that (Figure 4.7B). Necropsies performed following sacrifice to look for evidence of cardiotoxicity and signs of cardiomyopathy were negative. These data suggest that SPRL-E are more effective at limiting tumor growth than the clinically utilized SSL.

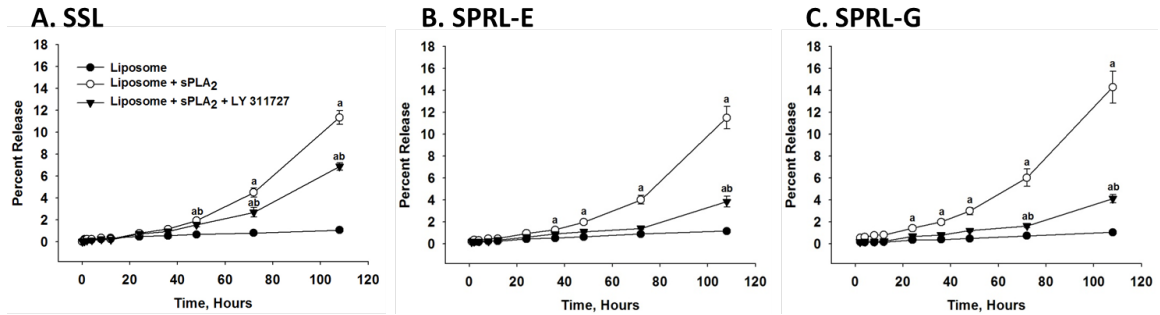


**Figure 4.1 Effect of sPLA<sub>2</sub> inhibition on 6-carboxyfluorescein (6-CF) release from SPRL and SSL.** 6-CF was loaded into liposomes that were then incubated in F-12K medium containing 10% FBS for 108 hours at 37°C in the presence and absence of 100  $\mu$ M LY311727 (sPLA<sub>2</sub> inhibitor). At the specified time points, samples were removed and analyzed for fluorescence. Data are presented as the mean  $\pm$  SEM of 5-6 different experiments. “a” Denotes a significant ( $p < 0.05$ ) difference compared to control and “b” represents a significant difference compared to liposomes + sPLA<sub>2</sub>.

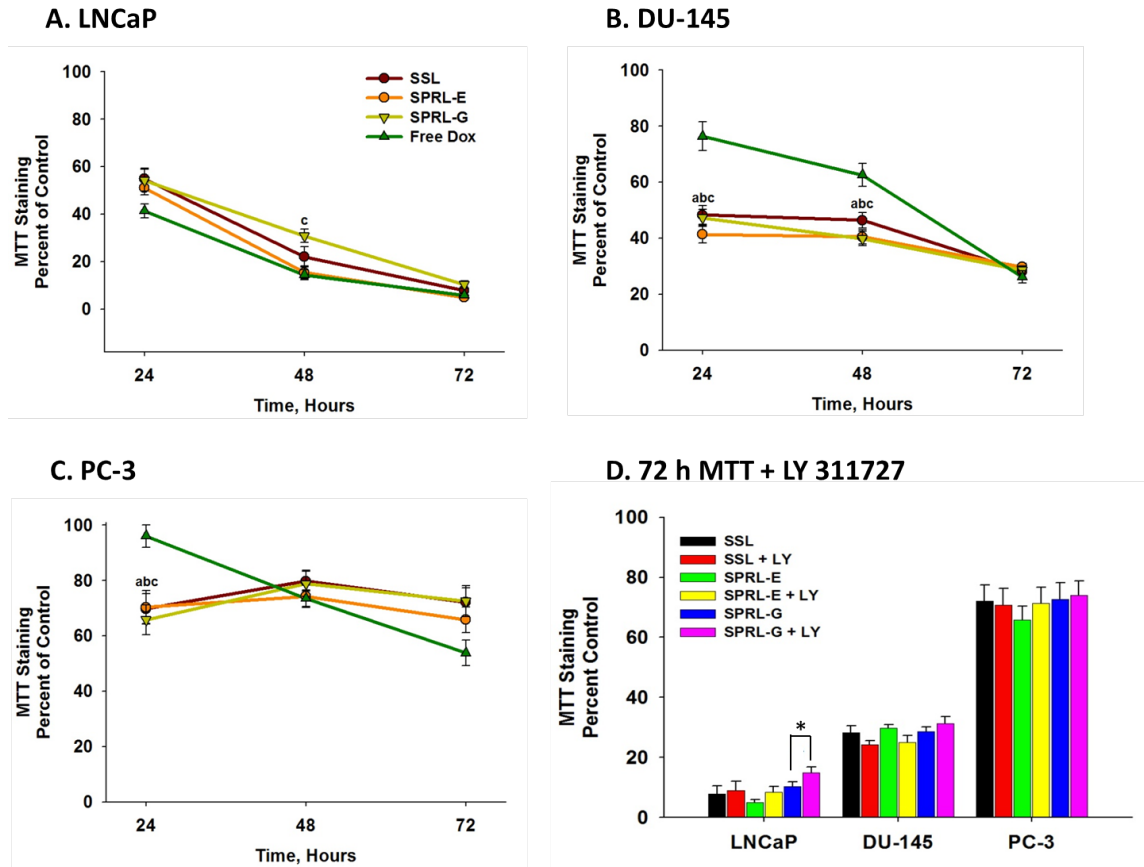


**Figure 4.2 Time-dependent effects of SPRL and SSL on MTT staining in human prostate cancer cells.** LNCaP (A), DU-145 (B) and PC-3 (C) cells were dosed with 2.5  $\mu$  M doxorubicin or liposomal equivalents and MTT staining was assessed at 24, 48 and 72 hours. Panel D shows the effect of LY311727 on MTT staining in the presence and absence of SSL and SPRL-E and G after 72 hours. Data are presented as the mean  $\pm$  SEM of at least 3 different experiments. In panels A-C “a” denotes a significant difference ( $p < 0.05$ ) between Free Dox and SSL, “b” denotes a significant difference between Free Dox and SPRL-E, and “c” denotes a significant difference between Free Dox and SPRL-G. In panel D “\*” denotes a significant difference between the presence and absence of LY311727.

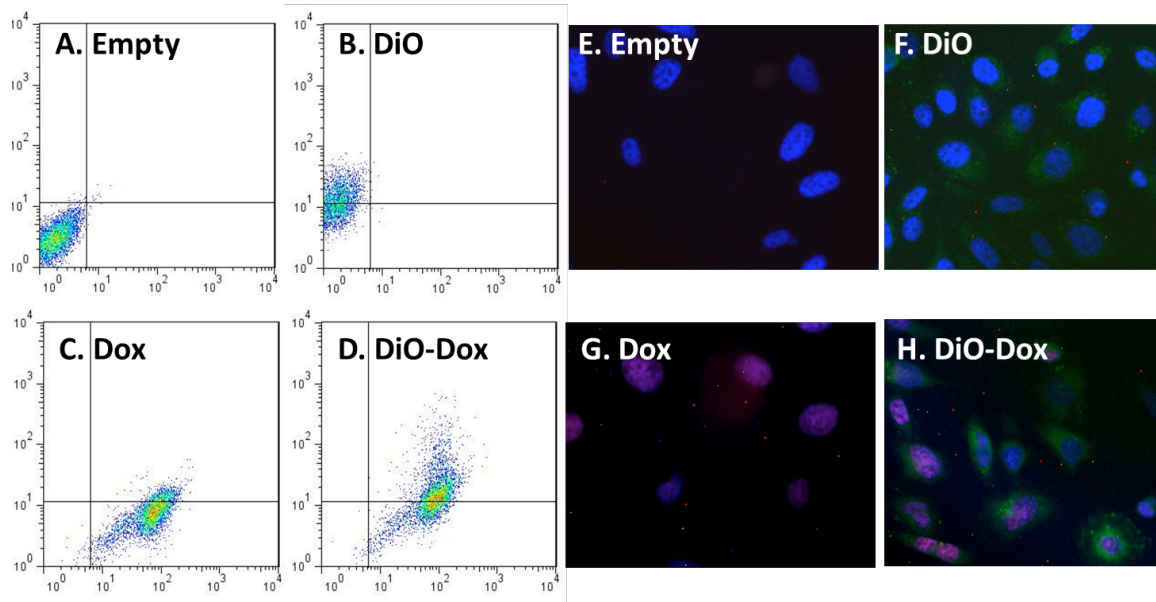


**Figure 4.3 Tandem tracking of doxorubicin, SPRL and SSL in prostate cancer cells using flow cytometry and fluorescence microscopy.** Cells were treated with DiO-labeled, doxorubicin loaded (Dox) liposomes and liposomes labeled with both doxorubicin and DiO (Dio-Dox). The above figures are representative scatter plots and microscopy images showing PC-3 cell treated with SPRL-E. Both liposomes and doxorubicin were tracked concurrently using flow cytometry (**A-D**) and fluorescent microscopy at 350X magnification (**E-H**). Panels **A-D** represent scatter plots showing fluorescence for empty liposomes (**A**), DiO-labeled liposomes (**B**) Dox-loaded liposomes (**C**) and doxorubicin-loaded liposomes labeled with DiO (**D**). Panels **E-F** represent fluorescence microscopy of these cells stained with DAPI and treated with empty liposomes (**E**), DiO-labeled liposomes (**F**), doxorubicin-loaded liposomes (**G**) and doxorubicin loaded liposomes labeled with DiO (**H**). Data are representative of at least 3 separate experiments.

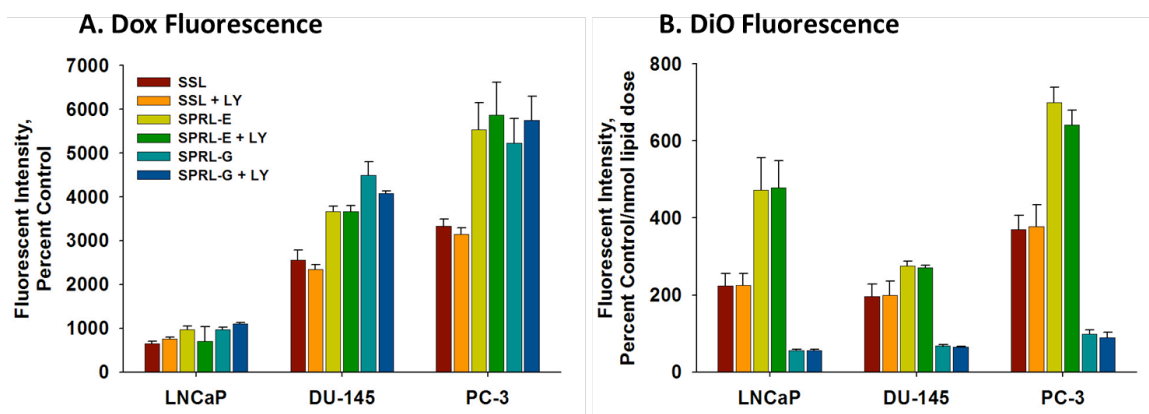


**Figure 4.4** Quantification of fluorescence of doxorubicin and DiO in prostate cancer cells exposed to SPRL and SSL. LNCaP, DU-145, and PC-3 cells were treated with dual-labeled liposomes for 72 hours and examined with flow cytometry. Panel **A** shows the intensity of doxorubicin fluorescence while panel **B** shows the intensity of DiO fluorescence normalized by the nmol dose of lipid. Data are presented as the mean  $\pm$  SEM of at least 3 different experiments. Differences were considered significant with a  $p < 0.05$ .

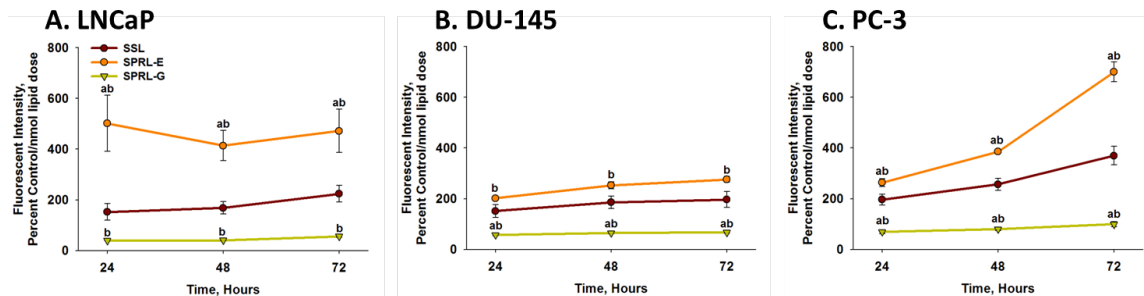


**Figure 4.5 Time-dependence of DiO uptake in prostate cancer cells exposed to SPRL and SSL.** LNCaP (A), DU-145 (B) and PC-3 (C) cells were exposed to DiO-labeled liposomes for 24, 48 and 72 hours, after which cells were detached, washed, and assessed for fluorescence using flow cytometry. Data are presented as the mean +/- SEM of at least 3 different experiments. Differences between SPRL formulations and SSL are denoted by “a” and differences between SPRL-E and G are denoted by “b”.

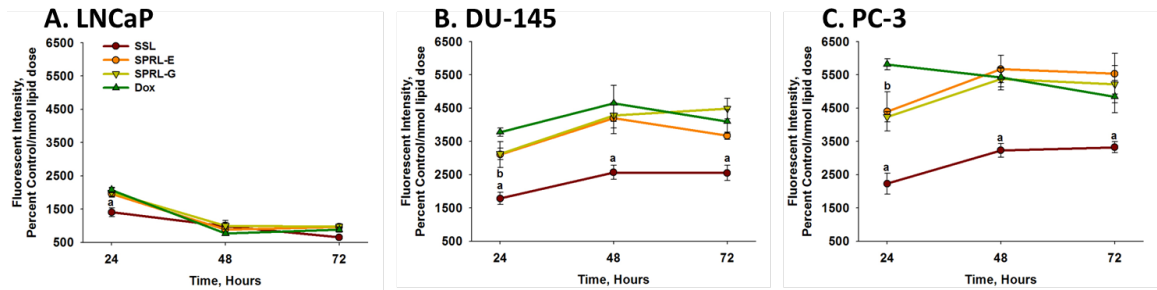


**Figure 4.6 Time-dependence of doxorubicin uptake in prostate cancer cells exposed to SPRL and SSL.** LNCaP (A), DU-145 (B) and PC-3 (C) cells were exposed to doxorubicin alone (Dox) or encapsulated in SPRL-E, G and SSL for 24, 48, and 72 hours, after which cells were detached, washed, and assessed for fluorescence using flow cytometry. Data are presented as the mean  $\pm$  SEM of at least 3 different experiments. “a” Denotes a significant ( $p < 0.05$ ) difference between Dox and SSL, “b” denotes a significant difference between Dox and SPRL-G. There were no significant differences between Dox and SPRL-E.

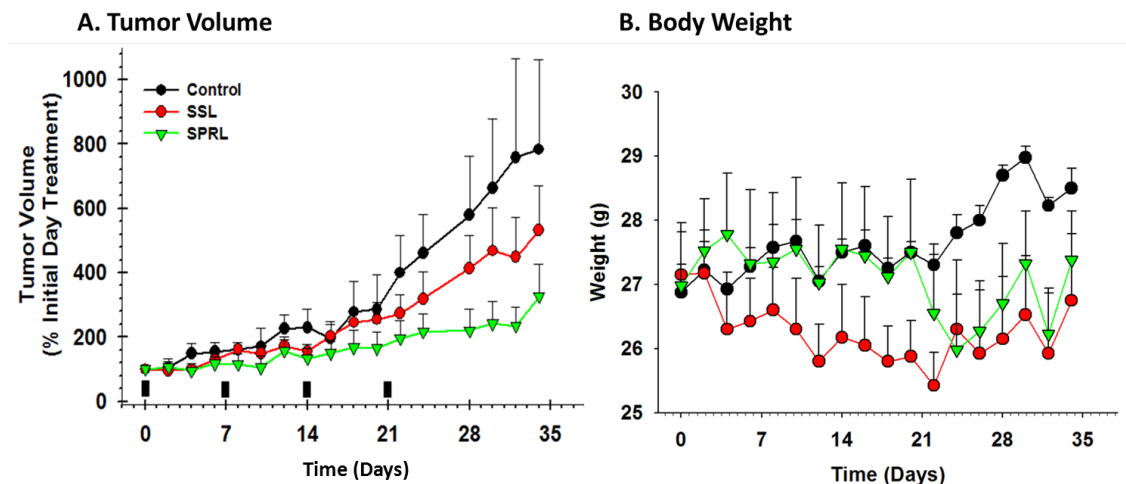


**Figure 4.7 Effect of doxorubicin containing SPRL and SSL on PC-3 xenograft tumor growth.** Nude mice bearing PC-3 xenograft tumors were treated (indicated by solid bars) with SSL and SPRL-E formulations on a weekly basis for 4 weeks after tumors reached 400 mm<sup>3</sup> and tumor volume (A) and mouse weight (B) were determined every 2 days for 34 days. Data are presented as the mean +/- SEM of at least 4 different mice.

## Discussion

This study demonstrated the novel finding that SRPL formulations containing doxorubicin were effective at decreasing human prostate cancer cell growth *in vitro* and *in vivo*. The data support the hypothesis that SPRL may be used to treat cancer, as well as other diseases where sPLA<sub>2</sub> is over expressed and may be more effective than the clinically utilized SSL. The increased efficacy of SPRL-E, compared to SSL, *in vivo* may have been a result of increased uptake. This hypothesis is supported by our *in vitro* studies in all three prostate cancer cells lines. However, SPRL-G was also more effective than SSL at delivering drug inside the cell, although uptake of these particles was limited by comparison. Thus, other mechanisms, in addition to uptake, may be mediating the increased efficacy of SPRL *in vivo*.

The fact that these nanoparticles induced cytotoxicity at levels comparable to free drug *in vitro* is an unexpected finding. Free drug typically displays greater antitumor activity than liposomes *in vitro*, as encapsulated drugs must first be released from nanoparticles. Toxicities equal to free drug suggests that there is enhanced release and/or uptake mechanisms at work beyond the simple diffusion of particles across the membrane. The nature of this mechanism is unknown, but must be cell mediated, as the release studies in Figure 4.1 demonstrate that drug release is effectively zero in the absence of cells or sPLA<sub>2</sub>.

SPRL were designed to interact with sPLA<sub>2</sub>, but all of the formulations, including SSL, had similar levels of *in vitro* cytotoxicity in spite of having different levels of DiO fluorescence. This shows that cytotoxicity does not

always correlate to cellular uptake and suggest that the mechanisms mediating cytotoxicity of these nanoparticles are distinct from those mediating uptake. One possible explanation for these differences may be a product of extracellular degradation of liposomes, resulting in the release and subsequent uptake of doxorubicin independent of the nanoparticle. It is unlikely that differences in cytotoxicity are mediated by differences in sPLA<sub>2</sub> activity between these cells as LY311727 had little to no effect on MTT staining, even though it decreased sPLA<sub>2</sub>-mediated release of payload in earlier studies. This suggests that the mechanism of cytotoxicity or uptake does not require enzyme activity, and again, points to the possibility of multiple mechanisms mediating cytotoxicity.

The inability of LY311727 to alter uptake or antitumor activity does not necessarily mean that these liposomes are not responsive to sPLA<sub>2</sub>. sPLA<sub>2</sub> have functions that are independent of their lipolytic activity and several proteins exist in mammalian cells that bind sPLA<sub>2</sub> independently of the sPLA<sub>2</sub> active site (Lambeau and Gelb, 2008b). One of these proteins is a receptor in the C-type lectin superfamily called PLA<sub>2</sub>R and it is responsible for internalizing sPLA<sub>2</sub> back inside the cell *via* endocytosis after it has been secreted (Hanasaki and Arita, 2002). Studies in other cells types show that binding of sPLA<sub>2</sub> to PLA<sub>2</sub>R does not require lipase activity (Lambeau and Gelb, 2008b). Thus, an alternative mechanisms for uptake of these formulations, independent of lipase activity, is that the liposome are interacting with sPLA<sub>2</sub>, which forms a complex with the PLA<sub>2</sub>R membrane

receptor that is then transported into the cell. This type of facilitated uptake has not been reported for liposomes or other drug carriers and may hold great potential in terms of developing a novel targeting strategy.

One clear finding in this study is that the mechanisms mediating SPRL uptake and drug delivery are cell-dependent. The cell lines used in this study differentially express multiple sPLA<sub>2</sub> isoforms (Menschikowski et al., 2008). It is possible that these differences may account for disparities in drug delivery and SPRL uptake, as each sPLA<sub>2</sub> isoform displays differential preferences for binding to lipid substrates, PLA<sub>2</sub>R and other extracellular features of the membrane (Hanasaki and Arita, 2002; Murakami et al., 2012).

In addition to cell-dependence, these data suggest that the mechanisms mediating the uptake of drug and nanoparticles are formulation-dependent. All of these nanoparticles were roughly identical in size (100 nm), but differed slightly in terms of phospholipid content. Our results demonstrate that incorporating as little as 10% of zwitterionic or anionic lipid into our liposome membranes can have a pronounced affect on whether or not they are taken up or release their contents extracellularly (Figures 4.5 and 4.6). This information will be invaluable for the development of future generations of SPRL, whether they are designed to treat cancer or any one of numerable other diseases.

SSL containing doxorubicin is a FDA approved treatment for some cancers, and goes under the name trade name Doxil™ (1995). SSL and

SPRL-E differ only by 10 mol% DSPE, which is abundant in eukaryotic cell membranes (Bakovic et al., 2007). This suggests that SPRL may be rapidly translated to clinical application with little fear of toxicity. The increased efficacy of SPRL against tumor growth *in vivo* suggests that SPRL may be viable for treating prostate cancers specifically, as well as other cancers that over express sPLA<sub>2</sub>.

This enhanced efficacy of SPRL-E *in vivo* was particularly interesting, given that all three of the formulations performed comparably *in vitro*. These data suggest that the responsiveness to sPLA<sub>2</sub> becomes more valuable in an *in vivo* platform. One reason for the discrepancy between the *in vitro* and *in vivo* data may be the increased uptake of both drug and carrier that SPRL-E compared to SSL (Figures 4.5 and 4.6). This uptake mechanism may be minimized *in vivo*, but play a more important role *in vivo*. Another possible explanation for this discrepancy is that in an *in vitro* setting there is no means of clearance, or interaction with additional organ systems. However, *in vivo* such events are critical to nanoparticle efficacy. It is unlikely that differences in EPR results in increased efficacy *in vivo* as both particles should deposit in the tumor tissue in relatively similar amounts based on previous studies (Maeda et al., 2000). Finally, it is well established that *in vitro* efficacy of nanoparticles does not always translate well *in vivo* and vice versa. Future studies focusing on differences in the mechanism of uptake and delivery *in vivo* are expected to provide answers to some of these questions.

Although the experiments in this study focused on the utility of SPRL in prostate cancer, this targeting strategy may hold greater potential. As mentioned above, sPLA<sub>2</sub> have a variety of physiological functions (Lambeau and Gelb, 2008b) and are commonly over expressed in a number of serious pathologies. Up regulation of sPLA<sub>2</sub> frequently occurs in atherosclerotic plaques and in arthritic joints (Bostrom et al., 2007; Fraser et al., 2009; Leistad et al., 2004; Pruzanski and Vadas, 1988; Rosengren et al., 2006), as well as other inflammatory conditions (Oka et al., 1990; Yamashita et al., 1994a; Yamashita et al., 1993). This suggests that SPRL may be integrated, or translated, to therapies outside of just prostate cancer.

In conclusion, we showed that engineering liposomes to specifically interact with sPLA<sub>2</sub> is a viable targeting strategy for inhibiting prostate cancer growth *in vitro* and *in vivo*. Data in this study also suggests that mechanisms independent of sPLA<sub>2</sub> activity may, in part, mediate the toxicity and disposition of liposomes, and that the efficacy of sPLA<sub>2</sub> targeted nanoparticles are mediated by mechanisms that are cell- and formulation-dependent. Identifying these mechanisms will be key to designing more efficacious targeting strategies for treatment of diseases that over express sPLA<sub>2</sub>.

## CHAPTER 5

# MECHANISTIC ROLES OF PHOSPHOLIPASE A<sub>2</sub> RECEPTOR AND GROUP X SECRETORY PHOSPHOLIPASE A<sub>2</sub> IN MODULATING ACTIVITY OF SECRETORY PHOSPHOLIPASE A<sub>2</sub> RESPONSIVE LIPOSOMES IN PROSTATE CANCER CELLS<sup>3</sup>

---

<sup>3</sup> Mock, Jason, Wilding, Stephanie, Arnold, Robert and Cummings, Brian. To be submitted to *Biochemical Pharmacology*.

## Abstract

Secretory phospholipase A<sub>2</sub> (sPLA<sub>2</sub>) are esterases associated with inflammation that cleave phospholipids at the *sn*-2 ester bond, releasing a lysophospholipid and a fatty acid. While they serve important physiological roles in defense and signaling, they are over expressed in several pathologies, including arthritis, atherosclerosis, sepsis and several cancers. Our lab previously engineered and evaluated liposomes that are responsive to different sPLA<sub>2</sub> isoforms. Use of these sPLA<sub>2</sub> responsive liposomes (SPRL) increased cellular uptake of both drug and formulations compared to clinically utilized sterically stabilized liposomes (SSL), and increased the efficacy of anti-cancer agents both in vitro and in vivo. The mechanisms mediating increased efficacy and uptake of SPRL are not fully understood. Phospholipase A<sub>2</sub> receptors (PLA<sub>2</sub>R) are membrane localized and mediate endocytosis of several sPLA<sub>2</sub> isoforms, including Group X sPLA<sub>2</sub>. We used wild type PC-3, a stable PLA<sub>2</sub>R knockdown of this cell line and recombinant Group sPLA<sub>2</sub> X to test the hypothesis that these two proteins mediate uptake of SPRL and their enhanced efficacy in prostate cancer cells. Knocking down PLA<sub>2</sub>R significantly increased the cytotoxicity and uptake of the anti-cancer drug doxorubicin in correlation with increased uptake of SPRL, in contrast, knockdown of PLA<sub>2</sub>R had no effect on the uptake of SSL. Conversely, addition of Group X sPLA<sub>2</sub> minimally altered the cytotoxicity of SPRL, but increased uptake of SPRL while decreasing drug uptake, suggesting that extracellular destabilization and dose dumping from nanoparticles occurred.

Taken in total, these data indicate that both PLA<sub>2</sub>R and Group X sPLA<sub>2</sub> modulate the behavior of SPRL and suggest that both are potential targets for future generations of delivery vectors and chemotherapeutics.

## **Introduction**

Nanoparticulate drug delivery is an ever-expanding area of research that holds great potential for improving the treatment of cancer. To date, several types of nanoparticles have made it into clinical use, including albumin-based nanoparticles containing paclitaxel used to treat metastatic breast cancer (Miele et al., 2009), iron-oxide nanoparticles used to treat anemia in testicular and prostate cancer patients (Duncan and Gaspar, 2011; Shih et al., 2005), and liposomal-doxorubicin approved to treat ovarian cancer and Kaposi's sarcoma (Safra et al., 2000). In addition, there are several nanoparticle-based technologies in the pipeline, ranging in purpose from treatment to diagnosis and imaging (Hu and Zhang, 2012; Salvador-Morales et al., 2012; Schroeder et al., 2012; Waite and Roth, 2012).

Liposomes are currently one of the most widely utilized nanoparticles, with multiple formulations approved for a variety of indications. Their development and clinical use has been ongoing for over two decades (Langer, 1998; Papahadjopoulos et al., 1991; Safra et al., 2000; Schroeder et al., 2012). Like most drug carriers, liposomes can provide continuous levels of drug in a desirable range, reduce harmful side effects, reduce the amount of drug needed for efficacy, increase patient compliance by lowering the

number of doses necessary, increase the bioavailability of drugs with short half-lives and provide a means of targeting specific tissues (Langer, 1998). Treating cancer with liposomes could take advantage of all of these benefits, and the clinical success of Doxil, a liposomal formulation of doxorubicin, is a testament to the power of these particles to alter kinetics and reduce dose-limiting toxicity (Barenholz, 2001).

The treatment solid tumors, such as breast and prostate cancer, with long circulating liposomes is also advantageous due to their ability to passively accumulate in the interstitial space through a phenomenon known as enhanced permeation and retention (EPR). This passive targeting results from the aberrant, leaky vasculature and lack of adequate lymphatic drainage characteristic of many solid tumors (Maeda et al., 2000).

Our laboratory previously engineered formulations that we deemed sPLA<sub>2</sub> responsive liposomes (SPRL) for their preferential interaction with this family of phospholipases (Zhu et al., 2011a; Zhu et al., 2011b). sPLA<sub>2</sub> are commonly over expressed during bouts of inflammation and in inflammatory diseases like arthritis, atherosclerosis and sepsis [41-50] as well as a variety of cancers (Dong et al., 2006; Yamashita et al., 1994a), including prostate (Graff et al., 2001; Jiang et al., 2002; Kallajoki et al., 1998; Sved et al., 2004). Over expression of sPLA<sub>2</sub>, particularly Group IIA sPLA<sub>2</sub>, has been observed in prostate cancer for a number of years, with tumors showing levels 22-fold higher than controls (Sved et al., 2004). Likewise, others reported that 91% of high-grade tumors were immunoreactive when probed for sPLA<sub>2</sub> (Jiang et

al., 2002). Additionally, primary cultures of cancer cells that over expressed sPLA<sub>2</sub> proliferated twice as fast as those that did not over express the enzyme, and over expression of sPLA<sub>2</sub> was inversely correlated with 5-year survival of prostate cancer patients (Graff et al., 2001).

We recently showed in diverse prostate cancer cells that targeting liposomes to interact with sPLA<sub>2</sub> increased payload release and enhanced liposomal degradation compared to clinically utilized sterically-stabilized liposomes (SSL) (manuscript in revision). These liposomes, termed sPLA<sub>2</sub> responsive liposomes or SPRL, also performed better than SSL at delivering drugs to several prostate cancer cell lines and were more effective at slowing tumor growth in a xenograft model. These studies tested two SPRL formulations, one containing 10% phosphatidylethanolamine, called SPRL-E, and one containing 10% phosphatidylglycerol, called SPRL-G, which behaved significantly differently in terms of in vitro behavior. While both induced similar levels of cytotoxicity, SPRL-E was characterized by comparatively higher levels of uptake of the carrier. Interestingly, SPRL-G had comparable levels of drug uptake, but dramatically lower levels of liposome uptake. This suggests that multiple mechanisms are involved in liposome uptake and release of interluminal contents. It is also possible that these differences result from the differential expression of the sPLA<sub>2</sub> isoforms in the cell lines tested (Menschikowski et al., 2008). Another hypothesis is that SPRL and SSL may be differentially interacting with the receptor for sPLA<sub>2</sub> called the phospholipase A<sub>2</sub> receptor, or PLA<sub>2</sub>R.

PLA<sub>2</sub>R is a M-type receptor in the C-type lectin superfamily that can internalize sPLA<sub>2</sub> inside the cell via endocytosis (Hanasaki and Arita, 2002). Others have shown that PLA<sub>2</sub>R does not require sPLA<sub>2</sub> to be catalytically active for endocytosis to occur (Lambeau and Gelb, 2008b). Given our previous findings that pharmacological inhibition of sPLA<sub>2</sub> did little to alter uptake of drug or liposome, it is possible that our SPRL formulations are interacting with sPLA<sub>2</sub> and forming a complex that is subsequently transported into the cell by PLA<sub>2</sub>R. This type of facilitated uptake has never been reported for any species of nanocarrier.

The differential expression of sPLA<sub>2</sub> may also alter the uptake of SPRL and account for differences in uptake between cell lines. The species specificity of sPLA<sub>2</sub> for PLA<sub>2</sub>R is well documented (Hanasaki and Arita, 1996, 2002; Lambeau and Lazdunski, 1999), and the differential expression of sPLA<sub>2</sub> in multiple prostate cancer cell lines has been previously reported (Menschikowski et al., 2008) and confirmed herein. Given our results, Group X sPLA<sub>2</sub> was distinct as an isoform of interest because of its status as a putative high affinity ligand for PLA<sub>2</sub>R and its widely varying levels of expression in the cell lines we tested (Menschikowski et al., 2008). Given the profile of this enzyme for being the most catalytically active sPLA<sub>2</sub> (Lambeau and Gelb, 2008b; Murakami et al., 2012) and a potential substrate for PLA<sub>2</sub>R (Rouault et al., 2007; Yokota et al., 2001), we believed that its role in the behavior of SPRL should be further examined.

The purpose of the work herein was to determine the molecular constituents mediating the differential behavior of our two SPRL formulations, and SSL. To this end, PLA<sub>2</sub>R was stably knocked down in PC-3 prostate cancer cells and the uptake and efficacy of dual labeled liposomes was determined. Additionally, the effect of exogenous Group X sPLA<sub>2</sub>, a putative substrate of human PLA<sub>2</sub>R (Hanasaki and Arita, 2002; Murakami et al., 2012), on the uptake and efficacy of dual labeled liposomes was also assessed.

## **Results**

### *Expression and Knock Down of sPLA<sub>2</sub> and PLA<sub>2</sub>R in PC-3*

Our laboratory previously determined (manuscript in revision) that the behavior of SPRL is cell-dependent. We hypothesized that this cell-dependence may have been, in part, influenced by the differential expression of various sPLA<sub>2</sub> isoforms. Using RT-PCR, we determined which of the conventional mammalian sPLA<sub>2</sub> are expressed in PC-3. As shown in Figure 5.1A, PC-3 cells expressed Groups IB, IIA, V and X sPLA<sub>2</sub>. Levels of each of these sPLA<sub>2</sub> and PLA<sub>2</sub>R were also quantified in LNCaP and DU-145 prostate cancer cell lines (Figure 5.1B), as these lines were used in our previous studies (manuscript in revision). Following quantification of these transcripts, we decided to move forward only using PC-3 cells, as they had the highest levels of transcription of sPLA<sub>2</sub>, and displayed differential expression of Group X sPLA<sub>2</sub>.

Expression of PLA<sub>2</sub>R was also examined in PC-3, LNCaP and DU-145 cells (data not shown). PLA<sub>2</sub>R expression was highest in PC-3 cells, making it an ideal candidate for studying the effects of knockdown. A representative RT-PCR gel in the Figure 5.2 Inset shows this robust level of transcription. The expression of PLA<sub>2</sub>R protein using immunoblot analysis was unsuccessful due to lack of antibody specificity.

To study the role of PLA<sub>2</sub>R in the uptake and efficacy of SPRL and SSL the expression of this receptor was stably inhibited, or knocked down, using shRNA in lentiviral vectors. Figure 5.2 shows that we were able to achieve sustained knockdown of greater than 80%, as determined by QRT-PCR, compared to the normal level of transcription in control cells. Knockdown of PLA<sub>2</sub>R did not alter the rate of growth of PC-3 cells based on doubling time and did not induce detectable cell death (data not shown).

#### *Cytotoxicity and Uptake of Liposomes and Drug in PLA<sub>2</sub>R Knockdown Cells*

To determine the effect of PLA<sub>2</sub>R knockdown on cytotoxicity and uptake of liposomes, PC-3 cells expressing the non-coding shRNA and shRNA against PLA<sub>2</sub>R cells were treated with SSL, SPRL-E and SPRL-G that were either loaded with doxorubicin, labeled with DiO, or both. As shown in Figure 5.3, knockdown of PLA<sub>2</sub>R resulted in a dramatic decrease in cell number and distinct changes in cell morphology following a 2.5 μM equivalent dose of encapsulated doxorubicin. Figure 5.3A and 5.3C show that knockdown of PLA<sub>2</sub>R did not alter either the apparent cell number or

morphology compared to wild type cells. Treatment of wild type cells with doxorubicin encapsulated in SSL resulted in slight decrease in cell number and cell rounding compared to control cells after 24 hours (Figure 5.3B). In contrast, exposure of PLA<sub>2</sub>R knockdown cells to SSL resulted in significantly less growth and increased cell rounding compared to wild type cells exposed to SSL (Figure 5.3D). Treatment of wild type cells with SPRL-E or G also resulted in slight changes in morphology compared to controls; however, once again, knockdown of PLA<sub>2</sub>R decreased the amount of cells compared to controls (Figure 5.3E-H). These data suggest that knocking down PLA<sub>2</sub>R increases the cytotoxicity of doxorubicin encapsulated in liposomes.

To confirm that changes in cell morphology were a result of cytotoxicity, the effect of PLA<sub>2</sub>R knockdown on MTT staining was determined (Figure 5.4). Knockdown of PLA<sub>2</sub>R caused a significant decrease in MTT staining in cells exposed to SSL compared to wild type controls (Figure 5.4A). Decreases in MTT staining were time-dependent, and PLA<sub>2</sub>R knockdown decreased MTT staining at all time points tested. In contrast to MTT staining, PLA<sub>2</sub>R knockdown did not alter DiO uptake into cells after SSL exposure and only altered doxorubicin uptake after 72 hours, as compared to controls (Figures 5.4B and C).

Similar to SSL, PLA<sub>2</sub>R knockdown decreased MTT staining at all time points measured, compared to controls after exposure to doxorubicin loaded into SPRL-E (Figure 5.5). Unlike SSL, PLA<sub>2</sub>R knockdown increased DiO fluorescence after both 48 and 72 hours, suggesting increased uptake of

SPRL-E (Figure 5.5B). Increases in DiO fluorescence in cells exposed to SPRL-E correlated to increased doxorubicin levels at both 24 and 72 hours (Figure 5.5C).

In contrast to SSL and SPRL-E, PLA<sub>2</sub>R knockdown did not alter MTT staining, as compared to control, after exposure to doxorubicin loaded SPRL-G at 24 and 48 hours, but decreased MTT staining significantly at 72 hours (Figure 5.6A). Interestingly, PLA<sub>2</sub>R knockdown increased DiO fluorescence at all time points measured (Figure 5.6B). Likewise, PLA<sub>2</sub>R knockdown increased doxorubicin fluorescence slightly at 24 hours and significantly at 48 and 72 hours, as compared to controls (Figure 5.6C).

#### *Cytotoxicity and Uptake of Liposomes and Drug in the Presence of Exogenous Group X sPLA<sub>2</sub>*

Since Group X sPLA<sub>2</sub> is a highly preferred substrate for PLA<sub>2</sub>R, we tested the hypothesis that addition of Group X sPLA<sub>2</sub> would alter the cytotoxicity and uptake of SPRL and SSL. To this end, 10 nM of Group X sPLA<sub>2</sub> was added to each well prior to dosing with liposomes and cytotoxicity and uptake were analyzed 24 hours later (Figure 5.7).

As shown in Figures 5.4-5.6, treatment of cells with SSL, or SPRL-E or G, for 24 hours did not decrease MTT staining below that of control. The addition of Group X sPLA<sub>2</sub>, prior to exposure to doxorubicin-loaded SSL, decreased MTT staining, compared to cells exposed only to SSL (Figure 5.7A) after 24 hours. Decreases in MTT staining were not accompanied by

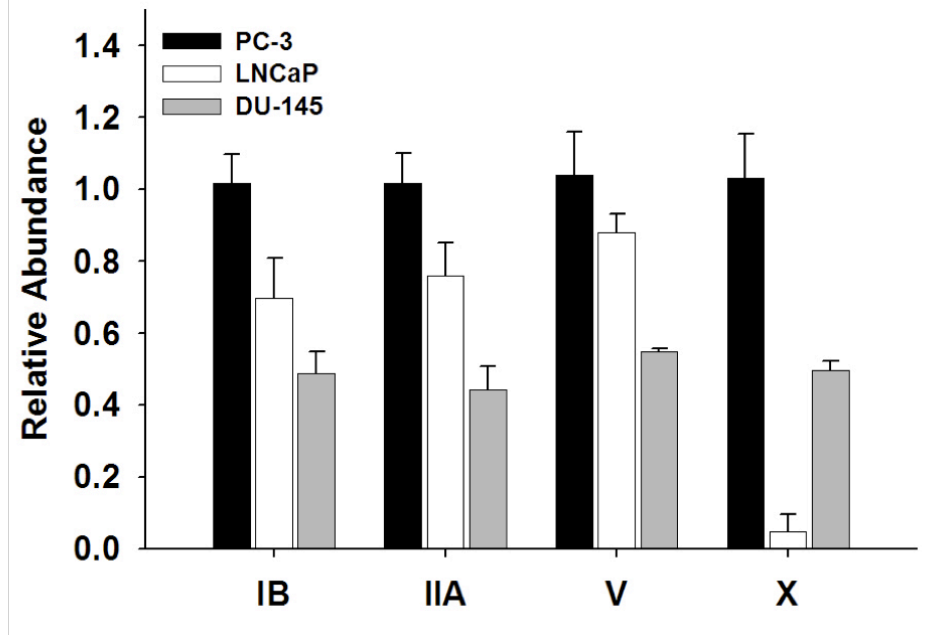
any changes in DiO fluorescence (Figure 5.7B), but there was a decrease in doxorubicin fluorescence in the presence of exogenous Group X sPLA<sub>2</sub>, as shown in (Figures 5.7C).

In contrast to SSL, addition of Group X sPLA<sub>2</sub> to cells exposed to doxorubicin loaded SPRL-E did not alter MTT staining (Figure 5.7D), but increased DiO fluorescence and decreased doxorubicin fluorescence compared to cells not exposed to Group X sPLA<sub>2</sub> (Figure 5.7D-F). Similar results were seen with SPRL-G (Figures 5.7G-7I).

### A. RT-PCR of sPLA<sub>2</sub> in PC-3



### B. QRT-PCR of sPLA<sub>2</sub> in Multiple Prostate Cancer Lines



44

**Figure 5.1 Expression of sPLA<sub>2</sub> in prostate cancer cells.** Total RNA was isolated from PC-3, LNCaP and DU-145 cells, converted to cDNA and RT-PCR was performed with primers specific for Groups IB, IIA, V and X sPLA<sub>2</sub> in PC-3 cells as well as LNCaP and DU-145 using qPCR. Panel **A** shows the products of the RT-PCR on an agarose gel in PC-3 cells. Panel **B** shows the results of qPCR performed to receive a quantitative comparison of the three cell lines. Data are presented as the mean +/- the SEM of at least 3 different experiments. Differences were considered significant with a  $p < 0.05$  and denoted by "\*\*".

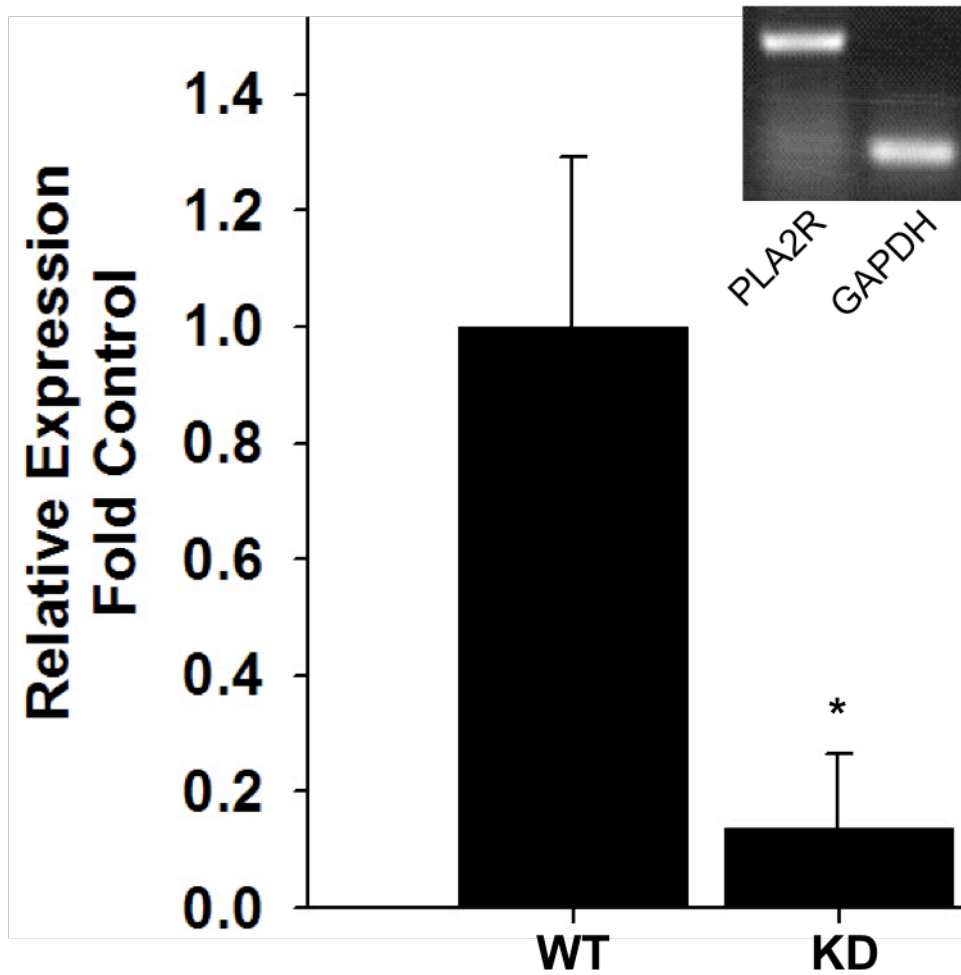


**Figure 5.2 Knockdown of PLA<sub>2</sub>R in PC-3 cells.** PC-3 cells were stably transduced with shRNA directed against PLA<sub>2</sub>R using a lentiviral vector to knockdown transcription, which is illustrated by the RT-PCR gel shown in the inset. The expression of PLA<sub>2</sub>R mRNA in wild type and knockdown cells was quantified using qPCR. Data are presented as the mean +/- the SEM of at least 3 different experiments. Differences were considered significant with a  $p < 0.05$  and denoted by "\*\*".

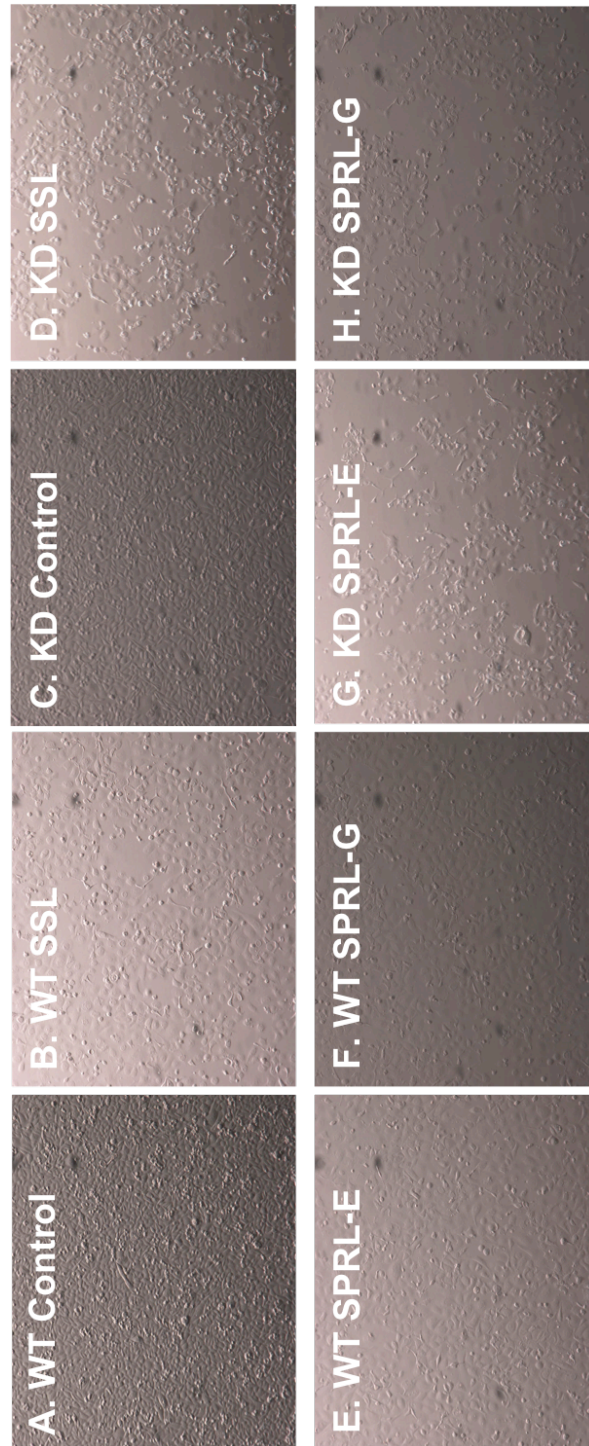


**Figure 5.3 Phase contrast microscopy of wild type and PLA<sub>2</sub>R knockdown PC-3 cells treated with SSL and SPRL.** Cells were seeded at  $7.0-8.0 \times 10^4$  cells per well and allowed to grow for 24 hours prior to treatment with  $2.5 \mu\text{M}$  equivalents of doxorubicin in SSL or SPRL and examined 24 hours later using a phase contrast microscope at 250X magnification. Data are representative of at least 3 ( $n = 3$ ) separate experiments.

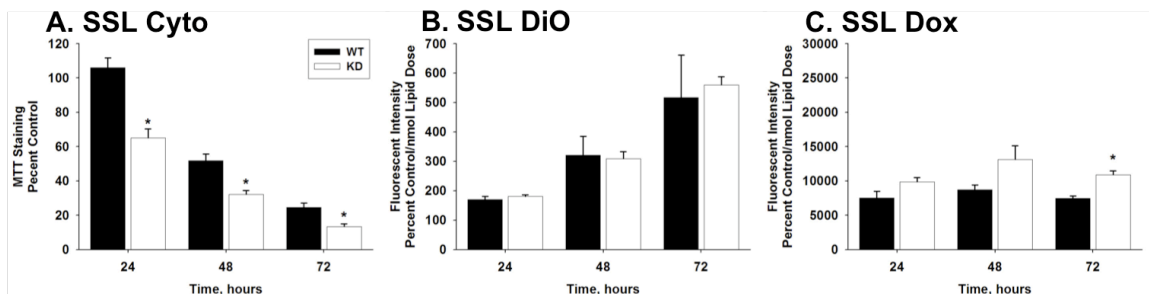


**Figure 5.4 Performance of SSL in WT and KD PC-3 Cells.** To determine cytotoxicity, wild type or PLA<sub>2</sub>R knockdown PC-3 cells were seeded at 30,000 cells/ml and allowed to grow for 24 hours prior to treatment with SSL containing doxorubicin for 24-72 hours. To determine uptake, wild type or PLA<sub>2</sub>R knockdown PC-3 cells were seeded at 7.0-8.0×10<sup>4</sup> cells/ml and allowed to grow for 24 hours prior to treatment with empty SSL (not shown) or SSL containing doxorubicin and DiO for 24-72 hours. Panel **A** shows results for MTT staining, Panel **B** shows uptake of DiO and Panel **C** shows uptake of doxorubicin. Data are presented as the mean +/- the SEM of at least 3 different experiments. Differences were considered significant with a p < 0.05 and denoted by ”\*”.

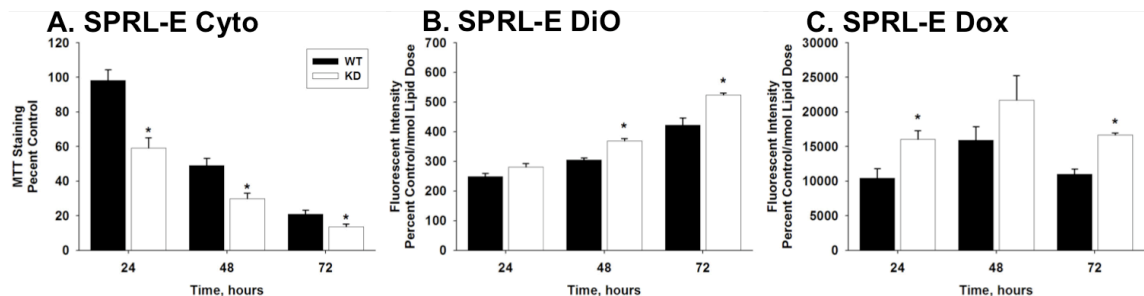


**Figure 5.5 Performance of SPRL-E in WT and KD PC-3 Cells.** To determine cytotoxicity, wild type or PLA<sub>2</sub>R knockdown PC-3 cells were seeded at 30,000 cells/ml and allowed to grow for 24 hours prior to treatment with SPRL-E containing doxorubicin for 24-72 hours. To determine uptake, wild type or PLA<sub>2</sub>R knockdown PC-3 cells were seeded at 7.0-8.0×10<sup>4</sup> cells/ml and allowed to grow for 24 hours prior to treatment with empty SPRL-E (not shown) or SPRL-E containing doxorubicin and DiO for 24-72 hours. Panel **A** shows results for MTT staining, Panel **B** shows uptake of DiO, and Panel **C** shows uptake of doxorubicin. Data are presented as the mean +/- the SEM of at least 3 different experiments. Differences were considered significant with a p < 0.05 and denoted by "\*".

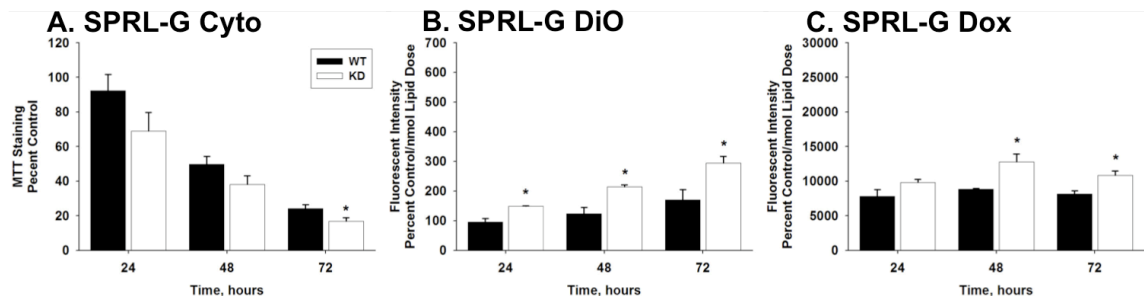


**Figure 5.6 Performance of SPRL-G in WT and KD PC-3 Cells.** To determine cytotoxicity, wild type or PLA<sub>2</sub>R knockdown PC-3 cells were seeded at 30,000 cells/ml and allowed to grow for 24 hours prior to treatment with SPRL-G containing doxorubicin for 24-72 hours. To determine uptake, wild type or PLA<sub>2</sub>R knockdown PC-3 cells were seeded at 7.0-8.0×10<sup>4</sup> cells/ml and allowed to grow for 24 hours prior to treatment with empty SPRL-G (not shown) or SPRL-G containing doxorubicin and DiO for 24-72 hours. Panel **A** shows results for MTT staining, Panel **B** shows uptake of DiO, and Panel **C** shows uptake of doxorubicin. Data are presented as the mean +/- the SEM of at least 3 different experiments. Differences were considered significant with a p < 0.05 and denoted by "\*\*".

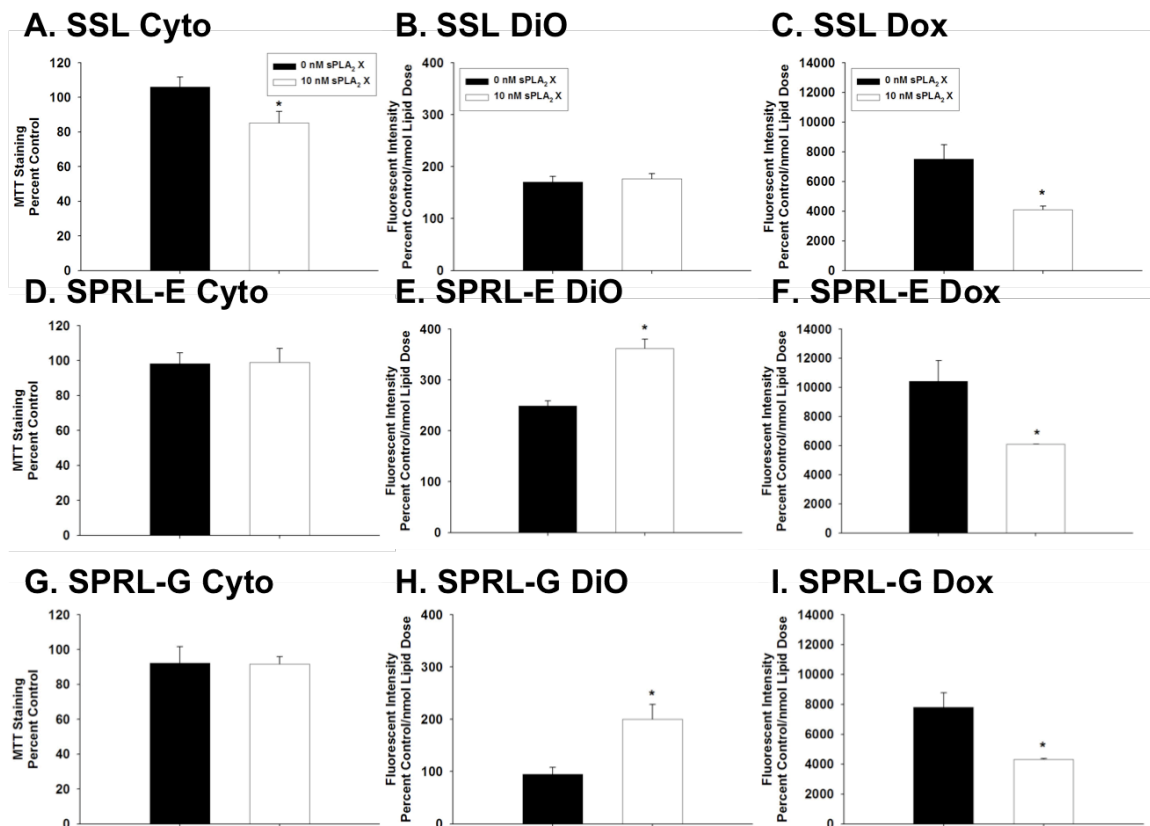


**Figure 5.7** Effect of Group X sPLA<sub>2</sub> on cytotoxicity and uptake of SSL and SPRL. PC-3 cells were seeded at 30,000 cells/ml for cytotoxicity studies or  $7.0\text{-}8.0 \times 10^4$  cells/ml for uptake studies and allowed to grow for 24 hours prior to treatment. Cells were either left alone before treating with liposomes (black bars) or pretreated with 10 nM Group X sPLA<sub>2</sub> for 30 minutes prior to treatment with liposomes (white bars). For cytotoxicity experiments cells were treated with liposomes that only contained doxorubicin while uptake experiments required liposomes that were labeled with DiO and loaded with doxorubicin. After 24 hours MTT staining (A, D and G), DiO fluorescence (B, E and H) and doxorubicin fluorescence (C, F and I) were determined. Panels A-C show the effect of Group X sPLA<sub>2</sub> on SSL. Panels D-F show the effect of Group X sPLA<sub>2</sub> on SPRL-E. Panels G-I show the effect of Group X sPLA<sub>2</sub> on SPRL-G. Data are presented as the mean  $\pm$  the SEM of at least 3 different experiments. Differences were considered significant with a  $p < 0.05$  and denoted by "\*".

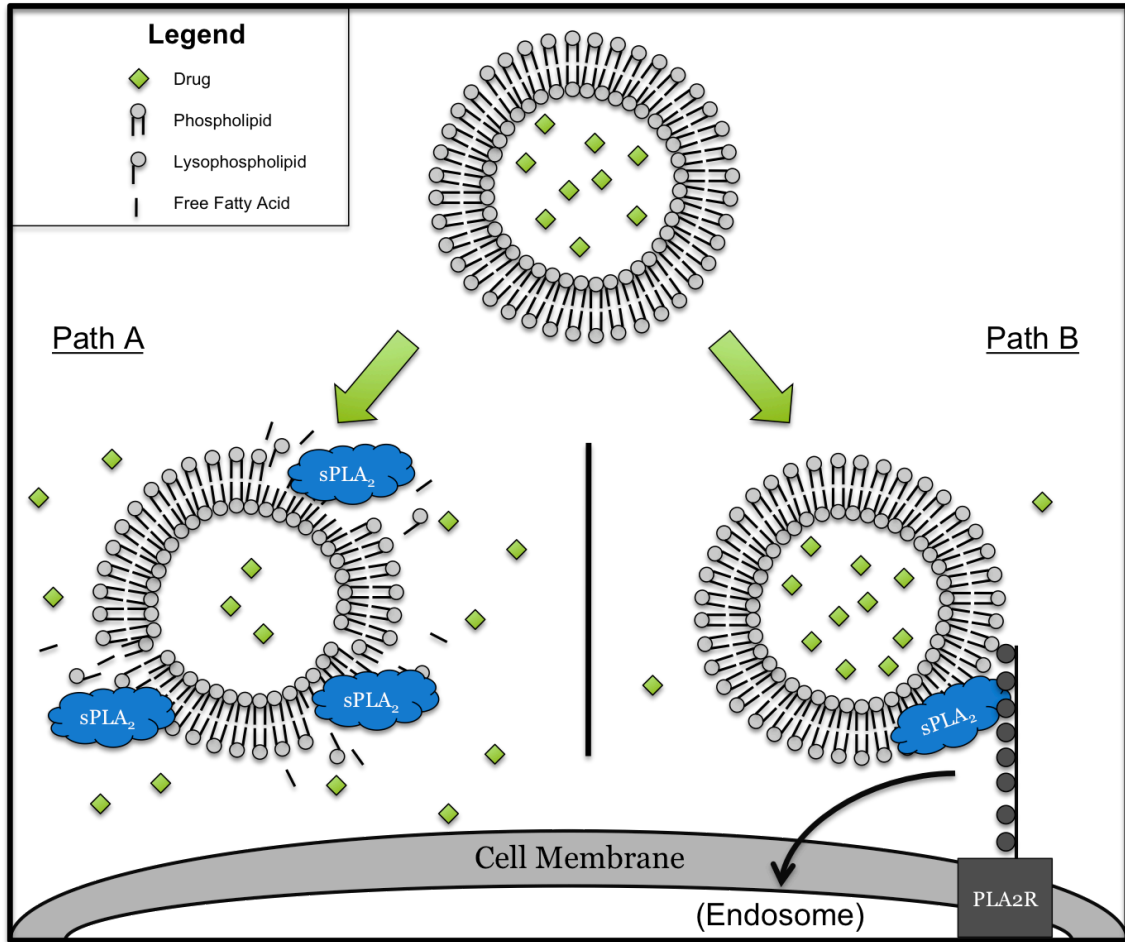


**Figure 5.8 Potential drug delivery pathways.** Our results suggest that SPRL are delivering drug across the cell membrane by more than one pathway. Path A illustrates one possibility, in which sPLA<sub>2</sub> hydrolyze the liposome membrane, allowing the encapsulated drug to leak out. Alternatively, in Path B, SPRL are interacting with sPLA<sub>2</sub>, which subsequently bind PLA<sub>2</sub>R to facilitate endocytosis.

## Discussion

This study showed that both PLA<sub>2</sub>R and Group X sPLA<sub>2</sub> modulate the behavior of SPRL in prostate cancer cells. We previously reported that sPLA<sub>2</sub> modulate the release of payload from SPRL (Zhu et al., 2011a; Zhu et al., 2011b), and that the uptake of liposomes is independent of enzymatic activity (manuscript in revision). This suggested the hypothesis that sPLA<sub>2</sub> can cause SPRL to release their payload in the extracellular space, or the media. This also suggested that liposomal uptake into cells may be facilitated by another mechanism independent of sPLA<sub>2</sub> activity. Data from the current study suggest that PLA<sub>2</sub>R may mediate one of these mechanisms and that the differential expression of sPLA<sub>2</sub> isoforms and PLA<sub>2</sub>R may mediate the differential behavior of SPRL.

The differential expression of sPLA<sub>2</sub> isoforms in different models of prostate cancer cells has been previously reported (Menschikowski et al., 2008). Data reported in this study show that similar levels of expression of Groups IIA and V in PC-3 and LNCaP cells, which were higher than that in DU-145 cells. In contrast, PC-3 cells expressed higher levels of Group X sPLA<sub>2</sub>, compared to both LNCaP and DU-145 cells. This is interesting because Group IIA and V sPLA<sub>2</sub> are generally associated with heparin-sulfate proteoglycans and are endocytosed via caveola-dependent processes. Additionally, both of these isoforms are low affinity substrates for human PLA<sub>2</sub>R (Hanasaki and Arita, 2002). In contrast, Group X sPLA<sub>2</sub> is hypothesized to be a higher affinity substrate for human PLA<sub>2</sub>R, but does not

participate in the heparin-sulfate proteoglycan shuttling pathway (Lambeau and Gelb, 2008b; Murakami et al., 2012) and is a high affinity PLA<sub>2</sub>R substrate in mice (Rouault et al., 2007; Yokota et al., 2001). Interestingly, PLA<sub>2</sub>R expression was also highest in PC-3 cells compared to LNCaP and DU-145 cells (data not shown). These data are the first to report the expression of PLA<sub>2</sub>R in any prostate cancer cell line. The significance of higher levels of PLA<sub>2</sub>R and Group X sPLA<sub>2</sub> in PC-3 cells, compared other cells lines is a topic of future studies.

Knockdown of PLA<sub>2</sub>R increased the uptake of both SPRL and doxorubicin in PC-3 cells, but had no effect on either SSL uptake or doxorubicin uptake (Figures 5.4-5.6). This finding further agrees with our recently published studies (Zhu et al., 2011a; Zhu et al., 2011b) (manuscript in revision) that SPRL behave differentially than SSL with regards to sPLA<sub>2</sub>, and extends these studies to PLA<sub>2</sub>R.

The increase in SPRL uptake in the cells where PLA<sub>2</sub>R expression is inhibited may result from the increases in the extracellular levels of sPLA<sub>2</sub>. The sPLA<sub>2</sub> most likely to be involved is Group X sPLA<sub>2</sub> as none of the other human sPLA<sub>2</sub> are believed to be substrates for this receptor (Hanasaki and Arita, 2002). Nevertheless, roles for other sPLA<sub>2</sub> isoforms cannot be ruled out. For example, liposomes may undergo facilitated uptake through interactions with Group IIA or V sPLA<sub>2</sub>, which are taken up via a caveola-dependent pathway (Han et al., 1999; Kim et al., 2001; Kim et al., 2002; Murakami et al., 2012), This may be a more efficient means of nanoparticle

uptake, but is otherwise masked by the high expression levels of Group X sPLA<sub>2</sub> and PLA<sub>2</sub>R.

Since PLA<sub>2</sub>R is essentially a negative regulator of sPLA<sub>2</sub> activity, as it internalizes these enzymes for recycling, the increased amounts of sPLA<sub>2</sub> that are likely found outside of the cell following knockdown may be mediating faster liposomal degradation. This increased degradation may result in dose dumping and a higher effective concentration of drug outside of the cell, leading to more rapid uptake. At this point, if the liposome has become completely degraded, a completely different process, like pinocytosis, may be responsible for the uptake of the lipid components and fluorescent markers. The exact mechanism is still under study.

PLA<sub>2</sub>R knockdown appeared to sensitize PC-3 cells to doxorubicin, based on decreases in MTT staining and alterations in cellular morphology. While cytotoxicity was generally higher in PLA<sub>2</sub>R knockdown cells, not all formulations responded similarly in terms of cytotoxicity. For example, the cytotoxicity of SRPL-G was only altered after 72 hours. Reasons for these differences are not known at this time. Regardless, these data are the first to demonstrate the knockdown of PLA<sub>2</sub>R increases the cytotoxicity of an anti-cancer agent delivered using nanoparticles.

PLA<sub>2</sub>R knockdown also altered the uptake of liposomes and drug, which is another novel finding of this work. Interestingly, increased liposome uptake was only seen using SPRL, and correlated to increased drug uptake. In contrast, PLA<sub>2</sub>R knockdown did not alter the uptake of SSL and only

slightly altered drug uptake after 72 hours. These data support the hypothesis that drug delivery induced by SPRL is partially mediated by PLA<sub>2</sub>R. These data also suggest that the incorporation of sPLA<sub>2</sub> sensitive lipids into SPRL may facilitate their dependence on PLA<sub>2</sub>R.

These data suggest that PLA<sub>2</sub>R may be viable target for inhibition of cancer cell growth, using nanoparticles, or small molecules. This hypothesis is supported by studies showing that PLA<sub>2</sub>R activity has been linked to several pathways involved in proliferation, migration, and senescence (Augert et al., 2009; Higashino et al., 1994; Kanemasa et al., 1992; Kinoshita et al., 1997; Kundu and Mukherjee, 1997).

Group X sPLA<sub>2</sub> is a putative, high-affinity substrate for PLA<sub>2</sub>R (Rouault et al., 2007). Addition of 10 nM Group X sPLA<sub>2</sub> did little to change the cytotoxicity of SPRL and caused a slight increase in cytotoxicity of SSL. In contrast, addition of Group X sPLA<sub>2</sub> significantly increased uptake of SPRL, but not SSL, and decreased the uptake of doxorubicin for all formulations. The increase in uptake of SPRL, but not SSL, in the presence of Group X sPLA<sub>2</sub> supports the hypothesis that SPRL are more sensitive to sPLA<sub>2</sub> than SSL. The non-effect of sPLA<sub>2</sub> on toxicity with our formulations suggests that the mechanisms mediating the uptake of liposomes and their cytotoxicity are independent.

The decrease in doxorubicin uptake seen with all formulations in the presence of Group X sPLA<sub>2</sub> is somewhat counter intuitive. It is possible that the abundance of sPLA<sub>2</sub> is causing a more rapid extracellular destabilization

of the particles and increased dumping of the drug prior to cellular uptake. This would suggest that uptake of intact particles that still contain some doxorubicin via sPLA<sub>2</sub>-facilitated uptake is a more efficient means of getting the drug across the membrane compared to simple diffusion of free doxorubicin after it has leaked out of the particle, as evidenced by decreased levels of doxorubicin fluorescence (Figure 5.7). In contrast, it is possible that the addition of Group X sPLA<sub>2</sub> results in uptake of intact liposomes, in which the fluorescence of doxorubicin is quenched due to the proximity of the drug molecules. This possibility seems unlikely though given that there was no increase in cytotoxicity.

Overall, our data show that PLA<sub>2</sub>R mediates the uptake of liposomes and the inclusion of sPLA<sub>2</sub> sensitive lipids alters the uptake and cytotoxicity of these liposomes. These data do not directly show that liposome uptake into cells is through PLA<sub>2</sub>R, but that its activity is somehow related to the behavior of SPRL. It is possible that PLA<sub>2</sub>R function to remove sPLA<sub>2</sub> from the media, and that knockdown of this receptor increases the concentration of these proteins in the extracellular space, or media in this case. This increase in enzyme would increase degradation and dose dumping (Figure 5.8). It is also possible that liposomes bind to sPLA<sub>2</sub> and that this complex binds to PLA<sub>2</sub>R and is transported into cells in endosomes (Figure 5.8). Further research is needed to support either of these hypothesis, but such work would have been premature had knockdown of PLA<sub>2</sub>R not altered liposome uptake or efficacy.

## CHAPTER 6

### SUMMARY

The overall hypothesis of this work was that PLA<sub>2</sub>, specifically iPLA<sub>2</sub> and sPLA<sub>2</sub>, can be utilized as therapeutic targets for the treatment of prostate cancer. Three specific aims were addressed in testing this hypothesis including (1) Evaluating the effectiveness of putative iPLA<sub>2</sub> inhibitors on cancer cell growth, (2) Demonstrating the ability of SPRL to treat multiple models of prostate cancer, and (3) Determining the molecular mechanisms that dictate the behavior of SPRL. First, conventional, small molecule inhibitors of iPLA<sub>2</sub> were screened for their potential to halt cancer cell growth by arresting the cell cycle. While several of the compounds tested had growth inhibiting IC<sub>50</sub>s in the low μM range and there was evidence of cell cycle arrest, there were issues with stability that will likely prevent any of the compounds tested from being clinically viable.

This above series of experiments did however demonstrate that compound based on iPLA<sub>2</sub> inhibitors have the potential to alter the cell cycle in proliferating cancer cells, and our results on the enantiomeric specificity of these inhibitors agrees with previously published findings. On the whole, these results suggest that iPLA<sub>2</sub> could be a putative drug target and future

generations of therapeutics may benefit from the structure-activity relationships that can be drawn from the screening performed in this study.

The second specific aim that was addressed dealt with the engineering and testing of liposomes designed to specifically interact with sPLA<sub>2</sub>. The resulting sPLA<sub>2</sub> responsive liposomes (SPRL) that we created were screened for activity in both *in vitro* and *in vivo* prostate cancer models. Two formulations stood out among all others in preliminary screens. These two formulations, deemed SPRL-E and SPRL-G for their inclusion of 10% phosphatidylethanolamine and phosphatidylglycerol, respectively, proved to be more adept than traditionally sterically stabilized liposomes at delivering drug inside the cell. Furthermore, both SPRL formulations achieved levels of cytotoxicity equivalent to free drug *in vitro*, which is unexpected for a delivery vector of this kind. Interestingly, neither cytotoxicity nor uptake of drug or particle was significantly altered by the pharmacological inhibition of sPLA<sub>2</sub>. Thus, while we had shown in the preliminary stages of screening that degradation of SPRL by sPLA<sub>2</sub> was sufficient to modulate drug release, it was not necessary for producing the observed *in vitro* effects. Finally, *in vivo* evaluation showed that at sub-toxic doses, SPRL-E was more effective than SSL at treating growing solid tumors, suggesting the potential clinical utility for this targeting scheme. This is particularly of note considering the marginal differences between SPRL and SSL, the latter of which has already been approved by the FDA for the treatment of multiple forms of cancer.

During evaluation of our SPRL, we found that although both SPRL-E and SPRL-G were more efficient at delivering drug inside the cell compared to SSL, there was a paradoxical disconnect between drug delivery and particle uptake. While SPRL-E rapidly crossed the membrane in all three prostate cancer lines tested and increased with time, uptake of SPRL-G was dramatically lower by comparison in spite of comparable levels of drug delivery. This suggested that there are multiple mechanisms at work in terms of dictating how SPRL behave.

This disconnect between uptake and efficacy of SPRL brought us to our third specific aim, which studied the molecular mechanisms responsible for the distinct profiles of SPRL-E and SPRL-G. To this end we assessed the relationship between Group X sPLA<sub>2</sub> and PLA<sub>2</sub>R at facilitating uptake. PLA<sub>2</sub>R is a C-type lectin receptor known to mediate the uptake and recycling of various sPLA<sub>2</sub> isoforms in different species. Group X sPLA<sub>2</sub> is a preferred substrate of PLA<sub>2</sub>R, and therefore we hypothesized that we may be achieving facilitated uptake of SPRL through transitive interactions between our liposomes, Group X sPLA<sub>2</sub> and PLA<sub>2</sub>R that result in the endocytosis of this complex. This type of uptake has not been previously described by other groups and would represent one possible alternative to process of sPLA<sub>2</sub>-mediated degradation of the liposomes that we had originally envisioned. The differences in these two pathways are illustrated in Figure 5.8.

To test the hypothesis that PLA<sub>2</sub>R mediates liposome uptake and efficacy we knocked down the expression of PLA<sub>2</sub>R and found that this

increased levels of uptake of both SPRL formulations and drug and increased cytotoxicity. While increases in cytotoxicity were also seen with SSL, these increases were not correlated with increases in uptake of the nanoparticles or drug. This suggests that the addition of sPLA<sub>2</sub> sensitive lipids allow SPRL to more efficiently interact with this pathway.

Although our data do not definitively prove that SPRL are being taken up through a PLA<sub>2</sub>R-facilitated mechanism, this is still a possible route of endocytosis, and at the very least, our data suggest that PLA<sub>2</sub>R is in some ways responsible for modulating the behavior of SPRL. Additionally, knocking down this receptor likely increased the extracellular concentration of sPLA<sub>2</sub>, as the PLA<sub>2</sub>R recycling pathway would no longer be operating optimally. This increase in extracellular enzyme might account for some of the changes in behavior due to increased lipolytic activity in the media, which would enhance degradation and dose dumping.

The addition of Group X sPLA<sub>2</sub> also appears to be important in mediating the behavior of SPRL. While the increased concentrations of Group X sPLA<sub>2</sub> had little effect on the cytotoxicity of SPRL, exogenous Group X sPLA<sub>2</sub> increased DiO fluorescence and decreased doxorubicin fluorescence. There are at least two alternative explanations for this. First, additional sPLA<sub>2</sub> may enhance degradation of liposomes in the extracellular space, releasing the drug. The release of drug would allow it to cross into the cell through diffusion while the degraded constituents of the liposome may be taken up by pinocytosis or another endocytotic mechanism, resulting in

increased intercellular fluorescence. Alternatively, the increase in Group X sPLA<sub>2</sub> may allow for more PLA<sub>2</sub>R-facilitated uptake, as Group X is a putative high-affinity substrate for the receptor and the only isoform expressed in this cell type that is capable of mediating this pathway.

Overall, the data presented herein suggest that PLA<sub>2</sub>, specifically iPLA<sub>2</sub> and sPLA<sub>2</sub>, may be used as drug targets for the treatment of prostate cancer. Inhibition of iPLA<sub>2</sub> is sufficient for slowing of tumor growth and altering cell cycle. Additionally, sPLA<sub>2</sub> overexpression can be utilized as a molecular trigger for the targeting on tumor-specific nanoparticles. This targeting can be achieved through complex interactions between sPLA<sub>2</sub> and PLA<sub>2</sub>R or independent of this receptor, but in either case enzyme activity is not required. More research will be required to optimize this targeting scheme and elucidate the exact molecular mechanism underlying their efficacy.

## REFERENCES

1995. DOXIL approved by FDA. *AIDS Patient Care* 9, 306.
- Abern, M. R., Dude, A. M., Tsivian, M., Coogan, C. L., 2012. The characteristics of bladder cancer after radiotherapy for prostate cancer. *Urol Oncol*.
- Al-Mamgani, A., Lebesque, J. V., Heemsbergen, W. D., Tans, L., Kirkels, W. J., Levendag, P. C., Incrocci, L., 2009. Controversies in the treatment of high-risk prostate cancer--what is the optimal combination of hormonal therapy and radiotherapy: a review of literature. *Prostate* 70, 701-709.
- Aljuffali, I. A., Mock, J. N., Costyn, L. J., Nguyen, H., Nagy, T., Cummings, B. S., Arnold, R. D., 2011. Enhanced antitumor activity of low-dose continuous administration schedules of topotecan in prostate cancer. *Cancer Biology & Therapy* 12, 407-420.
- Andresen, T. L., Jensen, S. S., Kaasgaard, T., Jorgensen, K., 2005. Triggered activation and release of liposomal prodrugs and drugs in cancer tissue by secretory phospholipase A2. *Curr Drug Deliv* 2, 353-362.
- Arnold, R. D., Mager, D. E., Slack, J. E., Straubinger, R. M., 2005. Effect of repetitive administration of Doxorubicin-containing liposomes on plasma pharmacokinetics and drug biodistribution in a rat brain tumor model. *Clin Cancer Res* 11, 8856-8865.
- Atsumi, G., Murakami, M., Kojima, K., Hadano, A., Tajima, M., Kudo, I., 2000. Distinct roles of two intracellular phospholipase A2s in fatty acid release in the cell death pathway. Proteolytic fragment of type IVA cytosolic phospholipase A2 $\alpha$  inhibits stimulus-induced arachidonate release, whereas that of type VI Ca<sup>2+</sup>-independent phospholipase A2 augments spontaneous fatty acid release. *J Biol Chem* 275, 18248-18258.
- Augert, A., Payre, C., de Launoit, Y., Gil, J., Lambeau, G., Bernard, D., 2009. The M-type receptor PLA2R regulates senescence through the p53 pathway. *EMBO Rep* 10, 271-277.

- Ayilavarapu, S., Kantarci, A., Fredman, G., Turkoglu, O., Omori, K., Liu, H., Iwata, T., Yagi, M., Hasturk, H., Van Dyke, T. E., 2010. Diabetes-induced oxidative stress is mediated by Ca<sup>2+</sup>-independent phospholipase A2 in neutrophils. *J Immunol* 184, 1507-1515.
- Bakovic, M., Fullerton, M. D., Michel, V., 2007. Metabolic and molecular aspects of ethanolamine phospholipid biosynthesis: the role of CTP:phosphoethanolamine cytidyltransferase (Pcyt2). *Biochem Cell Biol* 85, 283-300.
- Balboa, M. A., Perez, R., Balsinde, J., 2008. Calcium-independent phospholipase A2 mediates proliferation of human promonocytic U937 cells. *FEBS J* 275, 1915-1924.
- Balsinde, J., Bianco, I. D., Ackermann, E. J., Conde-Frieboes, K., Dennis, E. A., 1995. Inhibition of calcium-independent phospholipase A2 prevents arachidonic acid incorporation and phospholipid remodeling in P388D1 macrophages. *Proc Natl Acad Sci U S A* 92, 8527-8531.
- Balsinde, J., Dennis, E. A., 1997. Function and inhibition of intracellular calcium-independent phospholipase A2. *J Biol Chem* 272, 16069-16072.
- Bao, S., Li, Y., Lei, X., Wohltmann, M., Jin, W., Bohrer, A., Semenkovich, C. F., Ramanadham, S., Tabas, I., Turk, J., 2007. Attenuated free cholesterol loading-induced apoptosis but preserved phospholipid composition of peritoneal macrophages from mice that do not express group VIA phospholipase A2. *J Biol Chem* 282, 27100-27114.
- Barenholz, Y., 2001. Liposome application: problems and prospects. *Current Opinion in Colloid & Interface Science* 6, 66-77.
- Bartlett, G. R., 1959. Phosphorus assay in column chromatography. *J Biol Chem* 234, 466-468.
- Bingham, C. O., 3rd, Murakami, M., Fujishima, H., Hunt, J. E., Austen, K. F., Arm, J. P., 1996. A heparin-sensitive phospholipase A2 and prostaglandin endoperoxide synthase-2 are functionally linked in the delayed phase of prostaglandin D2 generation in mouse bone marrow-derived mast cells. *J Biol Chem* 271, 25936-25944.
- Bostrom, M. A., Boyanovsky, B. B., Jordan, C. T., Wadsworth, M. P., Taatjes, D. J., de Beer, F. C., Webb, N. R., 2007. Group v secretory phospholipase A2 promotes atherosclerosis: evidence from genetically altered mice. *Arterioscler Thromb Vasc Biol* 27, 600-606.
- Boukaram, C., Hannoun-Levi, J. M., 2010. Management of prostate cancer recurrence after definitive radiation therapy. *Cancer Treat Rev* 36, 91-100.

- Chakravarty, P. K., Krafft, G. A., Katzenellenbogen, J. A., 1982. Haloenol lactones: enzyme-activated irreversible inactivators for serine proteases. Inactivation of alpha-chymotrypsin. *J Biol Chem* 257, 610-612.
- Crawford, E. D., Flaig, T. W., 2012. Optimizing outcomes of advanced prostate cancer: drug sequencing and novel therapeutic approaches. *Oncology (Williston Park)* 26, 70-77.
- Crowl, R. M., Stoller, T. J., Conroy, R. R., Stoner, C. R., 1991. Induction of phospholipase A2 gene expression in human hepatoma cells by mediators of the acute phase response. *J Biol Chem* 266, 2647-2651.
- Cummings, B. S., McHowat, J., Schnellmann, R. G., 2000. Phospholipase A(2)s in cell injury and death. *J Pharmacol Exp Ther* 294, 793-799.
- Daniels, S. B., Cooney, E., Sofia, M. J., Chakravarty, P. K., Katzenellenbogen, J. A., 1983. Haloenol lactones. Potent enzyme-activated irreversible inhibitors for alpha-chymotrypsin. *J Biol Chem* 258, 15046-15053.
- Daniels, S. B., Katzenellenbogen, J. A., 1986. Halo enol lactones: studies on the mechanism of inactivation of alpha-chymotrypsin. *Biochemistry* 25, 1436-1444.
- Dennis, E. A., Cao, J., Hsu, Y. H., Magrioti, V., Kokotos, G., 2011. Phospholipase A2 enzymes: physical structure, biological function, disease implication, chemical inhibition, and therapeutic intervention. *Chem Rev* 111, 6130-6185.
- Dong, Q., Patel, M., Scott, K. F., Graham, G. G., Russell, P. J., Sved, P., 2006. Oncogenic action of phospholipase A2 in prostate cancer. *Cancer Lett* 240, 9-16.
- Dong, Z., Liu, Y., Scott, K. F., Levin, L., Gaitonde, K., Bracken, R. B., Burke, B., Zhai, Q. J., Wang, J., Oleksowicz, L., Lu, S., 2010. Secretory phospholipase A2-IIa is involved in prostate cancer progression and may potentially serve as a biomarker for prostate cancer. *Carcinogenesis* 31, 1948-1955.
- Drummond, M. F., Mason, A. R., 2007. European perspective on the costs and cost-effectiveness of cancer therapies. *J Clin Oncol* 25, 191-195.
- Duncan, R., Gaspar, R., 2011. Nanomedicine(s) under the microscope. *Mol Pharm* 8, 2101-2141.
- Fan, R., Vermesh, O., Srivastava, A., Yen, B. K., Qin, L., Ahmad, H., Kwong, G. A., Liu, C. C., Gould, J., Hood, L., Heath, J. R., 2008. Integrated barcode chips for rapid, multiplexed analysis of proteins in microliter quantities of blood. *Nat Biotechnol* 26, 1373-1378.

- Farooqui, A. A., Horrocks, L. A., 2006. Phospholipase A2-generated lipid mediators in the brain: the good, the bad, and the ugly. *Neuroscientist* 12, 245-260.
- Farooqui, A. A., Ong, W. Y., Horrocks, L. A., 2006. Inhibitors of brain phospholipase A2 activity: their neuropharmacological effects and therapeutic importance for the treatment of neurologic disorders. *Pharmacol Rev* 58, 591-620.
- Ferlay, J., Autier, P., Boniol, M., Heanue, M., Colombet, M., Boyle, P., 2007. Estimates of the cancer incidence and mortality in Europe in 2006. *Ann Oncol* 18, 581-592.
- Fraser, H., Hislop, C., Christie, R. M., Rick, H. L., Reidy, C. A., Chouinard, M. L., Eacho, P. I., Gould, K. E., Trias, J., 2009. Varespladib (A-002), a secretory phospholipase A2 inhibitor, reduces atherosclerosis and aneurysm formation in ApoE<sup>-/-</sup> mice. *J Cardiovasc Pharmacol* 53, 60-65.
- Galsky, M. D., Small, A. C., Tsao, C. K., Oh, W. K., 2012. Clinical development of novel therapeutics for castration-resistant prostate cancer: Historic Challenges and Recent Successes. *CA Cancer J Clin*.
- Gelb, M. H., Valentin, E., Ghomashchi, F., Lazdunski, M., Lambeau, G., 2000. Cloning and recombinant expression of a structurally novel human secreted phospholipase A2. *J Biol Chem* 275, 39823-39826.
- Geran, R. I., Schumacher, Abbott, B. J., Greenberg, Macdonald, 1972. Protocols for Screening Chemical Agents and Natural-Products against Animal Tumors and Other Biological-Systems. *Cancer Chemotherapy Reports Part 3* 3, 1-&.
- Graff, J. R., Konicek, B. W., Deddens, J. A., Chedid, M., Hurst, B. M., Colligan, B., Neubauer, B. L., Carter, H. W., Carter, J. H., 2001. Expression of group IIa secretory phospholipase A2 increases with prostate tumor grade. *Clin Cancer Res* 7, 3857-3861.
- Han, S. K., Kim, K. P., Koduri, R., Bittova, L., Munoz, N. M., Leff, A. R., Wilton, D. C., Gelb, M. H., Cho, W., 1999. Roles of Trp31 in high membrane binding and proinflammatory activity of human group V phospholipase A2. *J Biol Chem* 274, 11881-11888.
- Hanasaki, K., Arita, H., 1996. Structure and function of phospholipase A2 receptor. *Adv Exp Med Biol* 416, 315-319.
- Hanasaki, K., Arita, H., 2002. Phospholipase A2 receptor: a regulator of biological functions of secretory phospholipase A2. *Prostaglandins Other Lipid Mediat* 68-69, 71-82.

- Hanasaki, K., Ono, T., Saiga, A., Morioka, Y., Ikeda, M., Kawamoto, K., Higashino, K., Nakano, K., Yamada, K., Ishizaki, J., Arita, H., 1999. Purified group X secretory phospholipase A(2) induced prominent release of arachidonic acid from human myeloid leukemia cells. *J Biol Chem* 274, 34203-34211.
- Haran, G., Cohen, R., Bar, L. K., Barenholz, Y., 1993. Transmembrane ammonium sulfate gradients in liposomes produce efficient and stable entrapment of amphipathic weak bases. *Biochim Biophys Acta* 1151, 201-215.
- Harisinghani, M. G., Barentsz, J., Hahn, P. F., Deserno, W. M., Tabatabaei, S., van de Kaa, C. H., de la Rosette, J., Weissleder, R., 2003. Noninvasive detection of clinically occult lymph-node metastases in prostate cancer. *N Engl J Med* 348, 2491-2499.
- Herbert, S. P., Walker, J. H., 2006. Group VIA calcium-independent phospholipase A2 mediates endothelial cell S phase progression. *J Biol Chem* 281, 35709-35716.
- Higashino, K., Ishizaki, J., Kishino, J., Ohara, O., Arita, H., 1994. Structural comparison of phospholipase-A2-binding regions in phospholipase-A2 receptors from various mammals. *Eur J Biochem* 225, 375-382.
- Hite, R. D., Seeds, M. C., Jacinto, R. B., Balasubramanian, R., Waite, M., Bass, D., 1998. Hydrolysis of surfactant-associated phosphatidylcholine by mammalian secretory phospholipases A2. *Am J Physiol* 275, L740-747.
- Ho, I. C., Arm, J. P., Bingham, C. O., 3rd, Choi, A., Austen, K. F., Glimcher, L. H., 2001. A novel group of phospholipase A2s preferentially expressed in type 2 helper T cells. *J Biol Chem* 276, 18321-18326.
- Hoefl, B., Linseisen, J., Beckmann, L., Muller-Decker, K., Canzian, F., Husing, A., Kaaks, R., Vogel, U., Jakobsen, M. U., Overvad, K., Hansen, R. D., Knuppel, S., Boeing, H., Trichopoulou, A., Koumantaki, Y., Trichopoulos, D., Berrino, F., Palli, D., Panico, S., Tumino, R., Bueno-de-Mesquita, H. B., van Duijnhoven, F. J., van Gils, C. H., Peeters, P. H., Dumeaux, V., Lund, E., Huerta Castano, J. M., Munoz, X., Rodriguez, L., Barricarte, A., Manjer, J., Jirstrom, K., Van Guelpen, B., Hallmans, G., Spencer, E. A., Crowe, F. L., Khaw, K. T., Wareham, N., Morois, S., Boutron-Ruault, M. C., Clavel-Chapelon, F., Chajes, V., Jenab, M., Boffetta, P., Vineis, P., Mouw, T., Norat, T., Riboli, E., Nieters, A., 2010. Polymorphisms in fatty-acid-metabolism-related genes are associated with colorectal cancer risk. *Carcinogenesis* 31, 466-472.
- Hoozemans, J. J., Veerhuis, R., Janssen, I., Rozemuller, A. J., Eikelenboom, P., 2001. Interleukin-1beta induced cyclooxygenase 2 expression and

prostaglandin E2 secretion by human neuroblastoma cells: implications for Alzheimer's disease. *Exp Gerontol* 36, 559-570.

Hsu, Y. H., Burke, J. E., Li, S., Woods, V. L., Jr., Dennis, E. A., 2009. Localizing the membrane binding region of Group VIA Ca<sup>2+</sup>-independent phospholipase A2 using peptide amide hydrogen/deuterium exchange mass spectrometry. *J Biol Chem* 284, 23652-23661.

Hu, C. M., Zhang, L., 2012. Nanoparticle-based combination therapy toward overcoming drug resistance in cancer. *Biochem Pharmacol* 83, 1104-1111.

Huang, Y., He, S., Li, J. Z., Seo, Y. K., Osborne, T. F., Cohen, J. C., Hobbs, H. H., 2010. A feed-forward loop amplifies nutritional regulation of PNPLA3. *Proc Natl Acad Sci U S A* 107, 7892-7897.

Jemal, A., Siegel, R., Xu, J., Ward, E., 2010. Cancer statistics, 2010. *CA Cancer J Clin* 60, 277-300.

Jenkins, C. M., Han, X., Mancuso, D. J., Gross, R. W., 2002. Identification of calcium-independent phospholipase A2 (iPLA2) beta, and not iPLA2gamma, as the mediator of arginine vasopressin-induced arachidonic acid release in A-10 smooth muscle cells. Enantioselective mechanism-based discrimination of mammalian iPLA2s. *J Biol Chem* 277, 32807-32814.

Jiang, J., Neubauer, B. L., Graff, J. R., Chedid, M., Thomas, J. E., Roehm, N. W., Zhang, S., Eckert, G. J., Koch, M. O., Eble, J. N., Cheng, L., 2002. Expression of group IIA secretory phospholipase A2 is elevated in prostatic intraepithelial neoplasia and adenocarcinoma. *Am J Pathol* 160, 667-671.

Kallajoki, M., Alanen, K. A., Nevalainen, M., Nevalainen, T. J., 1998. Group II phospholipase A2 in human male reproductive organs and genital tumors. *Prostate* 35, 263-272.

Kamps, J. A., Morselt, H. W., Swart, P. J., Meijer, D. K., Scherphof, G. L., 1997. Massive targeting of liposomes, surface-modified with anionized albumins, to hepatic endothelial cells. *Proc Natl Acad Sci U S A* 94, 11681-11685.

Kanemasa, T., Hanasaki, K., Arita, H., 1992. Migration of vascular smooth muscle cells by phospholipase A2 via specific binding sites. *Biochim Biophys Acta* 1125, 210-214.

Kienesberger, P. C., Oberer, M., Lass, A., Zechner, R., 2009. Mammalian patatin domain containing proteins: a family with diverse lipolytic activities involved in multiple biological functions. *J Lipid Res* 50 Suppl, S63-68.

Kim, K. P., Rafter, J. D., Bittova, L., Han, S. K., Snitko, Y., Munoz, N. M., Leff, A. R., Cho, W., 2001. Mechanism of human group V phospholipase A2

(PLA2)-induced leukotriene biosynthesis in human neutrophils. A potential role of heparan sulfate binding in PLA2 internalization and degradation. *J Biol Chem* 276, 11126-11134.

Kim, Y. J., Kim, K. P., Rhee, H. J., Das, S., Rafter, J. D., Oh, Y. S., Cho, W., 2002. Internalized group V secretory phospholipase A2 acts on the perinuclear membranes. *J Biol Chem* 277, 9358-9365.

Kinoshita, E., Handa, N., Hanada, K., Kajiyama, G., Sugiyama, M., 1997. Activation of MAP kinase cascade induced by human pancreatic phospholipase A2 in a human pancreatic cancer cell line. *FEBS Lett* 407, 343-346.

Kinsey, G. R., Cummings, B. S., Beckett, C. S., Saavedra, G., Zhang, W., McHowat, J., Schnellmann, R. G., 2005. Identification and distribution of endoplasmic reticulum iPLA2. *Biochem Biophys Res Commun* 327, 287-293.

Kiyohara, H., Egami, H., Kako, H., Shibata, Y., Murata, K., Ohshima, S., Sei, K., Suko, S., Kurano, R., Ogawa, M., 1993. Immunohistochemical localization of group II phospholipase A2 in human pancreatic carcinomas. *Int J Pancreatol* 13, 49-57.

Kohli, M., Tindall, D. J., 2010. New developments in the medical management of prostate cancer. *Mayo Clin Proc* 85, 77-86.

Kudo, I., Murakami, M., Hara, S., Inoue, K., 1993. Mammalian non-pancreatic phospholipases A2. *Biochim Biophys Acta* 1170, 217-231.

Kundu, G. C., Mukherjee, A. B., 1997. Evidence that porcine pancreatic phospholipase A2 via its high affinity receptor stimulates extracellular matrix invasion by normal and cancer cells. *J Biol Chem* 272, 2346-2353.

Kuopio, T., Ekfors, T. O., Nikkanen, V., Nevalainen, T. J., 1995. Acinar cell carcinoma of the pancreas. Report of three cases. *APMIS* 103, 69-78.

Kupert, E., Anderson, M., Liu, Y., Succop, P., Levin, L., Wang, J., Wikenheiser-brokamp, K., Chen, P., Pinney, S. M., Macdonald, T., Dong, Z., Starnes, S., Lu, S., 2011. Plasma secretory phospholipase A2-IIa as a potential biomarker for lung cancer in patients with solitary pulmonary nodules. *BMC Cancer* 11, 513.

Lake, A. C., Sun, Y., Li, J. L., Kim, J. E., Johnson, J. W., Li, D., Revett, T., Shih, H. H., Liu, W., Paulsen, J. E., Gimeno, R. E., 2005. Expression, regulation, and triglyceride hydrolase activity of Adiponutrin family members. *J Lipid Res* 46, 2477-2487.

Lambeau, G., Gelb, M. H., 2008a. Biochemistry and physiology of mammalian secreted phospholipases A2. *Annu Rev Biochem* 77, 495-520.

- Lambeau, G., Lazdunski, M., 1999. Receptors for a growing family of secreted phospholipases A2. *Trends Pharmacol Sci* 20, 162-170.
- Lambeau, G. r., Gelb, M. H., 2008b. Biochemistry and Physiology of Mammalian Secreted Phospholipases A2. *Annual Review of Biochemistry* 77, 495-520.
- Langer, R., 1998. Drug delivery and targeting. *Nature* 392, 5-10.
- Leistad, L., Feuerherm, A. J., Ostensen, M., Faxvaag, A., Johansen, B., 2004. Presence of secretory group IIa and V phospholipase A2 and cytosolic group IValpha phospholipase A2 in chondrocytes from patients with rheumatoid arthritis. *Clin Chem Lab Med* 42, 602-610.
- Leung, S. Y., Chen, X., Chu, K. M., Yuen, S. T., Mathy, J., Ji, J., Chan, A. S., Li, R., Law, S., Troyanskaya, O. G., Tu, I. P., Wong, J., So, S., Botstein, D., Brown, P. O., 2002. Phospholipase A2 group IIA expression in gastric adenocarcinoma is associated with prolonged survival and less frequent metastasis. *Proc Natl Acad Sci U S A* 99, 16203-16208.
- Li, H., Zhao, Z., Wei, G., Yan, L., Wang, D., Zhang, H., Sandusky, G. E., Turk, J., Xu, Y., 2010. Group VIA phospholipase A2 in both host and tumor cells is involved in ovarian cancer development. *FASEB J* 24, 4103-4116.
- Liu, Y. M., Moldes, M., Bastard, J. P., Bruckert, E., Viguerie, N., Hainque, B., Basdevant, A., Langin, D., Pairault, J., Clement, K., 2004. Adiponutrin: A new gene regulated by energy balance in human adipose tissue. *J Clin Endocrinol Metab* 89, 2684-2689.
- Ma, Z., Ramanadham, S., Hu, Z., Turk, J., 1998. Cloning and expression of a group IV cytosolic Ca<sup>2+</sup>-dependent phospholipase A2 from rat pancreatic islets. Comparison of the expressed activity with that of an islet group VI cytosolic Ca<sup>2+</sup>-independent phospholipase A2. *Biochim Biophys Acta* 1391, 384-400.
- Ma, Z., Wang, X., Nowatzke, W., Ramanadham, S., Turk, J., 1999. Human pancreatic islets express mRNA species encoding two distinct catalytically active isoforms of group VI phospholipase A2 (iPLA2) that arise from an exon-skipping mechanism of alternative splicing of the transcript from the iPLA2 gene on chromosome 22q13.1. *J Biol Chem* 274, 9607-9616.
- Maeda, H., Wu, J., Sawa, T., Matsumura, Y., Hori, K., 2000. Tumor vascular permeability and the EPR effect in macromolecular therapeutics: a review. *J Control Release* 65, 271-284.
- Malik, I., Turk, J., Mancuso, D. J., Montier, L., Wohltmann, M., Wozniak, D. F., Schmidt, R. E., Gross, R. W., Kotzbauer, P. T., 2008. Disrupted membrane homeostasis and accumulation of ubiquitinated proteins in a

- mouse model of infantile neuroaxonal dystrophy caused by PLA2G6 mutations. *Am J Pathol* 172, 406-416.
- Mannello, F., Qin, W., Zhu, W., Fabbri, L., Tonti, G. A., Sauter, E. R., 2008. Nipple aspirate fluids from women with breast cancer contain increased levels of group IIA secretory phospholipase A2. *Breast Cancer Res Treat* 111, 209-218.
- McHowat, J., Creer, M. H., 2004. Catalytic features, regulation and function of myocardial phospholipase A2. *Curr Med Chem Cardiovasc Hematol Agents* 2, 209-218.
- Menschikowski, M., Hagelgans, A., Gussakovsky, E., Kostka, H., Paley, E. L., Siegert, G., 2008. Differential expression of secretory phospholipases A2 in normal and malignant prostate cell lines: regulation by cytokines, cell signaling pathways, and epigenetic mechanisms. *Neoplasia* 10, 279-286.
- Miele, E., Spinelli, G. P., Tomao, F., Tomao, S., 2009. Albumin-bound formulation of paclitaxel (Abraxane ABI-007) in the treatment of breast cancer. *Int J Nanomedicine* 4, 99-105.
- Mishra, R. S., Carnevale, K. A., Cathcart, M. K., 2008. iPLA2beta: front and center in human monocyte chemotaxis to MCP-1. *J Exp Med* 205, 347-359.
- Morgan, N. V., Westaway, S. K., Morton, J. E., Gregory, A., Gissen, P., Sonek, S., Cangul, H., Coryell, J., Canham, N., Nardocci, N., Zorzi, G., Pasha, S., Rodriguez, D., Desguerre, I., Mubaidin, A., Bertini, E., Trembath, R. C., Simonati, A., Schanen, C., Johnson, C. A., Levinson, B., Woods, C. G., Wilmot, B., Kramer, P., Gitschier, J., Maher, E. R., Hayflick, S. J., 2006. PLA2G6, encoding a phospholipase A2, is mutated in neurodegenerative disorders with high brain iron. *Nat Genet* 38, 752-754.
- Morioka, Y., Saiga, A., Yokota, Y., Suzuki, N., Ikeda, M., Ono, T., Nakano, K., Fujii, N., Ishizaki, J., Arita, H., Hanasaki, K., 2000. Mouse group X secretory phospholipase A2 induces a potent release of arachidonic acid from spleen cells and acts as a ligand for the phospholipase A2 receptor. *Arch Biochem Biophys* 381, 31-42.
- Munoz, N. M., Meliton, A. Y., Lambertino, A., Boetticher, E., Learoyd, J., Sultan, F., Zhu, X., Cho, W., Leff, A. R., 2006. Transcellular secretion of group V phospholipase A2 from epithelium induces beta 2-integrin-mediated adhesion and synthesis of leukotriene C4 in eosinophils. *J Immunol* 177, 574-582.
- Murakami, M., Kambe, T., Shimbara, S., Yamamoto, S., Kuwata, H., Kudo, I., 1999. Functional association of type IIA secretory phospholipase A(2) with the glycosylphosphatidylinositol-anchored heparan sulfate proteoglycan in the

cyclooxygenase-2-mediated delayed prostanoid-biosynthetic pathway. *J Biol Chem* 274, 29927-29936.

Murakami, M., Kudo, I., Inoue, K., 1989. In vivo release and clearance of rat platelet phospholipase A2. *Biochim Biophys Acta* 1005, 270-276.

Murakami, M., Masuda, S., Shimbara, S., Ishikawa, Y., Ishii, T., Kudo, I., 2005. Cellular distribution, post-translational modification, and tumorigenic potential of human group III secreted phospholipase A(2). *J Biol Chem* 280, 24987-24998.

Murakami, M., Shimbara, S., Kambe, T., Kuwata, H., Winstead, M. V., Tischfield, J. A., Kudo, I., 1998. The functions of five distinct mammalian phospholipase A2S in regulating arachidonic acid release. Type IIa and type V secretory phospholipase A2S are functionally redundant and act in concert with cytosolic phospholipase A2. *J Biol Chem* 273, 14411-14423.

Murakami, M., Taketomi, Y., Miki, Y., Sato, H., Hirabayashi, T., Yamamoto, K., 2012. Recent progress in phospholipase A research: from cells to animals to humans. *Prog Lipid Res* 50, 152-192.

Nakanishi, M., Montrose, D. C., Clark, P., Nambiar, P. R., Belinsky, G. S., Claffey, K. P., Xu, D., Rosenberg, D. W., 2008. Genetic deletion of mPGES-1 suppresses intestinal tumorigenesis. *Cancer Res* 68, 3251-3259.

Nakano, T., Arita, H., 1990. Enhanced expression of group II phospholipase A2 gene in the tissues of endotoxin shock rats and its suppression by glucocorticoid. *FEBS Lett* 273, 23-26.

Nevalainen, T. J., Graham, G. G., Scott, K. F., 2008. Antibacterial actions of secreted phospholipases A2. Review. *Biochim Biophys Acta* 1781, 1-9.

Ohtsuki, M., Taketomi, Y., Arata, S., Masuda, S., Ishikawa, Y., Ishii, T., Takanezawa, Y., Aoki, J., Arai, H., Yamamoto, K., Kudo, I., Murakami, M., 2006. Transgenic expression of group V, but not group X, secreted phospholipase A2 in mice leads to neonatal lethality because of lung dysfunction. *J Biol Chem* 281, 36420-36433.

Oka, S., Arita, H., 1991. Inflammatory factors stimulate expression of group II phospholipase A2 in rat cultured astrocytes. Two distinct pathways of the gene expression. *J Biol Chem* 266, 9956-9960.

Oka, Y., Ogawa, M., Matsuda, Y., Murata, A., Nishijima, J., Miyauchi, K., Uda, K., Yasuda, T., Mori, T., 1990. Serum immunoreactive pancreatic phospholipase A2 in patients with various malignant tumors. *Enzyme* 43, 80-88.

Ow, K. T., Mameghan, H., Lochhead, A., Fisher, R., Yang, J. L., Mameghan, J., Andersen, S., Russell, P. J., The prognostic significance of tumor-associated markers p53, HER-2/neu, c-myc, v-H-ras, PCNA and EGFr of local and distant recurrence in localized human prostatic adenocarcinoma. *Urologic Oncology: Seminars and Original Investigations* 1, 144-152.

Pan, Y. H., Yu, B. Z., Singer, A. G., Ghomashchi, F., Lambeau, G., Gelb, M. H., Jain, M. K., Bahnson, B. J., 2002. Crystal structure of human group X secreted phospholipase A2. Electrostatically neutral interfacial surface targets zwitterionic membranes. *J Biol Chem* 277, 29086-29093.

Papahadjopoulos, D., Allen, T. M., Gabizon, A., Mayhew, E., Matthay, K., Huang, S. K., Lee, K. D., Woodle, M. C., Lasic, D. D., Redemann, C., Martin, F. J., 1991. Sterically Stabilized Liposomes - Improvements in Pharmacokinetics and Antitumor Therapeutic Efficacy. *Proceedings of the National Academy of Sciences of the United States of America* 88, 11460-11464.

Perez, R., Balboa, M. A., Balsinde, J., 2006. Involvement of group VIA calcium-independent phospholipase A2 in macrophage engulfment of hydrogen peroxide-treated U937 cells. *J Immunol* 176, 2555-2561.

Peterson, B., Knotts, T., Cummings, B. S., 2007. Involvement of Ca<sup>2+</sup>-independent phospholipase A2 isoforms in oxidant-induced neural cell death. *Neurotoxicology* 28, 150-160.

Pfeilschifter, J., Muhl, H., Pignat, W., Marki, F., van den Bosch, H., 1993. Cytokine regulation of group II phospholipase A2 expression in glomerular mesangial cells. *Eur J Clin Pharmacol* 44 Suppl 1, S7-9.

Pruzanski, W., Lambeau, L., Lazdunsky, M., Cho, W., Kopilov, J., Kuksis, A., 2005. Differential hydrolysis of molecular species of lipoprotein phosphatidylcholine by groups IIA, V and X secretory phospholipases A2. *Biochim Biophys Acta* 1736, 38-50.

Pruzanski, W., Vadas, P., 1988. Secretory synovial fluid phospholipase A2 and its role in the pathogenesis of inflammation in arthritis. *J Rheumatol* 15, 1601-1603.

Radner, F. P., Streith, I. E., Schoiswohl, G., Schweiger, M., Kumari, M., Eichmann, T. O., Rechberger, G., Koefeler, H. C., Eder, S., Schauer, S., Theussl, H. C., Preiss-Landl, K., Lass, A., Zimmermann, R., Hoeffler, G., Zechner, R., Haemmerle, G., 2012. Growth retardation, impaired triacylglycerol catabolism, hepatic steatosis, and lethal skin barrier defect in mice lacking comparative gene identification-58 (CGI-58). *J Biol Chem* 285, 7300-7311.

- Rai, R., Katzenellenbogen, J. A., 1992. Guanidinophenyl-substituted enol lactones as selective, mechanism-based inhibitors of trypsin-like serine proteases. *J Med Chem* 35, 4150-4159.
- Ramanadham, S., Song, H., Hsu, F. F., Zhang, S., Crankshaw, M., Grant, G. A., Newgard, C. B., Bao, S., Ma, Z., Turk, J., 2003. Pancreatic islets and insulinoma cells express a novel isoform of group VIA phospholipase A2 (iPLA2 beta) that participates in glucose-stimulated insulin secretion and is not produced by alternate splicing of the iPLA2 beta transcript. *Biochemistry* 42, 13929-13940.
- Ramanadham, S., Wolf, M. J., Li, B., Bohrer, A., Turk, J., 1997. Glucose-responsivity and expression of an ATP-stimulatable, Ca(2+)-independent phospholipase A2 enzyme in clonal insulinoma cell lines. *Biochim Biophys Acta* 1344, 153-164.
- Rando, R. R., 1974. Chemistry and enzymology of kcat inhibitors. *Science* 185, 320-324.
- Reed, P. E., Katzenellenbogen, J. A., 1991. Beta-substituted beta-phenylpropionyl chymotrypsins. Structural and stereochemical features in stable acyl enzymes. *J Med Chem* 34, 1162-1176.
- Rosengren, B., Jonsson-Rylander, A. C., Peilot, H., Camejo, G., Hurt-Camejo, E., 2006. Distinctiveness of secretory phospholipase A2 group IIA and V suggesting unique roles in atherosclerosis. *Biochim Biophys Acta* 1761, 1301-1308.
- Roshak, A. K., Capper, E. A., Stevenson, C., Eichman, C., Marshall, L. A., 2000. Human calcium-independent phospholipase A2 mediates lymphocyte proliferation. *J Biol Chem* 275, 35692-35698.
- Rouault, M., Bollinger, J. G., Lazdunski, M., Gelb, M. H., Lambeau, G., 2003. Novel mammalian group XII secreted phospholipase A2 lacking enzymatic activity. *Biochemistry* 42, 11494-11503.
- Rouault, M., Le Calvez, C., Boilard, E., Surrel, F., Singer, A., Ghomashchi, F., Bezzine, S., Scarzello, S., Bollinger, J., Gelb, M. H., Lambeau, G., 2007. Recombinant production and properties of binding of the full set of mouse secreted phospholipases A2 to the mouse M-type receptor. *Biochemistry* 46, 1647-1662.
- Rydel, T. J., Williams, J. M., Krieger, E., Moshiri, F., Stallings, W. C., Brown, S. M., Pershing, J. C., Purcell, J. P., Alibhai, M. F., 2003. The crystal structure, mutagenesis, and activity studies reveal that patatin is a lipid acyl hydrolase with a Ser-Asp catalytic dyad. *Biochemistry* 42, 6696-6708.

- Saarela, J., Jung, G., Hermann, M., Nimpf, J., Schneider, W. J., 2008. The patatin-like lipase family in *Gallus gallus*. *BMC Genomics* 9, 281.
- Safra, T., Muggia, F., Jeffers, S., Tsao-Wei, D. D., Groshen, S., Lyass, O., Henderson, R., Berry, G., Gabizon, A., 2000. Pegylated liposomal doxorubicin (doxil): reduced clinical cardiotoxicity in patients reaching or exceeding cumulative doses of 500 mg/m<sup>2</sup>. *Ann Oncol* 11, 1029-1033.
- Salvador-Morales, C., Valencia, P. M., Thakkar, A. B., Swanson, E. W., Langer, R., 2012. Recent developments in multifunctional hybrid nanoparticles: opportunities and challenges in cancer therapy. *Front Biosci (Elite Ed)* 4, 529-545.
- Schonborn, I., Minguillon, C., Lichtenegger, W., Zschiesche, W., Spitzer, E., 1995. [C-erbB-2, EGF receptor, p53 and PCNA. The prognostic significance of recent tumor markers for lymph node negative breast cancer]. *Geburtshilfe Frauenheilkd* 55, 566-571.
- Schroeder, A., Heller, D. A., Winslow, M. M., Dahlman, J. E., Pratt, G. W., Langer, R., Jacks, T., Anderson, D. G., 2012. Treating metastatic cancer with nanotechnology. *Nat Rev Cancer* 12, 39-50.
- Seilhamer, J. J., Pruzanski, W., Vadas, P., Plant, S., Miller, J. A., Kloss, J., Johnson, L. K., 1989. Cloning and recombinant expression of phospholipase A2 present in rheumatoid arthritic synovial fluid. *J Biol Chem* 264, 5335-5338.
- Seilhamer, J. J., Randall, T. L., Yamanaka, M., Johnson, L. K., 1986. Pancreatic phospholipase A2: isolation of the human gene and cDNAs from porcine pancreas and human lung. *DNA* 5, 519-527.
- Seruga, B., Tannock, I. F., 2012. Chemotherapy-based treatment for castration-resistant prostate cancer. *J Clin Oncol* 29, 3686-3694.
- Shih, H. A., Harisinghani, M., Zietman, A. L., Wolfgang, J. A., Saksena, M., Weissleder, R., 2005. Mapping of nodal disease in locally advanced prostate cancer: rethinking the clinical target volume for pelvic nodal irradiation based on vascular rather than bony anatomy. *Int J Radiat Oncol Biol Phys* 63, 1262-1269.
- Shinzawa, K., Sumi, H., Ikawa, M., Matsuoka, Y., Okabe, M., Sakoda, S., Tsujimoto, Y., 2008. Neuroaxonal dystrophy caused by group VIA phospholipase A2 deficiency in mice: a model of human neurodegenerative disease. *J Neurosci* 28, 2212-2220.
- Sina, F., Shojaee, S., Elahi, E., Paisan-Ruiz, C., 2009. R632W mutation in PLA2G6 segregates with dystonia-parkinsonism in a consanguineous Iranian family. *Eur J Neurol* 16, 101-104.

Sofia, M. J., Katzenellenbogen, J. A., 1986. Enol lactone inhibitors of serine proteases. The effect of regiochemistry on the inactivation behavior of phenyl-substituted (halomethylene)tetra- and -dihydrofuranones and (halomethylene)tetrahydropyranones toward alpha-chymotrypsin: stable acyl enzyme intermediate. *J Med Chem* 29, 230-238.

Song, K., Zhang, X., Zhao, C., Ang, N. T., Ma, Z. A., 2005. Inhibition of Ca<sup>2+</sup>-independent phospholipase A2 results in insufficient insulin secretion and impaired glucose tolerance. *Mol Endocrinol* 19, 504-515.

Song, Y., Wilkins, P., Hu, W., Murthy, K. S., Chen, J., Lee, Z., Oyesanya, R., Wu, J., Barbour, S. E., Fang, X., 2007. Inhibition of calcium-independent phospholipase A2 suppresses proliferation and tumorigenicity of ovarian carcinoma cells. *Biochem J* 406, 427-436.

Sonoshita, M., Takaku, K., Sasaki, N., Sugimoto, Y., Ushikubi, F., Narumiya, S., Oshima, M., Taketo, M. M., 2001. Acceleration of intestinal polyposis through prostaglandin receptor EP2 in Apc(Delta 716) knockout mice. *Nat Med* 7, 1048-1051.

Sreekumar, A., Poisson, L. M., Rajendiran, T. M., Khan, A. P., Cao, Q., Yu, J., Laxman, B., Mehra, R., Lonigro, R. J., Li, Y., Nyati, M. K., Ahsan, A., Kalyana-Sundaram, S., Han, B., Cao, X., Byun, J., Omenn, G. S., Ghosh, D., Pennathur, S., Alexander, D. C., Berger, A., Shuster, J. R., Wei, J. T., Varambally, S., Beecher, C., Chinnaiyan, A. M., 2009. Metabolomic profiles delineate potential role for sarcosine in prostate cancer progression. *Nature* 457, 910-914.

Stavridi, F., Karapanagiotou, E. M., Syrigos, K. N., 2012. Targeted therapeutic approaches for hormone-refractory prostate cancer. *Cancer Treat Rev* 36, 122-130.

Sun, B., Lockyer, S., Li, J., Chen, R., Yoshitake, M., Kambayashi, J. I., 2001. OPC-28326, a selective femoral vasodilator, is an alpha2C-adrenoceptor-selective antagonist. *J Pharmacol Exp Ther* 299, 652-658.

Sun, B., Zhang, X., Talathi, S., Cummings, B. S., 2008. Inhibition of Ca<sup>2+</sup>-independent phospholipase A2 decreases prostate cancer cell growth by p53-dependent and independent mechanisms. *J Pharmacol Exp Ther* 326, 59-68.

Sun, B., Zhang, X., Yonz, C., Cummings, B. S., 2010. Inhibition of calcium-independent phospholipase A2 activates p38 MAPK signaling pathways during cytostasis in prostate cancer cells. *Biochem Pharmacol* 79, 1727-1735.

Sun, G. Y., Xu, J., Jensen, M. D., Yu, S., Wood, W. G., Gonzalez, F. A., Simonyi, A., Sun, A. Y., Weisman, G. A., 2005. Phospholipase A2 in astrocytes: responses to oxidative stress, inflammation, and G protein-coupled receptor agonists. *Mol Neurobiol* 31, 27-41.

Sved, P., Scott, K. F., McLeod, D., King, N. J., Singh, J., Tsatralis, T., Nikolov, B., Boulas, J., Nallan, L., Gelb, M. H., Sajinovic, M., Graham, G. G., Russell, P. J., Dong, Q., 2004. Oncogenic action of secreted phospholipase A2 in prostate cancer. *Cancer Res* 64, 6934-6940.

Tischfield, J. A., Xia, Y. R., Shih, D. M., Klisak, I., Chen, J., Engle, S. J., Siakotos, A. N., Winstead, M. V., Seilhamer, J. J., Allamand, V., Gyapay, G., Lusic, A. J., 1996. Low-molecular-weight, calcium-dependent phospholipase A2 genes are linked and map to homologous chromosome regions in mouse and human. *Genomics* 32, 328-333.

Valentin, E., Singer, A. G., Ghomashchi, F., Lazdunski, M., Gelb, M. H., Lambeau, G., 2000. Cloning and recombinant expression of human group IIF-secreted phospholipase A(2). *Biochem Biophys Res Commun* 279, 223-228.

Verheij, H. M., Slotboom, A. J., de Haas, G. H., 1981. Structure and function of phospholipase A2. *Rev Physiol Biochem Pharmacol* 91, 91-203.

Waite, C. L., Roth, C. M., 2012. Nanoscale drug delivery systems for enhanced drug penetration into solid tumors: current progress and opportunities. *Crit Rev Biomed Eng* 40, 21-41.

Wijewickrama, G. T., Kim, J. H., Kim, Y. J., Abraham, A., Oh, Y., Ananthanarayanan, B., Kwatia, M., Ackerman, S. J., Cho, W., 2006. Systematic evaluation of transcellular activities of secretory phospholipases A2. High activity of group V phospholipases A2 to induce eicosanoid biosynthesis in neighboring inflammatory cells. *J Biol Chem* 281, 10935-10944.

Wu, Z., Minhas, G. S., Wen, D., Jiang, H., Chen, K., Zimniak, P., Zheng, J., 2004. Design, synthesis, and structure-activity relationships of haloenol lactones: site-directed and isozyme-selective glutathione S-transferase inhibitors. *J Med Chem* 47, 3282-3294.

Yamashita, S., Ogawa, M., Sakamoto, K., Abe, T., Arakawa, H., Yamashita, J., 1994a. Elevation of serum group II phospholipase A2 levels in patients with advanced cancer. *Clin Chim Acta* 228, 91-99.

Yamashita, S., Yamashita, J., Ogawa, M., 1994b. Overexpression of group II phospholipase A2 in human breast cancer tissues is closely associated with their malignant potency. *Br J Cancer* 69, 1166-1170.

Yamashita, S., Yamashita, J., Sakamoto, K., Inada, K., Nakashima, Y., Murata, K., Saishoji, T., Nomura, K., Ogawa, M., 1993. Increased expression of membrane-associated phospholipase A2 shows malignant potential of human breast cancer cells. *Cancer* 71, 3058-3064.

Yokota, Y., Notoya, M., Higashino, K., Ishimoto, Y., Nakano, K., Arita, H., Hanasaki, K., 2001. Clearance of group X secretory phospholipase A(2) via mouse phospholipase A(2) receptor. *FEBS Lett* 509, 250-254.

Zhang, L., Peterson, B. L., Cummings, B. S., 2005. The effect of inhibition of Ca<sup>2+</sup>-independent phospholipase A2 on chemotherapeutic-induced death and phospholipid profiles in renal cells. *Biochem Pharmacol* 70, 1697-1706.

Zhang, X. H., Zhao, C., Seleznev, K., Song, K., Manfredi, J. J., Ma, Z. A., 2006. Disruption of G1-phase phospholipid turnover by inhibition of Ca<sup>2+</sup>-independent phospholipase A2 induces a p53-dependent cell-cycle arrest in G1 phase. *J Cell Sci* 119, 1005-1015.

Zhu, G., Alhamhoom, Y., Cummings, B. S., Arnold, R. D., 2011a. Synthesis of lipids for development of multifunctional lipid-based drug-carriers. *Bioorg Med Chem Lett* 21, 6370-6375.

Zhu, G., Mock, J. N., Aljuffali, I., Cummings, B. S., Arnold, R. D., 2011b. Secretory phospholipase A responsive liposomes. *J Pharm Sci* 100, 3146-3159.

## APPENDIX

## Haloenol pyranones and morpholinones as antineoplastic agents of prostate cancer

Jason N. Mock, John P. Taliaferro, Xiao Lu, Sravan Kumar Patel, Brian S. Cummings, Timothy E. Long\*

Department of Pharmaceutical and Biomedical Sciences, University of Georgia, Athens, GA 30602-2352, USA

### ARTICLE INFO

#### Article history:

Received  
Received in revised form  
Accepted  
Available online

#### Keywords:

Haloenol  
Pyranones  
Morpholinones  
Phospholipase A<sub>2</sub>  
Prostate cancer

### ABSTRACT

Haloenol pyran-2-ones and morpholin-2-ones were synthesized and evaluated as inhibitors of cell growth in two different prostate cancer cell lines (PC-3 and LNCaP). Analogs derived from L- and D-phenylglycine were found to be the most effective antagonists of LNCaP and PC-3 cell growth. Additional studies reveal that the inhibitors induced G2/M arrest and the (S)-enantiomer of the phenylglycine-based derivatives was a more potent inhibitor of cytosolic iPLA<sub>2</sub>β.

2009 Elsevier Ltd. All rights reserved.

Haloenol pyranones<sup>1</sup> are mechanism-based inhibitors of serine proteases due to their ability to alkylate enzyme active sites following ring hydrolysis and unmasking of a reactive  $\alpha$ -haloketone functionality (Figure 1). To date, the most evaluated of these inhibitors is bromoenol lactone, (*E*)-6-(bromomethylene)tetrahydro-3-(1-naphthalenyl)-2*H*-pyran-2-one (**4**) or BEL. Interestingly, the popularity of BEL stems not as a deactivator of serine proteases, but rather for its ability to inhibit Ca<sup>2+</sup>-independent phospholipases A<sub>2</sub> (iPLA<sub>2</sub>), which are responsible for the catabolism of membrane glycerophospholipids. Over the last 20 years, BEL has enabled researchers to probe the role of iPLA<sub>2</sub> in pathologies involving oxidative stress and inflammation including cardiovascular<sup>2</sup>, Alzheimer's<sup>3</sup> and Parkinson's diseases<sup>4</sup>, diabetes mellitus<sup>5</sup>, and more recently, carcinogenesis<sup>6,7</sup>.

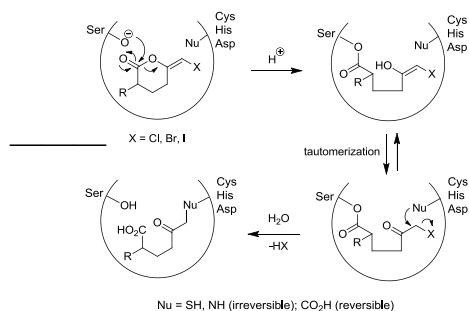


**Figure 1.** Mechanism of serinase inhibition by haloenol pyran-2-ones.

Mammalian cells possess multiple isoforms of iPLA<sub>2</sub><sup>8</sup>. The most studied are cytosolic iPLA<sub>2</sub>β, (Group VIA-1 and A-2 PLA<sub>2</sub>) and the membrane localized iPLA<sub>2</sub>γ (Group VIB PLA<sub>2</sub>), which together govern the release of fatty acids arachidonic acid and 2-lysophospholipids from membrane phospholipids. For many years, phospholipid remodeling<sup>8,9</sup> was thought to be the only function of these enzymes; however, beginning in the 1990's researchers began finding evidence that iPLA<sub>2</sub> participates in cell signaling<sup>10</sup>, proliferation<sup>11</sup>, and death<sup>4,12</sup>. It was established that the products arising from the breakdown of phospholipids functioned as signaling molecules for promoting cell growth and that the enzymes responsible for generating the lipids

(i.e. PLA<sub>2</sub>) are in greater abundance in carcinoma cells<sup>13</sup>.

The effects of iPLA<sub>2</sub> $\gamma$  and iPLA<sub>2</sub> $\beta$  on cell signaling and proliferation have recently been studied by enantiomer-based inhibition<sup>6,14</sup> strategies using (*R*)- and (*S*)-BEL, respectively (Figure 2). The mechanisms involved in their selectivity are currently under study although it was demonstrated that LNCaP and PC-3 prostate cancer cells display moderate increases in chemosensitivities to racemic BEL compared to the individual enantiomers<sup>6</sup>. These results suggest that the (*R*)- and (*S*)-conformers could be acting in a synergistic manner as cell growth inhibitors. The studies further established that enantiomers of haloenol pyranones may be used to selectively and pharmacologically inhibit iPLA<sub>2</sub> $\gamma$ , iPLA<sub>2</sub> $\beta$ , and possibly other enzymes involved in critical cell processes. In this Letter, we report on the antineoplastic activities of haloenol pyran-2-one analogs of BEL against prostate cancer. In addition, the evaluation of novel haloenol morpholin-2-ones constructed from L- and D-amino acids and their inhibitory effects on the cell cycle and iPLA<sub>2</sub> activity are described.

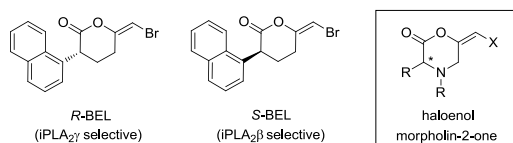
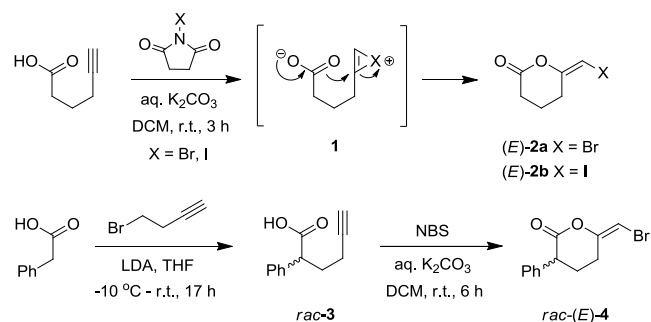


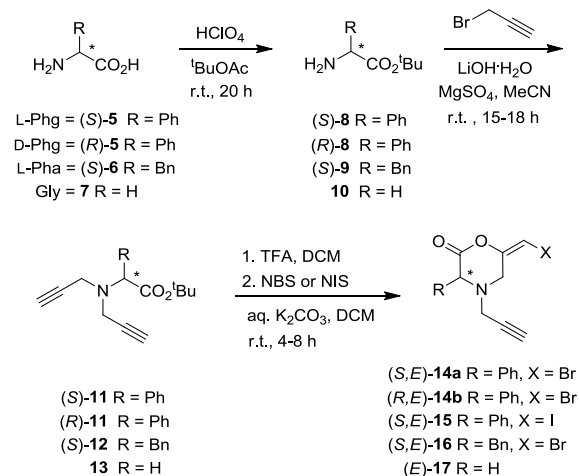
**Figure 2.** Chemical structures of BEL and haloenol morpholinones.

To evaluate whether analogs of BEL could have similar inhibitory effects on iPLA<sub>2</sub> and prostate cancer growth, we set forth to synthesize various haloenol pyran-2-ones from  $\alpha$ -substituted and unsubstituted acetylenic acids. Standard *E*-specific haloenol lactonization procedures<sup>1,15</sup> with *N*-halosuccinimides (X = Br, I) were used to generate the pyranone analogs (Scheme 1). In the case of the phenyl analog **4**, the acid precursor **3** required preparation from phenylacetic acid and 4-bromobut-1-yne using classical enolate chemistry<sup>18</sup>. Subsequent attempts to separate the (*R*)- and (*S*)-enantiomers of lactone **4** by chiral HPLC were unsuccessful, which led to us to consider the use of chiral pool amino acids to construct novel iPLA<sub>2</sub> inhibitors containing a *E*-haloenol morpholin-2-one framework (Figure 2).



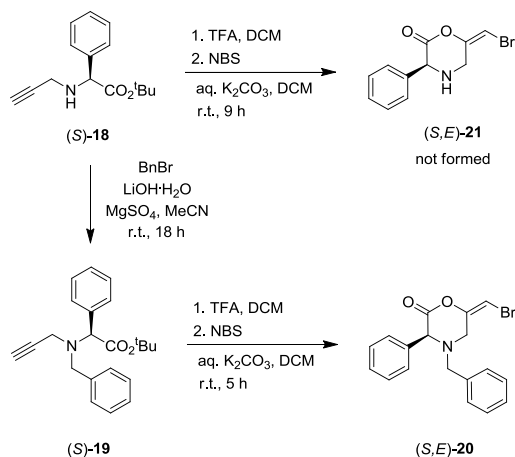
**Scheme 1.** Synthesis of unsubstituted and monophenyl BEL analogs.

L- and D-phenylglycine (Phg), L-phenylalanine (Pha), and glycine (Gly) were chosen as base materials to perform the asymmetrical synthesis of morpholinone analogs. Protected *tert*-butyl esters forms of the amino acids were first prepared from *tert*-butyl acetate<sup>16</sup> then converted to the corresponding *N,N*-propargyl  $\alpha$ -amino esters **11–13**<sup>17</sup>. Following deprotection of the carboxylic acid, bromo- and iodoenol morpholin-2-one analogs **14–17** were generated in 6–23% yield under the conditions described for pyranones **2** and **4**.



**Scheme 2.** Synthesis of *N*-propargyl bromoenol morpholin-2-ones **14–17**.

The synthesis of additional L-Phg-based analogs was also attempted from the monopropargyl intermediate **18**. Benzylation of the secondary amine followed by acid deprotection and cyclization gave the corresponding *N*-benzyl bromoenol morpholin-2-one **20**. Efforts to prepare the unsubstituted analog **21** were unsuccessful however, which was attributed to chemical instability of the *N*-proton ring system.



**Scheme 3.** Synthesis of N-benzyl bromoenol morpholin-2-one **20**.

Minimum inhibitory concentrations ( $IC_{50}$ s) were determined by MTT staining for the haloenol pyranones (**2**, **4**) and morpholinones (**14-17**, **20**) against LNCaP cells, and the more resistant PC-3 human prostate cancer cell line. With racemic BEL as a haloenol standard,  $IC_{50}$  measurements were taken at 24, 48, and 72 h (Table 1). BEL was found to inhibit growth in a time-dependent manner at 5-13  $\mu$ M and 14-34  $\mu$ M of LNCaP and PC-3, respectively, over 72 h which corroborated previous findings<sup>6</sup>. Activity comparison of BEL to pyranones **2** revealed that the unsubstituted analogs were equally efficacious inhibitors at 5-10 and 14-32  $\mu$ M for the

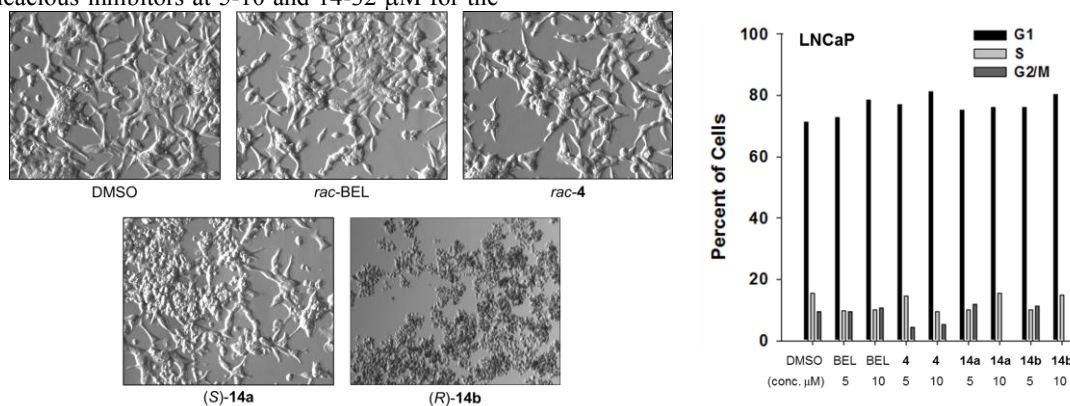


**Figure 3.** Changes in morphology (left-40X magnification) and cell cycle (right) of LNCaP cells following treatment with *rac*-BEL, *rac*-**4**, (*S*)-**14a**, and (*R*)-**14b**.

( $IC_{50}$  3-8  $\mu$ M). As a compound derived from the unnatural D-form of Phg, the augmented activity of (*R*)-**14b** was attributed in part to higher proteolytic susceptibility (e.g. chymotrypsin) that the L-Phg-based (*S*)-**14a** may have in the cell.

Other haloenol morpholinones were found to have weaker inhibitory activities including the L-Pha- and Gly-derived analogs **16** and **17**, respectively. Surprisingly, chemosensitivity for the iodoenol derivative **15** was also considerably lower than its bromoenol counterparts **14**. Conversely, the N-

corresponding cell lines. For the  $\alpha$ -substituted phenyl analog **4**, slightly enhanced activities were observed with  $IC_{50}$ s ranging from 6-27  $\mu$ M against PC-3.

**Table 1:**  $IC_{50}$ s ( $\mu$ M) against human prostate cancers after 24, 48, and 72 h exposure to haloenol inhibitors.<sup>a</sup>

compd	LNCaP			PC-3		
	24	48	72	24	48	72
<i>rac</i> -BEL	13	5	9	34	26	14
<b>2a</b>	10	5	5	19	23	14
<b>2b</b>	9	5	7	32	15	16
<i>rac</i> - <b>4</b>	31	5	4	27	10	6
( <i>S</i> )- <b>14a</b>	8	3	3	15	13	5
( <i>R</i> )- <b>14b</b>	6	6	3	8	6	3
( <i>S</i> )- <b>15</b>	26	23	20	21	21	25
( <i>S</i> )- <b>16</b>	41	26	32	33	57	39
<b>17</b>	25	29	28	13	10	7
( <i>S</i> )- <b>20</b>	3	4	3	4	1	4

<sup>a</sup>Data represent the calculated  $IC_{50}$  using data assessed 3-5 experiments ran in duplicate using separate passages of cells assessing alteration in MTT staining.

The morpholinones analogs similarly demonstrated antineoplastic activity with  $IC_{50}$ s reaching 3  $\mu$ M for the Phg-based derivatives **14** (Table 1). The inhibitors also appeared to be more rapid-acting antagonists of prostate cancer growth compared to BEL and its phenyl pyranone analog **4**. Moreover, activity comparison of the enantiomers revealed that (*R*)-**14b** was a more effective inhibitor than (*S*)-**14a** particularly against PC-3 cells

benzyl L-Phg-based analog **20** proved to be the most potent antagonist in the study ( $IC_{50}$  1-4  $\mu$ M). The compound demonstrated rapid and sustained inhibitory effects on cell proliferation for both LNCaP and PC-3 cells over the 72 h evaluation period.

To determine if growth inhibition was due to cytostatic or cytotoxic effects by the antagonists, cell viability was assessed by phase-contrast microscopy<sup>18</sup>. Comparisons of morphology were made by visual inspection of LNCaP cells following 72 h treatment with *rac*-BEL, *rac*-**4**, (*S*)-**14a**, and (*R*-

**14b** (Figure 3). Exposure to 5  $\mu\text{M}$  of BEL and its monophenyl analog **4** induced little to no morphological changes in cell shape, differentiation, and death compared to the vehicle (DMSO) control. For the morpholinone analogs **14**, apoptosis and/or necrosis was evident at the same concentrations particularly for the (*R*)-enantiomer. It was concluded from these microscopic images that prostate cancer cells had greater chemosensitivity to haloenol morpholinones than to the analogous haloenol pyranones which corroborated the IC<sub>50</sub> data.

The inhibitory effects by *rac*-BEL, pyranone **4**, and morpholinones **14** were additionally assessed by monitoring changes in the cell cycle by flow cytometry with propidium iodide<sup>6b</sup> (Figure 3). Moderate increases of LNCaP cell counts in the G1 phase were observed following 24 h treatment with 5 and 10  $\mu\text{M}$  of the test compounds. It is believed that the elevated G1 levels led to the decrease in S and G2/M phase cell percentages and the effects were greatest for **14a** and **14b** which induced complete cell cycle arrest at 10  $\mu\text{M}$ . Likewise, on comparison to cultures treated with the 5  $\mu\text{M}$  of the inhibitors, the increase of cells residing in S phase may have been due to the lack of cells entering the G2/M phase. These results further suggest that the cytotoxic effects of morpholinone-based analogs may be the result of DNA hypoploidy, which is associated with DNA fragmentation and apoptosis. Examples of agents that block mitosis by inhibiting chromosome replication include DNA alkylating agents (e.g. nitrogen mustards) and antagonists of glutathione S-transferase (e.g.

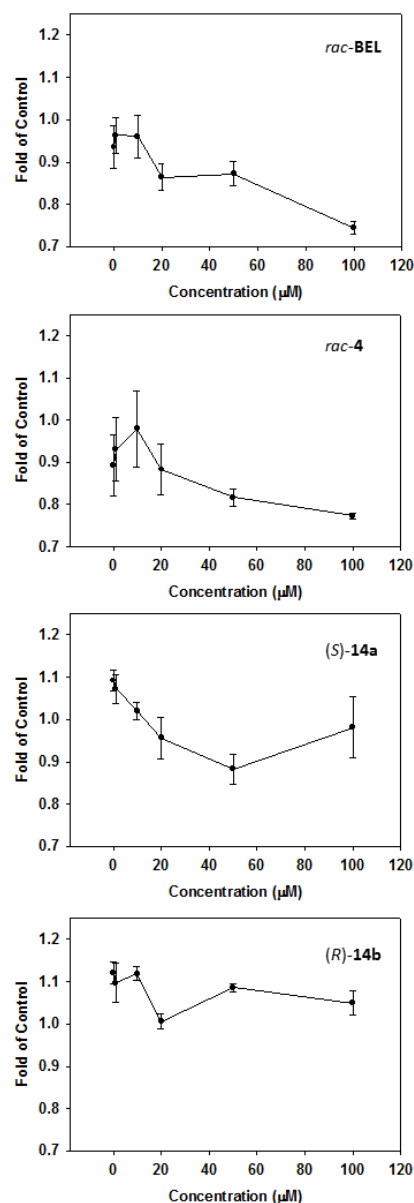


**Figure 4.** Inhibitory effects of *rac*-BEL, *rac*-4, (*S*)-**14a**, and (*R*)-**14b** on iPLA<sub>2</sub> $\beta$  activity in rat kidney cytosol in the presence of 4 mM EGTA. Data are represented as the mean  $\pm$  the S.E.M. of at least 3 separate experiments.  $\alpha$ -chloroacetamides<sup>19</sup>), which protect cells from oxidative DNA damage.

Lastly, *rac*-BEL, pyranone **4**, and morpholinones **14** were evaluated for their ability to inhibit iPLA<sub>2</sub> $\beta$  from rat kidney. Cytosolic fractions were treated for 0.5 h with 0-100  $\mu\text{M}$  of the compounds prior to inoculation with the arachidonoyl thio-phosphatidylcholine, a hydrolysable thioester-containing probe of PLA<sub>2</sub> activity<sup>6b</sup>. Both *rac*-BEL and its phenyl-substituted analog **4** demonstrated nearly identical efficacy to inhibit the enzyme in a concentration-dependent manner (Figure 4). Inhibitory activity was also noted for (*S*)-**14a** but to a lesser degree compared to pyranone-based antago-

nists. Little to no effects on iPLA<sub>2</sub>β activity was observed for (*R*)-**14b** which correlates to earlier findings<sup>6,14</sup> that the (*S*)-enantiomer of BEL selectively inhibits cytosolic iPLA<sub>2</sub>β while (*R*)-BEL possesses higher affinity for microsomal iPLA<sub>2</sub>γ.

In summary, haloenol pyran-2-ones were found to be efficacious inhibitors of prostate carcinoma cell growth and iPLA<sub>2</sub>β activity however, as with BEL, a definitive correlation could not be made. Novel haloenol morpholin-2-ones constructed asymmetrically from chiral amino acids were also discovered to be antagonists of cell proliferation. Differences in the effects on the cell cycle and iPLA<sub>2</sub>β activity suggested that the morpholinone analogs **14** may have a greater capacity to directly or indirectly cause DNA damage. Glutathione S-transferase which has a role in protecting DNA from oxidative damage is known to be inhibited by haloenol lactones<sup>20</sup> and could be a primary or secondary target for the Phg-based derivatives. Finally, during the course of these studies it became apparent that the chemical instability of the haloenol pyranones and morpholinones would likely preclude them from being viable drug candidates for prostate cancer. Their use as research tools in the study of tumorigenesis and validation of new therapeutic targets may be of great value though to the drug discovery community.

#### Acknowledgements

Financial support was generously provided by the College of Pharmacy at the University of Georgia and in part by a Georgia Cancer Coalition Distinguished Scholar Grants and a NIH NIBIB (EB08153) to B.S.C.

#### References and notes

- (a) Rai, R.; Katzenellenbogen, J. A. *J. Med. Chem.* **1992**, *35*, 4150; (b) Reed, P. E.; Katzenellenbogen, J. A. *J. Biol. Chem.* **1991**, *266*, 13; (c) Sofia, M. J.; Katzenellenbogen, J. A. *J. Med. Chem.* **1986**, *29*, 230; (d) Daniels, S. B.; Katzenellenbogen, J. A. *Biochemistry* **1986**, *25*, 1436; (e) Daniels, S. B.; Cooney, E.; Sofia, M. J.; Chakravarty, P. K.; Katzenellenbogen, J. A. *J. Biol. Chem.* **1983**, *258*, 15046; (f) Chakravarty, P. K.; Krafft, G. A.; Katzenellenbogen, J. A. *J. Biol. Chem.* **1982**, *257*, 610; (g) Krafft, G. A.; Katzenellenbogen, J. A. *J. Am. Chem. Soc.* **1981**, *103*, 5459; (h) Rando, R. R. *Science* **1974**, *185*, 320.
- McHowat, J.; Creer, M. H. *Curr. Med. Chem. Cardiovasc. Hematol. Agents* **2004**, *2*, 209.
- (a) Sun, G. Y.; Xu, J.; Jensen, M. D.; Yu, S.; Wood, W. G.; González, F. A.; Simonyi, A.; Sun, A. Y.; Weisman, G. A. *Mol. Neurobiol.* **2005**, *31*, 27; (b) Hoozemans, J. J. M.; Veerhuis, R.; Janssen, I.; Rozemuller, A. J. M.; Eikelenboom, P. *Exp. Gerontol.* **2001**, *36*, 559.
- (a) Farooqui, A. A.; Horrocks, L. A. *Neuroscientist* **2006**, *12*, 245; (b) Farooqui, A. A.; Ong, W. Y.; Horrocks, L. A. *Pharmacol. Rev.* **2006**, *58*, 591.
- (a) Song, K.; Zhang, X.; Zhao, C. Y.; Ang, N. T.; Ma, Z. M. A. *Mol. Endocrinol.* **2005**, *19*, 504; (b) Ramanadham, S.; Song, H. W.; Hsu, F. F.; Zhang, S.; Crankshaw, M.; Grant, G. A.; Newgard, C. B.; Bao, S. Z.; Ma, Z. M.; Turk, J. *Biochemistry* **2003**, *42*, 13929; (c) Ma, Z.; Wang, X.; Nowatzke, W.; Ramanadham, S.; Turk, J. *J. Biol. Chem.* **1999**, *274*, 9607; (d) Ma, Z.; Ramanadham, S.; Hu, Z.; Turk, J. *Biochim. Biophys. Acta* **1998**, *1391*, 384.
- (a) Sun, B.; Zhang, X. L.; Yonz, C.; Cummings, B. S. *Biochem. Pharmacol.* **2010**, *79*, 1727; (b) Sun, B.; Zhang, X.; Talathi, S.; Cummings, B. S. *J. Pharmacol. Exp. Ther.* **2008**, *326*, 59.
- (a) Song, Y.; Wilkins, P.; Hu, W. H.; Murthy, K. S.; Chen, J.; Lee, Z.; Oyesanya, R.; Wu, J. H.; Barbour, S. E.; Fang, X. *J. Biochem. J.* **2007**, *406*, 427; (b) Zhang, X. H.; Zhao, C.; Seleznev, K.; Song, K.; Manfredi, J. J.; Ma, Z. A. *J. Cell Sci.* **2006**, *119*, 1005; (c) Zhang, L.; Peterson, B. L.; Cummings, B. S. *Biochem. Pharmacol.* **2005**, *70*, 1697.
- (a) Cummings, B. C. *Biochem. Pharmacol.* **2007**, *74*, 949; (b) Schaloske, R. H.; Dennis E. A. *Biochim. Biophys. Acta* **2006**, *1761*, 1246; (c) Balsinde, J.; Perez, R.; Balboa, M. A. *Biochim. Biophys. Acta* **2006**, *1761*, 1344; (d) Casas, J.; Gijon, M. A.; Vigo, A. G.; Crespo, M. S.; Balsinde, J.; Balboa, M. A. *J. Biol. Chem.* **2006**, *281*, 6106. (e) Balboa, M. A.; J. Balsinde, J.; Dennis E. A. *Biochem. Biophys. Res. Commun.* **2000**, *267*, 145.
- (a) Balsinde, J.; Balboa, M. A.; Dennis, E. A. *J. Biol. Chem.* **1997**, *272*, 29317; (b) Balsinde, J.; Dennis, E. A. *J. Biol. Chem.* **1997**, *272*, 16069; (c) Balsinde, J.; Dennis, E. A. *J. Biol. Chem.* **1996**, *271*, 31937.
- (a) Hooks, S. B.; Cummings, B. S. *Biochem. Pharmacol.* **2008**, *76*, 1059; (b) Xu, J.; Weng, Y. I.; Simonyi, A.; Krugh, B. W.; Liao, Z.; Weisman, G. A.; Sun, G. Y. *J. Neurochem.* **2002**, *83*, 259; (c) Balsinde, J.; Balboa, M. A.; Li, W. H.; Llopis, J.; Dennis, E. A. *J. Immunol.* **2000**, *164*, 5398; (d) Bonventre, J. V. *J. Lipid Mediat. Cell Signal.* **1997**, *17*, 71; (e) Ramanadham, S.; Wolf, M. J.; Li, B.; Bohrer, A.; Turk, J. *Biochim. Biophys. Acta* **1997**, *1344*, 153.
- (a) Hassan, S.; Carraway, R. E. *Regul. Pept.* **2006**, *133*, 105; (b) Saavedra, G.; Zhang, W.; Peterson, B.; (b) Cummings, B. S. *J. Pharmacol. Exp. Ther.* **2006**, *318*, 1211; (c) Bao, S.; Bohrer, A.; Ramanadham, S.; Jin, W.; Zhang, S.; Turk, J. *J. Biol. Chem.* **2006**, *281*, 187; (d) Longo, W. E.; Grossmann, E. M.; Erickson, B.; Panesar, N.; Mazuski, J. E.; Kaminski, D. L. *J. Surg. Res.* **1999**, *84*, 51; (e) Teslenko, V.; Rogers, M.; Lefkowitz, J. B. *Biochim. Biophys. Acta* **1997**, *1344*, 189.
- (a) Cummings, B. S.; McHowat, J.; Schnellmann, R. G. *J. Pharmacol. Exp. Ther.* **2000**, *294*, 793; (b) Atsumi, G.; Tajima, M.; Hadano, A.; Nakatani, Y.; Murakami, M.; Kudo, I. *J. Biol. Chem.* **1998**, *273*, 13870;
- (a) Dong, Q.; Patel, M.; Scott, K. F.; Graham, G. G.; Russell, P. J.; Sved, P. *Cancer Lett.* **2006**, *240*, 9; (b) Jiang, J.; Neubauer, B. L.; Graff, J. R.; Chedid, M.; Thomas, J. E.; Roehm, N. W.; Zhang, S.; Eckert, G. J.; Koch, M. O.; Eble, J. N.; Cheng, L. *Am. J. Pathol.* **2002**, *160*, 667; (c) Graff, J. R.; Konicek, B. W.; Deddens, J. A.; Chedid, M.; Hurst, B. M.; Colligan, B.; Neubauer, B. L.; Carter, H. W.; Carter, J. H. *Clin. Cancer Res.* **2001**, *7*, 3857; (d) Yamashita, S.; Yamashita, J.; Ogawa, M. *Br. J. Cancer* **1994**, *69*, 1166; (e) Yamashita, S.; Ogawa, M.; Sakamoto, K.; Abe, T.; Arakawa, H.; Yamashita, J. *Clin. Chim. Acta* **1994**, *228*, 91; (f) Yamashita, S.; Yamashita, J.; Sakamoto, K.; Inada, K.; Nakashima, Y.; Murata, K.; Saishoji, T.; Nomura, K.; Ogawa, M. *Cancer* **1993**, *71*, 3058.
- (a) Kinsey, G. R.; Cummings, B. S.; Beckett, C. S.; Saavedra, G.; Zhang, W.; McHowat, J.; Schnellmann, R. G. *Biochem. Biophys. Res. Commun.* **2005**, *327*, 287; (b) Jenkins, C. M.; Han, X.; Mancuso, D. J.; Gross, R. W. *J. Biol. Chem.* **2002**, *277*, 32807.
- Dai, W.; Katzenellenbogen, J. A. *J. Org. Chem.* **1991**, *56*, 6893.

16. Chen, H.; Feng, Y.; Xu, Z.; Ye, T. *Tetrahedron* **2005**, *61*, 11132.
17. Cho, J. H.; Kim, B. M. *Tetrahedron Lett.* **2002**, *43*, 1273.
18. Cummings, B. S.; Schnellmann, R. G. *J. Pharm. Exp. Therap.* **2002**, *302*, 8.
19. Tsuboi, K.; Bachovchin, D. A.; Speers, A. E.; Spicer, T. P.; Fernandez-Vega, V.; Hodder, P.; Rosen, H.; Cravatt, B. F. *J. Am. Chem. Soc.* **2011**, *133*, 16605.
20. Wu, Z.; Minhas, G. S.; Wen, D.; Jiang, H.; Chen, K.; Zimniak, P.; Zheng, J. *J. Med. Chem.* **2004**, *47*, 3282.